Advanced Instrumentation and Sensor Fusion Methods in Input Devices for Musical Expression

Carolina Brum Medeiros

Input Devices and Music Interaction Laboratory
Schulich School of Music
McGill University
Montreal, Canada

April 2015

A thesis submitted to McGill University in partial fulfillment of the requirements for the degree of Doctor of Philosophy.

2015/04/15

Abstract

Advanced electronic instrumentation and sensor signal processing in Input Devices for Musical Expression must meet several requirements: they should be accurate, reproducible, monotonic, and robust. Despite these demanding design requirements, a large number of input devices are currently being developed in a Do-It-Yourself manner using simple sensing techniques. The aim of this thesis is to raise awareness of the limitations of this approach. As a solution, we propose state-of-the-art engineering tools to improve the sensing design: use of specialized sensor technologies, better electronic instrumentation, coherent calibration and data regression methods, and advanced signal processing through the sensor fusion filters. We have reviewed the Proceedings of the International Conference on New Musical Interfaces for Musical Expression, the major academic event in this field, from 2009 to 2013. Based on this review, we identify the generalized use of unsophisticated engineering solutions and easily available sensors, which are simple to assemble and require uncomplicated signal conditioning circuits. We then propose several methods of instrumentation and sensor signal processing that can deal with the above issues. Using these solutions, we evaluate the sensing design of one Digital Musical Instrument — The Rulers, an instrument containing several beams that can be bent or plucked, where beam motion can be assessed by either infrared, Hall effect, or strain gage sensors. We show that none of them are an optimal measurement solution. We then take advantage of the best features of each sensor technology, by applying sensor fusion techniques, optimally achieved by a linear Kalman filter. However, the Kalman filter implementation on human input signals is not obvious because several parameters of the system and its operation modes cannot be predefined, given the unpredictable nature of these signals. We therefore propose a framework for Kalman filter application based on gesture segmentation and classification, multiple sensors, multiple-model system and measurements, several candidate process models, filter evaluation, and Monte Carlo optimization. We confirm the validity of this framework by showing that it reduces the error covariance of the estimate. These results will hopefully lead to robust, reproducible, and responsive input devices more likely to provide skilled performers with instruments that could rival acoustic musical instruments in terms of expressive potential.

Résumé

Pour créer des instruments numériques qui permettent de s'exprimer musicalement, l'utilisation d'instrumentation électronique sophistiquée et de techniques avancées en traitement du signal répond à des besoins spécifiques: la précision, la reproductibilité, la robustesse et la monotonie des mesures. Souvent, au détriment de ces besoins, un grand nombre d'instruments numériques sont constitués de capteurs de qualité limitée assemblés à des systèmes de traitement du signal artisanaux. L'objet de cette thèse est de révéler les limites de ce type de développement et de proposer des solutions pour pallier ces limites. Nous proposons des outils qui visent à améliorer le procédé de traitement et d'acquisition des données via l'utilisation de capteurs spécifiques, d'instrumentation électronique de meilleure qualité, et de méthodes de calibration et de régression cohérentes. De plus, nous proposons des méthodes de traitement de signal avancées à partir de l'implémentation de filtres de Kalman. Nous avons travaillé à partir des Actes de la Conférence Internationale "New Musical Interfaces for Musical Expression" publiés entre 2009 et 2013. Cette conférence regroupe la communauté académique la plus représentative de la discipline. À travers ces recherches antérieures, nous avons constaté l'utilisation répandue de solutions rudimentaire couplées à l'utilisation de capteurs très abordables, faciles à assembler et qui nécessitent des conditionneurs de signal simples. Nous présentons donc des instrumentations électroniques et des systèmes de traitement de signal appropriés aux besoins spécifiques explicités en introduction. Avec ces solutions, nous évaluons le procédé de traitement et d'acquisition des données d'un instrument de musique numérique, "The Rulers", composé de plusieurs lames pouvant être ployée ou pincées. Le mouvement des lames est acquis soit par des capteurs infrarouges, soit par des capteurs magnétiques à effet Hall, ou encore l'utilisation de jauges de déformation. Nous montrons qu'aucun des capteurs ne présente une solution optimale pour nos mesures. Partant de ce constat, nous avons développé une technique de combinaison de données multi-capteurs qui exploite le meilleur de chaque technologie de capteurs grâce à un filtre de Kalman. L'implémentation de ce type de filtre n'est cependant pas évidente, l'absence d'un modelé d'action d'utilisateur rend un grand nombre de paramètres du système et de son fonctionnement à première vue indéfinissables. C'est pourquoi nous proposons une méthode d'utilisation des filtres de Kalman construite à partir de la décomposition et de la classification du mouvement, de plusieurs capteurs, de configurations multiples pour le système et les mesures, de l'évaluation des filtres et de l'optimisation Monte Carlo. La réduction de la covariance des erreurs dans nos estimés démontre la validité de notre méthode.

Dedication

This thesis is dedicated to my best friend and mom Maria.

Some smart kid wanted it.
For the love of a bald and terrified mathematician.
It should be obvious.
It's your Karma.

Acknowledgments

First, I would like to have 1/0 space here to thank not only those that directly contributed for this work, but also to those that help me on the adventure of learning, i.e. living.

This thesis counts with many contributions. The main one is the wise thoughts of my supervisor, Marcelo M. Wanderley, which are inspiring lessons for life. I am also indebted to Darryl Cameron, Yves Methot, Jullien Boissinot and Harold Kilianski, for their friendly help. I wish to thank the engineers that helped on assembling mechanical and electronic systems for this research: Pietro Verrecchia and Anthony Piciacchia. Also, I would like to thank former and current researchers of IDMIL Laboratory that shared, discussed and criticized this work. A nerdy thanks to the Vanessa Yaremchuk, for the machine learning implementation on The Rulers, for constant revisions and for the delightful discussions. My gratitude to the reviewers and editors of my published papers. An infinite loop thanks to all my proof-readers and best conceilling core: Matt Aldrich, Vanessa Yaremchuk, Chuck Bronson, Steve Sinclair, Thor Kell, John Sullivan, and Johnty Wang. I also would like to thank Amandine Pras for helping me with French and for not fitting in. My deep gratitude to Helene Drouin, Linda Mannix, and Eleanor Stubley for their kindness and help. My gratitude to my professors back home: Schneider, Carpes Jr. and da Rosa. The inspiring educator Philippe Depalle has all my respect and gratitude. I would like to thank Joseph Paradiso for having me as a visiting researcher in the Responsive Environments Group. My enourmous gratitude to Tom Kepple and Michael Lapinski, for so many lessons. It is an honor to work with the resenv colleagues, especially to Matt Aldrich, Brian Mayton and Nan-Wei Gong, precious inspiration sources. My gratitude also to Eric Berkson and his team, and for Visual3D for their software license and mentoring. Finally, financial support from the Coordenacao de Aperfeicoamento de Pessoal de Nivel Superior (Capes/Brazil), extra financial support from my advisor through a NSERC Discovery Grant, and other financial supports from Integrated Sensor System (ISS–CREATE), Center for Interdisciplinary Research in Music Media and Technology (CIRMMT), and Center for Research on Brain, Language and Music (CRBLM) were indispensable to accomplish this mission.

A deep gratitude to my families (gifted and cultivated), for being educators for life. I would also like to thank all friends, lovers, and colleagues for the support and the patience with my socially awkward math-mode. My deep thanks to Drs. Queiroz, Theodozio, and Farah, for keeping me up and almost running.

Full list of acknowledgments at carolinabrum.com/thesis.

Contents

List of Figures

List of Tables

List of Acronyms

AC	Alternate Current
ADC	Analog-to-Digital Converter
AHRS	Attitude and Heading Reference System
CMR	Common-Mode Rejection
CSI	Common Slopes and Intercepts
DC	Direct Current
DIY	Do-It-Yourself
DMI	Digital Musical Instrument
DSI	Different Slopes and Intercepts
DUT	Device Under Test
EEG	ElectroEncephalography
EKF	Extended Kalman Filters
EMG	ElectroMyoGraphy
FFT	Fast-Fourier Transform
FSR	Force Sensing Resistor
GF	Gage Factor
GUM	Guide to the Expression of Uncertainty in Measurement
HCI	Human-Computer Interaction
HL	Hall effect sensor
IC	Integrated Circuits
IEEE	Institute of Electrical and Electronics Engineers
in-amp	instrumentation amplifier
IR	Infrared
LKF	Linear Kalman Filters

MARG	Magnetic, Angular Rate, and Gravity
NIME	International Conference on New Interfaces for Musical Expression
op-amp	operational amplifier
RSS	Root-Sum-Square
SMC	Sound Music Computing Conference
SNR	Signal-to-Noise Ratio
ST	Schmitt Trigger
VIM	Vocabulary of Basic and General Terms in Metrology

Chapter 1

Introduction

Digital Musical Instruments (DMIs) are musical instruments typically composed of a control surface where user interaction is measured by sensors whose values are mapped to sound synthesis algorithms [1]. These instruments have gained interest among skilled musicians and performers in the last decades, leading to artistic practices including musical performance, interactive installations, and dance.

The creation of DMIs typically involves several areas, among them: arts, design, and engineering. The balance between these areas is an essential task in DMI design so that the resulting instruments can be aesthetically appealing, robust, and allow responsive, accurate, and repeatable sensing.

Although it has been claimed that specifications for artistic tools are stricter than those for military applications [2], this research raises a paradox. In most cases, DMIs are based on a few basic sensor types and unsophisticated engineering solutions, therefore they do not take advantage of more advanced sensing instrumentation and signal processing techniques that could dramatically improve their response. We aim to raise awareness regarding limitations of any engineering solution and assert the benefits of advanced electronic instrumentation

design in DMIs. For this, we propose the use of specialized sensors such as strain gages, advanced conditioning circuits and signal processing tools, and sensor fusion. We believe that careful electronic instrumentation design may lead to more responsive instruments.

The use of sensors and associated signal conditioning to measure physical quantities involves the fields of metrology and electronic instrumentation. Metrology is the science of measurement and its application, and has its own terminological dictionary which determines the "basic principles governing quantities and units": the International Vocabulary of Basic and General Terms in Metrology (VIM) [3]. The VIM, along with the GUM (Guide to the Expression of Uncertainty in Measurement), defines uncertainty and errors involved in measurements [4]. Electronic instrumentation is the measurement chain of an electronic measuring system, resulting in an analog or digital electrical output quantity. Electronic instrumentation typically includes all signal conditioning techniques on the path of a sensor signal towards an output electrical value. A sensor is considered the "element of a measuring system that is directly affected by a phenomenon carrying a quantity to be measured" [3]. Signal conditioning techniques include procedures and circuits devoted to adjusting, amplifying, filtering, selecting, and transducing signals.

Instrumentation of any sensor signal implies errors and uncertainties. Peter K. Stein states that a critical question concerning measurements is: "Could these data have been acquired by that measurement system without distortion, contamination and without affecting the process being observed" [5]. In order to answer this question, he developed the Unified Approach to the Engineering of Measurement Systems for Test and Evaluation. This Approach summarizes techniques to test and evaluate measuring systems [5, 6]. However, advanced electronic instrumentation is not sufficient to deal with the limited capability of measuring systems. Techniques such as calibration, regression, physical modeling, classification, and sensor fusion are helpful tools to enhance measurements. A reminder

about the importance of evaluating measured data is given by Stein: "Bad data look just as believable as Good Data! We ask a Measurement System for the Facts, not for its Opinion! [sic]" [5].

The development of sensing design for artistic applications is even more complicated. Buxton states that "in the grand scheme of things, there are three levels of design: standard spec, military spec and artist spec. Most significantly, I learned that the third, artist spec, was the hardest (and most important). If you could nail it, then everything else was easy [sic]" [2]. We believe that this applies to the design of musical tools, such as musical instruments. Indeed, over several years, expert musicians develop very high motor control skills to perform their acoustic instruments. For this, they rely on generally stable, robust, and responsive acoustic musical instruments that result from centuries of *lutherie* knowledge. Stable instruments are a necessary, but not sufficient requirement for musical expression. As Dobrian and Koppelman state: "sophisticated musical expression requires not only a good control interface but also virtuosic mastery of the instrument it controls" [7]. In the last few decades, Digital Musical Instruments have gained popularity among a large population. Several performers use DMIs in their practice, and some of them have developed very high motor control skills to perform these instruments. DMI design offers few physical constraints, and it is a highly creative endeavor involving a variety of knowledge fields such as art, design, human factors, and engineering. The balance between these areas is a delicate issue. Cook states that "Musical interface construction proceeds as more art than science, and possibly this is the only way that it can be done" [8]. We would rather advocate for a balanced approach between art and science because highly artistic instruments with poor engineering solutions might actually hinder musical expression, as they might not satisfy skilled performers' needs.

Dobrian and Koppelman wrote their 2006 NIME paper in order to "draw attention to

the question of whether musical expression in performance is being adequately addressed in much current research on real-time computer music interfaces" [7]. In this thesis, we have similar goals concerning sensing design. We are convinced that by applying advanced engineering techniques, one can achieve the specific requirements expressed above and create responsive instruments that join highly artistic design with state-of-the-art engineering solutions.

As most DMIs are meant for real-time performance, stable, robust, accurate, reproducible, and fast response sensing design is essential. Despite these demanding design requirements, a large number of DMIs are currently being developed in a Do-It-Yourself (DIY) manner using techniques that often result in unsophisticated engineering solutions prioritizing easily available sensors which are simple to assemble and require uncomplicated signal conditioning circuits [9, 10]. Furthermore, the main academic event related to DMIs, the International Conference on New Interfaces for Musical Expression (NIME), presents a similar trend. A review of the first eight ears of this conference showed that the majority of NIME DMIs are also based on a few common sensor technologies [11, 12].

Nevertheless, the use of electronic and more recent digital technologies for musical expression predates the NIME Conference. Since the end of 19th Century, electric, and later, electronic musical instruments have been created, tested, and performed. Several works show this diversity of devices. For instance, Chadabe's book presenting the history and evolution of electronic and digital music [13], Paradiso's overview of electronic music interfaces [14], Wanderley and Battier's trends in gesture controllers in music [15], Piringer's exhaustive list of electronic instruments [16], Miranda and Wanderley's review of digital musical instruments [1], and Marshall's review of sensors and actuators in digital musical instruments [11]. Sensing technologies, such as touch-sensitive keys, photocells, video, potentiometers, switches, buttons, infrared, piezoelectric, ultrasound, Hall effect, breath

pressure, radio frequency receptors, contact microphones, and strain gages were already being used in instruments design from 1958–1992 [13]. We have selected a few examples of these early instruments to illustrate their sensing design as compared to current sensing trends.

Works involving electronic or digital music and dance were the result of collaborations between several domains, such as dance, music, engineering, designers etc. Among them are works including the 1965 performance by John Cage, Merce Cunningham, Malcolm Goldstein, Frederick Lieverman, James Tenney, David Tudor, Stan VanDerBeek, and Nam June Paik, as well as the Dancer's Belt by Gordon Mumma in 1971, Isadora software and MidiDance by Mark Coniglio in the 1980s, the Very Nervous System by David Rokeby in 1989, and Paradiso's et al. Dancing Shoes in late 1990s [13, 14, 17]. It is interesting to note that several of these works were based on computer vision, a trend which has been decreasing recently, possibly due to the introduction of the Microsoft Kinect©, s.f. Chapter 2. Before the Kinect, other game controllers were used for musical expression, for instance the Wii in mid 2000 and the Power Glove by Mattel Toys in the mid-1980s.

While recent works point to a widespread application of micromachined accelerometers [11, 12, 18], non-miniaturized accelerometers had been already used in the 1970s, for example in Gordon Mumma's Dancer's Belt in 1971 [13]. The strain gage, recommended as an advanced sensing technology in this dissertation, was used by Max Mathews and Jay Kadis for "translating bow motion into MIDI" in the Celletto instrument in 1988, played by Chris Chafe [19]. Later in 2002, Diana Young used strain gages to build her HyperBow [20].

It is interesting to observe the evolution of digital musical instruments. Most of them do not go beyond a prototype version, while only a few have been built in several versions to improve their robustness and reliability. Two examples of instruments that continue to evolve after their first versions are The Hands and The Continuum. The first version of The

Hands was created by Michel Waisvisz and his team in 1984, and was used in performance until 1989 [21]. The second version, built by Waisvisz and Bert Bongers, was used from 1989 to 2000 [22]. The improvements included better mechanical structure and sensor placement, "better components and a more reliable wiring-system" [22]. Yet another version was used until his death in 2008 [1]. The Continuum has undergone three versions based on very different sensing strategies. The original version was based on light polarization and video, the second one on resistive-based sensing, and the third version on Hall effect sensors [23, 1].

Furthermore, while some instruments such as The Hands use several sensing technologies, others use only one, such as the well-known Lightning by Don Buchla and the Radio Baton by Max Matthews. Both of these have undergone multiple versions [13, 24].

These instruments and other equally important ones motivated a community to design new interfaces for musical expression. A core concern while designing them is their sensing. This thesis is dedicated to improved sensing in DMIs through the use of advanced engineering techniques to guarantee quality of measuring. We expect the concerns discussed throughout the text to inspire DMI design.

1.1 Motivation

The quality of sensing design is essential for systems engineering. Once quality observations—inputs—are available, mathematic components are used to control outputs. Measurement errors might be tolerated if confidence in the system is still guaranteed. Therefore, the definition of an acceptable error depends on the application and the role of sensing in the system. Some systems perform more stable tasks requiring lower confidence in the measurements (home temperature monitoring), whereas others are more strongly tied to the accuracy of the measurements (medical or surgical instruments). This implies that sensing

systems need to be evaluated [6], and that the evaluation product should be analyzed in respect to the system/user requirements.

We believe that the role of sensing in DMIs is equally critical. Faults and errors in sensing may lead to mapping errors, latency, or non-responsive outputs. Most of these issues can be solved by appropriate treatment of non-linear and non-monotonic sensor responses. Aside from this, it might be easy for musicians to perceive these errors and incoherence, given that musicians have refined motor control and awareness of the sound response of their motor actions. This leads the DMI designer to four tasks: 1) designing coherent sensor systems; 2) quantitatively evaluating the sensing techniques; 3) defining tolerable levels of error, latency, and non-responsive outputs; 4) audience experience. This dissertation focuses on the first two tasks. The third could, for instance, be performed by musicians in user studies. The fourth has been suggested by Bongers and Kunsten as the evaluation of the audience experience and the interaction [25], and has also been discussed by Gurevich et al. [26, 27]. The third and fourth tasks are out of the scope of this thesis.

Our contribution focuses on improving and evaluating sensing design in the context of DMIs. Traditional metrological evaluation is a necessary, but not sufficient, tool used to achieve sensing efficiency for DMIs. Advanced instrumentation design and sensor signal processing are useful tools to improve sensing in DMIs.

At the same time, computational intelligence techniques such as machine learning, estimation, and statistical tools may also contribute to sensing in DMIs. However, the variability of human gestures and motion techniques across subjects might be incompatible with the limited number of functions, clusters and patterns of computational intelligence algorithms. Therefore, these algorithms alone might not be a sufficient solution to improve sensing design. Similarly, sensor fusion algorithms such as the Kalman filter rely on knowing the process that might not be predefinable for human input signals.

The design of sensing systems to be used in the analysis of skilled motor performers—musicians, dancers, and athletes—should be responsive and accurate across the large variability of gestures and their biomechanical parameters. In order to achieve this, we propose the cooperation of several techniques and tools, namely advanced instrumentation design, coherent calibration and regression techniques, advanced sensor signal processing, sensing evaluation, and optimal sensor fusion.

Finally, we believe that DMIs and their interaction boundaries define a unique problem which requires dedicated solutions for sensing, processing, mapping, composing, and performing. For this reason, this thesis cannot propose a general solution for DMIs. However, it can offer possibilities brought in by state-of-the-art engineering tools, which could be replicated to other instruments. In order to accomplish this, we first raise awareness of the possible limitations of simple solutions for sensor signal processing and instrumentation. Secondly, we propose advanced signal conditioning and specialized sensors to improve sensing. Finally, we propose a framework for applying sensor fusion on unpredictable signals. The framework is tested, and its efficiency is proven using DMI signals as a testbed.

1.2 Structure of the Thesis

Instrumentation and signal processing techniques have been used in engineering for decades and have led to reliable measurements essential for areas such as medicine, navigation, and defense [28, 29]. In this thesis, we focus on applying these techniques to human input signals derived from DMIs. Concerning instrumentation, we propose the use of specialized sensors and sensor signal conditioning as an alternative to the trend of using uncomplicated sensing techniques in DMIs. In regards to sensor fusion, we have developed a method to apply a linear Kalman filter—which relies on an accurate model for the system process and

measurements—on human input signals, which are inherently unpredictable.

We start by reviewing the sensing techniques on DMIs as manifested in NIME Proceedings from 2009 to 2013. A total of 266 instruments were reported, and their sensing methods registered. The objective is to verify possible quality gaps and propose improvements on weak areas of sensing design. This review is presented in Chapter 2: Review of Sensors and Instrumentation Methods in DMIs.

In Chapter 3, Evaluation of sensing design for DMIs, we perform an in-depth review of techniques suggested in Chapter 2, using DMI The Rulers as a testbed. The sensing design of this DMI was kept as it was used in performance. Purposely, no improvements were performed in the infrared and Hall effect sensing design, in order to demonstrate the advantages that can arise using better instrumentation design. An alternative sensing solution using strain gages, suggested in Chapter 2, is reviewed and demonstrated. As a conclusion, even if the quality of strain gages is superior in several aspects, the complexity in their installation and conditioning circuits, their initial cost, and their mechanical robustness can be prohibitive. Therefore, in DMI design, we conclude that it is hard to define a unique optimal sensing solution, given that both ordinary sensors—such as infrared and Hall effect sensors— and specialized sensors— such as strain gages— have drawbacks and interesting features. This has led us to believe that taking advantage of the best features of each sensor could result in a better performance.

In Chapter 4, Multiple-model linear Kalman filter framework for unpredictable signals, we demonstrate all the improvements brought by enhancing the mechanical and sensing designs proposed in Chapter 3. We then work towards the application of a linear Kalman filter for The Rulers. The solution for the problem is not obvious, as driven motions — led by human input — cannot be modeled by a known pattern, sequence, rule, or probability, especially when it comes to a skilled motor performance. We believe that enclosing musical

gestures into defined models is more limiting than classifying gestures according to the knowledge of their physical model.

Chapter 5 presents the main findings of the thesis and the future direction this work is going to take.

Chapters 2 to 4 are based in manuscripts published in conferences and journal articles. Chapter 2 has been published in Sensors Journal (under Creative Commons license). Chapter 3 was based on a conference paper. However, its text differs significantly from the original published paper (Sound Music Computing Conference 2011), as several topics were improved and added to the original text. Chapter 4 is an augmented version of another journal article, published in IEEE Sensors Journal (copyright terms are presented in Appendix B). The arguments provided to the IEEE Sensor Journals reviewers, during the review process, were included in the chapter, as we understand that they help clarify some technical choices. As different areas are included in this thesis, each chapter presents its own literature review section.

1.3 Reading Guidelines

As this thesis covers multidisciplinary topics, it may be interesting for the reader to focus on his/her area of interest. The contributions of our thesis target multiple areas, including music technology, engineering, and biomechanics. In order to facilitate the exploration of these topics, we present guidelines for readers of various backgrounds.

1.3.1 For musicians and DMI designers

We have aimed to contribute to the music technology community by using knowledge from electrical and mechanical engineer to improve DMI design. This is a hard task that includes

several fronts, and we do not intend to cover them all. Instead, we will focus on sensing design only. Throughout our work, we claim that DMI designers can benefit from advanced engineering techniques such as coherent instrumentation design and sensor signal processing. The techniques proposed by these works range from basic and intermediate (Chapters 2 and 3) to advanced (Chapter 4).

The review of these engineering concepts, focused on DMI applications, could lead to improvements in electronic instrumentation design and measurement accuracy. A good example of this prospect is the deepness of electronics and engineering techniques given in the book New Digital Musical Instruments: Control and Interaction Beyond the Keyboard, essential for music technologists working on sensing, gestures, and music [1]. Supplying a special focus on the application of relatively simple electrical and mechanical engineering concepts to the creation and improvement of DMIs will allow this knowledge to become more applicable and relevant to this community, even if portions of it are already part of standard electronics textbooks [29, 30].

Aside from this review, original studies were presented in Chapters 2 and 3, such as:

- data gathering and analysis of sensor use in NIME publications;
- statistical studies using original data: co-occurrence of sensor technologies, trends, degrees (statistics on network connections), use of portable electronic devices, use of MARG sensors, etc.;
- method for evaluating sensor technologies for a DMI, including quantitative and qualitative analyses.

Chapters 2 and 3 focus on contributing to the music community, as they review concepts that are trivial for engineers but may be new to the music technology community (which

includes musicians, designers, psychologists, etc). As may be noticed, we have not explored musical expressivity since it is out of the scope of this thesis.

We agree that it would be good to see a validation made by musicians. By running a user experiment, the improvements brought by a better sensing design would likely appear. However, DMIs are usually original designs, and validation experiments cover many areas: human factors, mechanical design, sensing, mapping, composition, etc. That is to say, we believe that is hard to draw conclusions on the redesign of sensing through a validation study of a DMI. We do not believe we would have been able to isolate the issues having to do with sensing, so we have chosen to maintain our focus on sensing design, digging deep on statistics and estimation.

1.3.2 For engineers

The differences, challenges, and appealing features of working with human data include intention, consciousness, and unpredictability, and these features are observed when measuring the physical quantities of a human body or an object directly manipulated by it. Some engineering techniques might work very well when dealing with machines, but might be frail when dealing with human interaction or input. The DMI area makes this obvious at every stage of design and evaluation. In this work, we will include basic engineering concepts for the music community, as well as advanced engineering techniques particularly focused on human input signals and their challenging measuring.

Chapter 2 makes use of several exploratory analysis tools related to occurrence, including social network analysis. These tools help in drawing some conclusions about sensor use, and this might highlight development gaps that engineers might want to focus on. That is, this chapter could serve as an unintentional guide for what should be improved in DMI sensing design, considering the limitations of current designs.

Chapter 3 consists of simple but powerful electronic instrumentation techniques, which could be skipped altogether by engineers. Chapter 4 presents advanced engineering techniques that have been adapted to be effective with human input signals, and specifically discusses requirements for the implementation of a multiple model Kalman filter for human input signals. A multiple model Kalman filter implementation is not novel, but this work, in contrast, proposes a framework for it in the specific case where the signals are unpredictable since their source is human input. The implementation provided, using The Rulers as a testbed, is a practical validation of this framework, which includes a filter evaluation scheme for Kalman filter implementations. This evaluation includes various descriptors. One of them is introduced for the first time in this work, while others reference the other works cited throughout Chapter 4. The framework can also be used in several other circumstances where the definition of a process model is not straightforward.

Similar problems have been solved by using other filtering solutions, including extended Kalman filtering, Interacting Multiple Model (IMM) filters, and particle filters. In Section 4.2, we discuss the reasons why we have opted for the standard Kalman filter instead of these alternatives. To summarize, the standard Kalman filter is an optimal estimation filter – it respects the orthogonality principle, which states that the estimate and the estimation error are orthogonal to each other. This implies that the estimation error is the real value of the error instead of an estimation of the estimation error, as is the case of the extended Kalman filter. It is important to note that our own perspective for the Kalman filter design follows a signal processing approach instead of a control engineering approach. The first focuses on improving the accuracy and understanding of the system and its signals, whereas the second focuses on tracking and makes use of tuning strategies which might not be related to the physical modelling of the system and its signals.

1.3.3 For professionals on biomechanics, kinesiology, and other areas

As this thesis focuses on human input signals (especially Chapter 4), any professionals and researchers dealing with measuring these signals could benefit from this work. The framework presented in Chapter 4 is particularly designed for human input signals, and aside from DMI signals, this also includes human motion and data from wearable sensors. The framework prioritizes the physical modelling of the signals as much as possible, restricting the bandwidth for noisy sensor data. Human motion usually presents different kinematic physical models, including constant velocity, constant acceleration, jerk, bouncing, etc. A reasonable filter design might include multiple models, exactly as presented in this work, and the classification between models should not be obtained by restricting the motion with sequences or rules. Instead, we suggest the use of recursive classification based on sensor data or an extra data source. Guidelines for the application of this framework for various problems are provided in Section 4.10.

In the field of biomechanics, this framework has been successfully applied for fusing data from MARG sensors for ballistic human motions including baseball pitching. This project, called sportsemble, is a collaboration between the author, MIT Media Lab (Prof. Joseph Paradiso, Mickael Lapinski), Massachussets General Hospital (Dr. Eric Berkson, Donna Dscarborough), the Red Sox, Thomas J. Gill, and C-Motion (Tom Kepple) [31].

1.4 Publications

- Medeiros, C.B. and Wanderley, M.M., *A Comprehensive Review of Sensors and Instrumentation Methods in Devices for Musical Expression*, Sensors, 2014, 14, 13556-13591;
- Medeiros, C.B. and Wanderley, M.M., *Evaluation of Sensor Technologies for The*

Rulers: a Kalimba-like Digital Musical Instrument. In Proceedings of the Sound and Music Computing Conference (SMC 2011), Padova, Italy, 2011;

- Medeiros, C.B. and Wanderley, M.M., *Multiple-model linear Kalman filter framework for unpredictable signals*, IEEE Sensors Journal, 2014, 14, 979-991.

1.5 Terminology

In this dissertation, the use of some words need further explanation. The word instrumentation is used as a synonym for electronic instrumentation, previously defined. The word unpredictable is used in the colloquial sense, meaning undefinable instead of representing the capability to measure in prediction-estimation systems. Sensor fusion is herein defined as an advanced sensor signal processing technique employed to obtain information or data accuracy otherwise impossible to achieve with the individual data sources.

1.6 Disclaimer

Throughout the thesis, we will describe processing cost as an important variable for choosing signal processing techniques for DMIs. The reason for this is that processing data in DMIs is done locally by microcontrollers and microprocessors. At the beginning of this work in 2010, the Arduino boards Mega and UNO were the most common platforms used by DMI designers. We had intended to propose a sensor fusion protocol that could run over a firmware whose processing power was just above the average used by most DMI designs. Today, in 2015, it is still difficult to find DMI designs with powerful processing platforms, despite the fact that the availability of lightweight powerful processing devices has grown incredibly, including single board computers, PSOCs, etc. The reader might consider these

options in order to have faster and powerful signal processing techniques embedded in their DMIs.

Chapter 2

Review of Sensors and Instrumentation Methods in DMIs

In this chapter, we focus our attention on the engineering design of DMIs, particularly the choice of electronic instrumentation strategies. We present an overview of the electronic instrumentation strategies used in 266 papers by the NIME community from 2009 to 2013. We report the most commonly used sensors as well as their concomitant use with the same application. These results confirm the previous observations by Marshall *et al.* [11], which state that most of DMI sensing is based on simple ubiquitous sensing technologies. In the past few years, we identify the increased use of portable consumer electronic devices such as cell phones, tables and game controllers [32]. Following this trend, we verify the usage of sensors embedded in these devices. In addition, we survey the motion capture methods used by the community. We further identify another significant trend of measuring force-related quantities, using either accelerometers or Force Sensing Resistors (FSRs). Several of these force measurements do not follow application guidelines and sometimes their data analysis do not relate to any physical meaning. Due to that, we conclude that there is

room for improvement in the instrumentation design of DMIs and here we introduce three main directions for improvement: the use of specialized sensors, advanced instrumentation techniques and signal processing tools such as sensor fusion.

We introduce strain gages as an option for force measurement. Although these sensors present complex application and conditioning circuits, they provide high reproducibility, linearity and monotonicity. Our suggestion for advanced electronic techniques focuses on ordinary sensors and include circuits for gain and offset control, amplification, common-mode rejection and stable switching for discrete state measurements. Furthermore, we show that the use of sensor fusion techniques can lead to results whose errors are smaller than the error of each individual data source. In order to offer the reader a perspective of alternative ways to develop electronic instrumentation and sensor signal processing for DMIs, we comment on the development of a few NIME papers, offering progressive solutions using one of the three solutions: specialized sensors, advanced instrumentation techniques and signal processing tools.

Previous Work

Several studies are dedicated to the review of physical interfaces for musical expression. Some works borrow concepts of HCI (Human-Computer Interaction) to define a physical interface features and evaluation [33, 34]. Bongers' description of sensor types and uses is based on an association of those with human muscle action [33]. His classes of muscle action are reproduced in Figure 2.1. For each one of these classes, he cites several sensors. It is interesting to note that the author was able to classify a huge variety of sensor types using the variables pressure and displacement. These two variables are highly correlated to the two biomechanical factors on human motion: kinetics and kinematics. Bongers' paper is part of an electronic publication of articles discussing trends in gestural control [15]. A

more recent publication in the physical interfaces for musical expression reviews gesture definitions in music and simple sensing technologies [1].

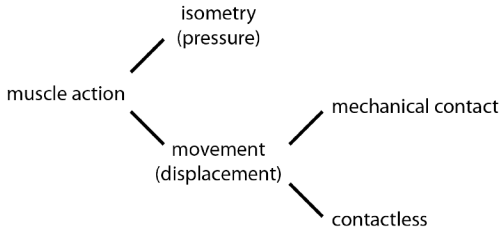

Fig. 2.1 Taxonomy used by Bongers [33]. Movements starts with human muscle action and can be further distinguished into isometric or movement [33]. Reproduced with permission.

Although several studies introduce different techniques for gesture acquisition and analysis using motion capture and/or sensors [35, 36, 37, 38, 39], not many studies are devoted to the interface between DMI design and sensor technology [33, 12, 11]. Existing surveys of sensor use in DMIs show that only a restricted number of common sensors are used in most applications [11, 12]. There are nevertheless several sensors, conditioning circuits and processing techniques that, due to their complexity and processing times, remain unknown among DMI designers [29, 40]. It is worth noting that concerning conditioning circuits, it is hard to find a unique solution that fits a variety of sensors, measurement ranges and applications. This might explain why just a few engineering books describe conditioning circuits for each sensor type [29].

The literature on sensing technology is vast and not restricted to academic publications. Manufacturers of sensor and signal conditioning ICs (Integrated Circuits) have made a huge contribution with their datasheet and application guideline publications [41, 42, 43, 44]. For testing and evaluation of measuring systems, the GUM Guide and the Unified Approach of Stein are essential references [4, 6]. Sensor fusion techniques are discussed by several works [28, 45, 46, 47, 48, 49], but only a few of them focus on sensor fusion specifically for

human body applications [50, 51, 52, 53, 54, 55, 56]. Indeed, the most popular application of fusion algorithms such as Kalman filters is devoted to navigation and tracking estimates using inertial and magnetic sensors, including those for human body applications [57, 58]. A few studies are dedicated to sensor fusion using other sensor types and sensor fusion with uncertain process models [59, 60]. A handful of publications describe instrumentation and/or processing techniques in detail such as calibration for inertial and magnetic sensor data [61, 62, 63].

Several NIME papers are dedicated to survey relevant sensing/processing techniques in the community: motion capture tools [64, 65, 66], machine learning [67] and the use of mobile devices [68]. Related studies are based on advanced engineering techniques and sensor technologies, both published in NIME and elsewhere. For instance, the use of specialized sensors—which require advanced conditioning circuit techniques—can be found in a few papers [69, 70, 59, 71, 72, 73]. Also, sensor fusion approaches are cited in some studies, although their implementation is not reported [74].

This chapter is organized as follows. In Section 2.1, we provide an overview of sensor use as reported in the NIME proceedings from 2009 to 2013, presenting interesting trends and co-occurrence analyses. Section 2.2 provides a brief review of motion analysis sensing used by the community. In Section 2.3, we focus on force assessment using accelerometers, FSRs, and strain gages. Section 2.4 reviews interesting examples of DMI sensing solutions, that could take advantage of specialized sensors, conditioning circuits and sensor fusion. Also, sensor fusion is further discussed by introducing basic concepts of complementary filtering and linear Kalman filtering. Conclusions are presented in Section 2.5.

2.1 Review of Sensor Use

First, we investigate the use of sensors in the DMI community from the last five years as manifested in the NIME conference proceedings (NIME 2009–2013) yielding a critical evaluation of sensor application and data interpretation. Table 2.1 presents the sensor use summary, compared with the dataset of previous study [11]. Some remarks about these categories are presented below in Table 2.1 and numbered according to the superscripted and numbered marks. We aimed to classify sensor use in DMIs in terms of the type of sensors and quantity to be measured. However, due to the varying clarity of NIME manuscripts, it is not always possible to distinguish and classify the DMIs according to the quantities being measured and the sensors used. Often, these two concepts are somewhat blurred. For example, some authors say that "we have used a touch sensor". In this case, touch is the quantity to be quantified, whereas a touch sensor can be a capacitive or resistive sensor. Despite the effort towards classifying sensors and quantities in DMIs, sometimes it was not possible to determine the technology used nor the physical quantity to be measured. These cases are categorized as non-definable.

Sensors that were similarly classified in both studies have their average incidence per area presented in Table 2.2. A quick glance at Tables 2.1 and 2.2 shows some interesting facts that require further exploration:

- Accelerometers and FSRs are the most used ones, similar to previous findings [11];
- The most popular sensors measure force indirectly, e.g., FSRs and accelerometers.

Table 2.3 shows the non-exclusive classification of occurrences per class. The non-exclusive occurrence means that a NIME application can be classified in multiple classes according to the resources (sensors/devices/equipments) it uses. The criteria for the classes are described as follows:

Table 2.1 Dataset of sensor use in NIME conference proceedings from 2009 to 2013, compared with respective dataset of a previous study [11]. Accelerometers, gyroscopes, and magnetometers have two occurrence values: the total number, and the embedded number of occurrences (in parentheses). The embedded occurrences are those in which these sensors are part of a consumer electronic device. Some of the sensors considered in this study were ignored in the previous study. These are described with the letter NM (Not Mentioned)

Sensors	**Occurrence (2009–2013)**	**Occurrence (2001–2008) [11]**
accelerometer	75 (30)	56
FSR^{TM} (Force Sensing Resistors^{TM}) [1]	38	68
gyroscope	30 (9)	NM
buttons and potentiometers [2]	29	110
conventional standalone video camera [3]	23	54
IR (infrared) [4]	22	27
magnetometer	16 (4)	NM
capacitive	15	NM
biosensing [5]	13	NM
piezoelectric disc	12	NM
non-definable [6]	12	NM
microphone	11	29
textiles	11 [7]	NM
photo/light [8]	10	NM
bend	9	21
Hall effect	7	NM
ultrasound	4	NM
pressure/flow	4 [9]	NM
fiber optic	2	NM

[1] *FSR* and Force Sensing Resistors are trademark of Interlink Electronics. In this text, we adopt the community's understanding of these terms: resistive sensors for measuring pressure. Therefore, we excluded the ^{TM} symbol to refer to any alike sensor, disregarding the brand [72, 75]; [2] This work combined all *potentiometers and switches* used as sensors within one category, whereas the previous work classified these sensors as button and switches (51 occurrences), rotary potentiometers (31 occurrences) and linear potentiometers (28 occurrences) [11]; [3] *conventional standalone video camera* category does not include video from Kinect©; [4] *infrared* category does not include the infrared sensing embedded in the Wii©; [5] the *biosensing* category refers to all biosignal sensing: EMG (ElectroMyoGraphy), EEG (ElectroEncephalography), etc.; [6] the *non-definable* category includes the instances where neither the sensor used nor the quantity being measured were possible to determine; [7] *textiles* were mostly used as resistive sensors; [8] *pressure/flow* category relates to any sensor measuring light as a potential or pixels of an image, [9] *pressure/flow* category relates to airflow measurements.

Analog sensors: sensors that output a continuous electrical signal [29];

Digital sensors: sensors that output a discrete electrical value: step or state [29]. They might be part of a consumer electronic device or not, we call these cases "embedded use of sensors";

Consumer electronics: portable devices primarily commercialized as devices for everyday use, mostly for entertainment or communication. In this context, it includes portable music players, cell phones, Wii©, Kinect© and tablets. Some NIME applications use the device's own functions modified for a particular function, whereas others use data from the device's embedded sensors;

Motion capture: refers to Kinect©, near-infrared or infrared camera-based systems such as Qualisys©, commercially available bodysuit sensor nodes such as the Xsens© and electromagnetic sensors nodes such as Polhemus©. Two remarks concerning this classification must be made. The first one refers to labeling the Kinect© as both consumer electronics and a motion capture tool. The second one refers to the distinction made between body sensor systems, such as the commercially available Xsens©, and dedicated solutions using sensors—classified as digital sensors. Both solutions are usually based on the same sensors: accelerometers, gyroscopes and magnetometers, however the first is presented like a black-box system whereas the second is a compound of sensors placed together and configured throughout. Accelerometers, gyroscopes and magnetometers are called MARG—Magnetic, Angular Rate, and Gravity—sensors.

It is hard to define whether a sensor has analog or digital output, so for this reason, we have classified each sensor according to their most usual output type (analog or digital). For instance, accelerometers are considered digital sensors.

Additional survey analyses on sensor use in DMIs follow. These analyses show interesting

Table 2.2 Average sensor use per year according to our survey (2009–2013) [18], compared with previous study (2001–2008) [11].

Sensors	**Average Use per year (2009–2013) [18]**	**Average Use per year (2001–2008) [11]**
accelerometer (embedded or not)	15	7
FSR	7.6	8.5
buttons and potentiometers (all)	5.8	13.8
video/image	4.6	6.75
infrared	4.4	3.4
microphone	2.2	3.6
bend	1.8	2.6

Table 2.3 Non-exclusive occurrence by class.

Occurrence by Class		
sensors	analog	172
	digital	134
others	consumer electronics	71 [1]
	motion capture	30

[1] at least one type of MARG sensor is used in 43 occurrences.

trends and sensor co-occurrences of the NIME designs.

2.1.1 Interesting Trends

According to Figure 2.2, some interesting trends in NIME 2009–2013 are noticeable:

- Accelerometers (embedded or not) were the most popular sensor across the years;
- FSR use is stable over the years;
- Potentiometers and switches are substantially used;
- The latest years (2012–2013) show that video has not been used recently;
- IR, microphone and bend sensors do not present a clear trend.

(a) accelerometer, FSR, potentiometer/switch (b) IR, video, microphone, bend

Fig. 2.2 Trends for some sensors within the interval 2009–2013

2.1.2 Use of Portable Consumer Electronics

The use of consumer electronics was not mentioned in the previous DMI survey listing: "Most popular sensors from NIME instruments" [11]. Figure 2.3 shows the use of these devices over the past five years. The percentage numbers reflect the percent of portable device use as compared with the total number of measuring techniques reviewed per year. Note that since the use dropped in 2010, the use of portable consumer electronic devices in DMIs has monotonically increased. The increase falls farther than 2 standard deviations away from the mean within the interval 2009–2012, therefore, is statistically significant.

Embedded Use of MARG Sensors

MARG sensors comprise accelerometer, gyroscope and magnetometer sensors. Table 2.4 expresses the embedded use of these sensors in portable consumer electronic devices, through

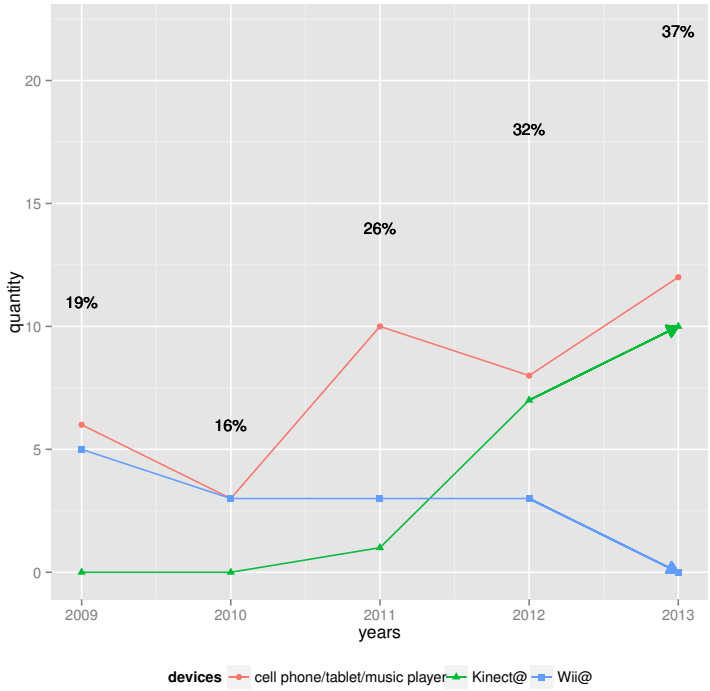

Fig. 2.3 Consumer electronics use within the interval 2009–2013. The percentage numbers reflect the percent of portable devices use compared with the total number of measuring techniques reviewed per year.

the study of their co-occurrence. The numbers show that most of the cell phone, music players and tablet applications make use of their embedded accelerometer. The embedded use of gyroscopes and magnetometers has fewer occurrences as their availability on portable consumer electronics is more recent.

2.1.3 Clusters

In this section, the co-occurrence of two sensors is analyzed through their adjacency matrix. This matrix quantifies the concomitant use of two sensors within the same application. Mapping the co-occurrence matrix results in Figure 2.4. A Ward hierarchical cluster algorithm was run for 3, 4 and 5 clusters [76]. The results for the choice of 3 clusters are

Table 2.4 Co-occurrence matrix of MARG sensors in portable consumer electronic devices.

MARG Sensors	Devices	
	Wii©	**cell phones/tablets/music players**
accelerometer	7	24
gyroscope	1 (MotionPlus©)	8
magnetometer	0	4

highlighted in Figure 2.4, which also depicts the results for 4 clusters. This algorithm uses the minimum variance within clusters as the criterion. Therefore, the clusters are formed for sensors that have similar co-occurrence values among each other. Given an approach with 3 clusters, the first cluster includes inertial and magnetic sensing (MARG sensing). These sensors along with well-designed sensor fusion techniques can provide accurate orientation data. As such, they are often deployed for navigation and more recently for human motion analysis. This will be discussed in Section 2.2.1. A second cluster is formed by infrared, FSR, potentiometers/switches, Hall effect, ultrasound and bend sensors. A common feature among all these sensors is that they can be easily assembled and they have a relatively low cost. They are cited among the most commonly used sensors in musical applications [1, 11]. Also, they are ubiquitous in forums and tutorials on sensors and microcontrollers [77, 78, 79]. The remaining cluster groups the sensors that tend to be used alone or with a few other types of sensing technologies; these are: microphone, light, video, biosensor, fabric, pressure/flow, capacitive and piezoelectric disc. For the 4 clusters solution, the clusters are: MARG sensors; infrared, FSR and potentiometer/switch, microphone, light and video; and the remaining.

Simple econometrics for social network analysis was deployed in order to better describe the concomitant use of sensors in DMIs. In this analogy, sensors are seen as users connected through a network of DMIs. In addition, the cited clusters can be seen as communities. The graph in Figure 2.5 is designed using an algorithm for undirected graphs called Kamada

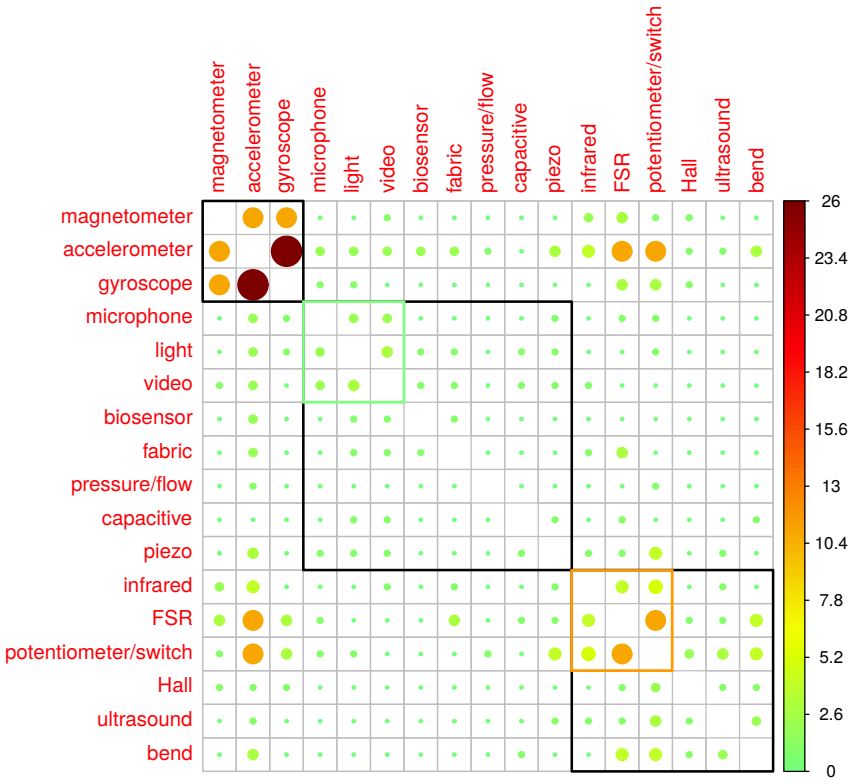

Fig. 2.4 Co-occurrence matrix map plus Ward hierarchical clustering for 3 clusters. As the co-occurrences of an aspect with itself were shown in Table 2.1, the main diagonal is left blank for clarity. Upper and lower matrices report the same information. The green and orange squares present the 4 clusters solution.

Kawai. This algorithm defines the ideal distance between the elements in order to provide a total balance of the graph and a small amount of edge crossings [80].

The image clearly shows the two strong clusters: one formed by the MARG sensors and another by resistive-based sensors (potentiometer/switch, FSR). It is noticeable that the accelerometer is placed in the center of the network. This comes from the fact that this sensor presents the highest degree of the network. The degree of a node expresses the number of connections that an object has [81]. The accelerometer is concomitantly used

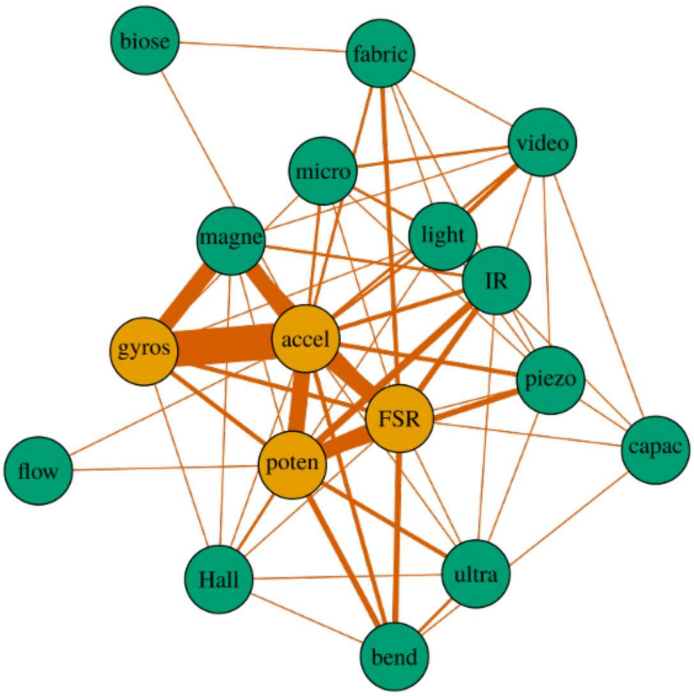

Fig. 2.5 Co-occurrence of sensors: line thickness is proportional to the number of instances the connected sensors were used in the same application. Sensor names were shortened as: *biose*, biosensor; *micro*, microphone; *flow*, pressure/flow; *accel*, accelerometer; *gyros*, gyroscope; *magne*, magnetometer; *poten*, potentiometer/switch; *capac*, capacitive; *ultra*, ultrasound. Sensors with the highest *degree* appear in orange.

with 17 other sensing types. Potentiometers/switches and FSR have the second highest degree. Similar analysis was performed including consumer electronics and motion capture tools. The results, not shown, indicate the following:

Motion capture: the incidence of motion capture tools coincides with a limited variety of other sensing techniques. Motion capture tools are only used in conjunction with other motion analysis sensing techniques—MARG sensors and Wii©—and video. This finding suggests that designers aiming to perform motion analysis do not consider motion capture tools as a unique and sufficient method to do so. This discussion will

be presented in Section 2.2;

Wii©: the measuring capabilities of this device used in DMIs are its infrared camera and its accelerometer. Seven out of fourteen times this device was used, its embedded accelerometer data was used;

Kinect©: of the 18 times the Kinect© was used, only once was another sensing technique—accelerometer—used.

2.2 Motion Analysis Sensing

DMIs are controlled by human input, thus their signals are difficult to predict or to classify. Most of human input to DMIs is essentially motion, which comprises kinematic and kinetic features. Kinematics is the study of motion and its variables, whereas kinetics is the study of internal and external forces and their momentum [35]. Regarding the sensor use, accelerometers, gyroscopes and FSRs can provide kinetic data, whereas Kinect©, infrared- and electromagnetic-based tools can provide kinematic data.

In this section we discuss MARG sensors and motion capture tools for biomechanical analysis of human motion. The appeal of MARG sensing had a large impact on many recent NIME papers. This can be observed in the numerous works willing to use the body itself as a DMI controller, instead of using an object for sensing human motion [1, 82, 83, 84]. Several NIME papers report the use of more than one motion analysis tool in the same application, some including kinetic and kinematic methods. This suggests that sensor fusion techniques could have been used to take advantage of the best features of each sensing technique.

2.2.1 MARG Sensors

First, a remark must be made about terminology. Often, DIY and NIME literature use the term IMU—Inertial Measurement Unit—to refer to concomitant use of accelerometer, gyroscope and magnetometer [66]. Accelerometer and gyroscopes are indeed inertial sensors, but magnetometers are not. The scientifically accurate terms are MARG sensors or AHRS. MARG—Magnetic, Angular Rate, and Gravity—sensors refer to the concomitant use of the three cited sensors, whereas AHRS—Attitude and Heading Reference System—refers to a system that provides an orientation data given the availability of MARG sensors and sensor fusion algorithms. These sensors can either be part of a consumer electronic device—called embedded—or part of a dedicated design—called independent. Figure 2.6 depicts the embedded and independent use of MARG sensors.

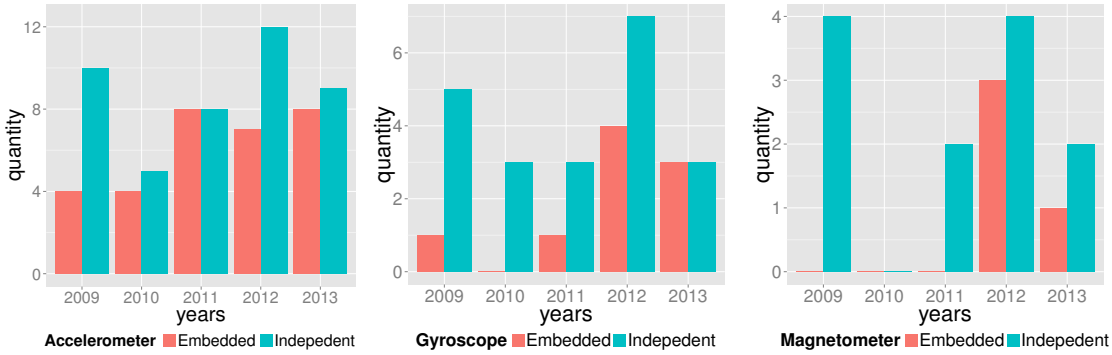

(a) accelerometer (b) gyroscope (c) magnetometer

Fig. 2.6 Embedded and independent use of MARG sensors

A brief overview of IMU and MARG sensors use in NIME follows:

- IMU: 24 out of 75 projects using accelerometers also use gyroscopes;
- MARG: 11 out of 75 projects using accelerometers also use both gyroscopes and magnetometers.

The simultaneous use of accelerometer, gyroscope and magnetometer allows the application of sensor fusion filters to provide orientation estimate. Few works (3 out of 266) implement complementary filtering, which has application and processing requirements that are more suitable for embedded applications than Kalman filtering [74]. The implementation of Kalman filters combined with system physical modeling result in estimates with considerable improvement in their error profile. Accelerometer data analysis will be further analyzed in Section 2.3. Sensor fusion will be discussed in Section 2.4.2.

2.2.2 Motion Capture

The motion capture techniques used by NIME researchers are infrared-based cameras, magnetic-based sensors, Kinect© and commercially available sensor networks. Many researchers have used the Kinect©—primarily available as a video game accessory—due to its price and simplicity, in comparison with the infrared- and magnetic- based methods [85]. All of these systems present advantages and drawbacks and the choice depends on the resources available, the problem to be solved and the level of accuracy desired [64, 65].

2.3 Force Assessment

In this section, we provide a literature review on force assessment, and discuss techniques to improve results, highlighting the most common flaws in the use of FSRs and accelerometers.

2.3.1 Accelerometer

This sensor has become increasingly present in portable consumer electronics, due to advances in micro-machinery technologies. This trend has also made them available at relatively low cost for engineers and designers interested in measuring acceleration in their

custom design. In fact, accelerometers can provide information not only about translational acceleration, but also about force, vibration, shock and tilt [86].

The use of accelerometers for inclination measurement is not linear unless a narrow range of inclination is considered. Another requirement for inclination measurement is that the Root-Sum-Square (RSS) of the three axes must equal one times gravity [87].

Regarding accelerometer data, it is impossible to distinguish gravity and acceleration due to motion. For this reason, when determining the sensor orientation, other sources of data and calibration are necessary.

Rotational motions result in an apparent AC (Alternating Current) acceleration, even if there is no translational acceleration. This apparent acceleration is a consequence of the variable projection of gravity on the axes [87].

In recent times, accelerometers have been used together with gyroscopes and magnetometers, allowing for the full description of orientation, through the use of sensor fusion techniques such as the Kalman filter.

Error Sources

Several sources of errors on accelerometers are described in the literature: nonlinear effects in scale factor, cross-axis coupling, measurement bias, vibro-pendulous error (for pendulous design), drift terms, misalignment errors, vibration rectification error, quantization, thermo-mechanical white noise, ratiometric errors, and random noise [88, 89, 90, 91, 92].

An error model can consider different amounts of error sources [93, 90]. According to several authors, the major deterministic error sources are the zero-offset bias and the first order scale factor [94, 90]. In addition to that, it is necessary to stochastically model the random noise. This modeling requires a minimum span of observation time, which depends on the time constant of the process and on the accepted error level.

Calibration

A calibration process must be able to account for deterministic errors such as bias and scale factor errors. In order to eliminate stochastic sources of error, additional information is required. Several calibration protocols can be found in the literature [61, 88, 94, 95]. Here, we focus on describing one of them due to its high measurement range and the familiarity of the author with the procedure [61].

The studied calibration protocol is based on properties of the centripetal acceleration. There is a centripetal acceleration when an object is rotated at a given radius greater than zero:

$$a = \omega^2 r \tag{2.1}$$

where a is the acceleration, ω is the angular velocity and r is the radius. Therefore, an accurate motor delivers stable angular rates that are correlated to calibration points for acceleration [61]. The angular velocity is sustained for some seconds—sufficient time to gather the minimum amount of samples to guarantee calibration coherence. The stability of the rotation radius is given by placing the sensor node in customized 3D fabricated brackets that are firmly attached to the shaft.

In this calibration set, the main challenge is to generate positive and negative centripetal acceleration with positive angular velocity [61]. A positive acceleration is generated when the accelerometer is rotated in such a position that the rotation axis is positively displaced on the orthogonal plane from its center axis. Alternatively, a negative acceleration is generated by a rotation in which the axis is negatively displaced in relation to the orthogonal plane [61].

Common Issues on Accelerometer Use

In this section, we focus on common issues in the NIME literature, concerning the accelerometer's application and data interpretation. A common application of accelerometer data is to estimate beat through the analysis of gestures of conducting, bouncing, percussion and dance [96, 97].

There are several accelerometer data processing solutions that can be found in DIY tutorials and NIME papers, and most of them are meant to extract beat information. Some solutions for a three-axis accelerometer are presented below. The order of presentation goes from a physical interpretation of the measurement itself, to a more complex analysis of the measurement features.

(1) Sum of the value of the axes;
(2) Use of the highest component of the acceleration;
(3) Norm of the acceleration;
(4) Norm less gravity;
(5) Peak detection;
(6) Acceleration integration (speed or position);
(7) FFT (Fast-Fourier Transform);
(8) Machine learning techniques.

The first solution does not present any physical meaning. The second one does not take into account the orientation of the sensor. Changes in orientation will bleed gravity and motion acceleration throughout the axes. The designer should reject any conclusions when the highest component is not sufficiently greater than gravity.

Concerning processing cost, the least expensive solutions that have connection with the physical world are the options 3 and 4. The norm of the acceleration is the length of the

acceleration vector, and is calculated as the root square of the squared sum of all axes. The norm subtracted by the absolute value of the gravity acceleration provides the magnitude of the acceleration due to motion.

Peak detection might be a coherent metric to identify impact, but it is limited for any further interpretation. The designer may remember that physical interpretation of zero-crossings and peaks on position data, velocity data, and acceleration data are different. Only for a simple stationary periodical signal, the acceleration peaks relate frequency-wise to those in the position domain. Solution 6 presents the integration in order to obtain position or velocity data. It is important to note that integration leads to errors due to uncertain integration constants.

FFT—possibly along with windowing techniques—and acceleration integration have the most expensive processing cost. The FFT is not a possibility for all types of signals though. Finally, pattern recognition, feature selection and a variety of other machine learning tools, usually aiming at gesture classification, could be used [98, 67].

2.3.2 FSR

Most FSRs are a polymer thick film device that vary their resistance according to the pressure applied to the active surface. The FSR manufacturer Interlink^{TM} claims FSRs are not load cells or strain gages, although they have similar properties [99]. Also, Interlink^{TM} claims that FSRs are not suitable for precision measurements: force accuracy ranges from 5% to 25% [99]. According to the analysis of commercially available FSRs, these sensors are not linear and they present considerable drift and hysteresis [75]. FSR response is usually an inverse power-law, i.e., there is a turn-on threshold, which is a substantial resistance drop at the beginning of the force measurement range. In addition, saturation occurs at the end of the force measurement range. Finally, some authors mention latency and robustness

problems in the use of FSR in DMIs [100]. In addition to calibration using curve fitting and a reference measuring system, it is recommended to use conditioning circuits that are able to protect the sensor and the electronics circuits and reduce the measurement error.

FSR Application

As an example, for a particular FSR, the suggested tips for application are listed below [99]:

- Apply the sensor to a firm, flat and smooth mounting surface;
- Use thin, uniform adhesives;
- Protect the sensor from sharp objects;
- Avoid excessive shear forces;
- Limit the applied current to 1 mA/cm^2 of applied force, as FSRs have a limited power dissipation.

Signal Conditioning

The simplest and most commonly deployed conditioning circuit is the voltage divider. The voltage divider is limited due to a couple of reasons. First, in this circuit, the current applied to the sensor depends on the resistances involved: sensor resistance and series resistor. A careless choice of series resistor values can be dangerous in terms of exceeding the maximum power requirement for the sensor, which can be permanently damaged. Another issue is that the voltage output is dependent on the load that it is connected to. This means that load impedance variations affect the measurement directly, unless the load impedance is much higher than the voltage divider resistances. Finally, voltage dividers are vulnerable to noise and are not capable of providing amplification.

This section deals with signal conditioning for FSRs and other resistive sensors. The

detailed explanation on voltage divider, buffer, instrumentation amplifier, and comparator with hysteresis could be skipped by Electrical Engineering readers.

The simplest way to adjust the output sensitivity of a voltage divider is shown in Figure 2.7a. This voltage divider does not allow output offset adjustment. In order to allow for this adjustment, the fixed resistor has to be substituted by a potentiometer (Figure 2.7b). This solution using only two terminals of the potentiometer is troublesome because the current through the FSR depends on not only its own resistance (R_{FSR}) but also the adjustment of the potentiometer resistance (R_1). As the adjustment of R_1 ranges from its minimum value (0 Ω) to its nominal resistance R_1^{max}, the following problems can arise when the potentiometer resistance tends to zero:

- The output can be connected directly to the ground, therefore not measuring the sensor output;
- The maximum current allowance for the sensor can be exceeded, permanently damaging the sensor;
- The power supply might not be capable of providing the demanded power, reducing its voltage and altering the output voltage.

An improvement is the solution presented in Figure 2.7c. In this case, a fixed resistor is added to the series circuit in order to guarantee the maximum power requirement. The protection considerations determine the value for R_2. Let V_s be the power supply voltage, I_A^{max} the maximum current per area of applied force given by the manufacturer (in A/cm^2), $Area$ the area of the sensor's active surface (in cm^2), R_{FSR}^{min} the minimum FSR resistance (maximum pressure) and R_1 as the nominal potentiometer resistance. Considering a 10%

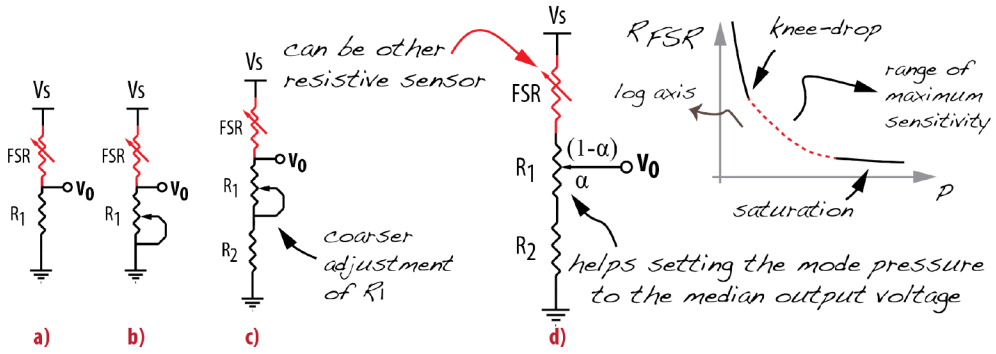

Fig. 2.7 Voltage divider topologies. (**a**) simplest solution; (**b**) output offset adjustment; (**c**) safety improvement; (**d**) safety and finer adjustment. Solution **a** is suggested by one FSR manufacturer, solutions **b** and **c** are often found on DIY designs, and solution **d** is proposed by us.

safety factor, the condition for sensor safety is:

$$R_{FSR}^{min} + R_1 + R_2 > \frac{V_s}{0.9\, I_A^{max}\, Area} \tag{2.2}$$

Note that in this case, the current through the sensor changes according to its own resistance (R_{FSR}) and the resistance variation of R_1. In order to overcome this issue, we recommend the circuit in Figure 2.7d. This is the most efficient manner to use a voltage divider as an FSR conditioning circuit. This topology using the three terminals of the potentiometer provides a finer adjustment of the output sensitivity, which depends on the measurement range, as the sensor response is not linear. Therefore, the R_1 adjustment helps setting the output offset—the minimum voltage output—and consequently the sensitivity level. The designer may avoid operating on the troublesome initial and final measurement range of the FSRs, exploring the range of maximum sensitivity free of saturation.

Practical considerations for resistor selection and adjustment are:

- The ratio R_1/R_2 along with the FSR resistance range defines the measurement range;
- R_1 adjustment defines the offset of the output value;

- Choose R_2 much smaller than R_1, and enough for protecting the sensor (Equation (2.2));
- Center the output voltage to the most frequent pressure (mode). For that, simulate this pressure and adjust R_1 in ways to obtain half of the supply voltage in the output. If $R_1 = \alpha\, R_1 + (1 - \alpha)\, R_1$, this is obtained when $(2\,\alpha - 1)\, R_1 = R_{FSR}^{mode} - R_2$.

The optimal choices for R_1 (nominal and adjustment) and R_2, according to the pressure measurement range, can lead to a design whose output measurement range lies within the maximum sensitivity of the sensor, saturating the output during FSR's initial or final measurement range [101]. This improves the curve fitting and takes advantage of the maximum sensor sensitivity.

An improved version of the voltage divider is to have its output applied to a voltage buffer amplifier. This circuit exploits the fact that op-amps have very high input impedance and very low output impedance. The impedance correction protects the sensor from excessive loads coming from the circuit connected to the op-amp output and isolates the output from the high impedance of the voltage divider. In this configuration, the load resistance does not influence the voltage divider output. The op-amp connected as a buffer works as a follower, that is, the op-amp output voltage follows the op-amp input voltage. The schematic for this circuit is included in Figure 2.8, which consists of the connection and use of the following components: R_1 as FSR, R_2, R_3 and B.

An improved conditioning circuit provides not only output offset adjustment, but also amplification factor (gain) adjustment. The independent adjustment of these two variables can yield a better voltage output range to the given pressure measurement range. For this, an uncomplicated set of op-amps can be deployed, as depicted in Figure 2.8.

The output for this circuit is:

$$V_o = \frac{Vs\,R_4}{\beta\,(R_4 + R_{FSR})} - \frac{V_b\,(1-\beta)}{\beta} \tag{2.3}$$

$$V_b = \frac{(R_3 + \alpha\,R_2)}{R_1 + R_2 + R_3}\,Vs \tag{2.4}$$

where R_2 adjusts the offset, R_5 adjusts the gain, and α and β are the resistance ratios for the two potentiometers. An important remark is that the offset and gain adjustments by software do not have the same role as by hardware. If the choices for resistances in the voltage divider result in a short measurement range, an offset adjustment by software would not improve the poor sensitivity and/or resolution. Software adjustments are meant for fine adjustments, rather than Signal-to-Noise Ratio (SNR) improvements.

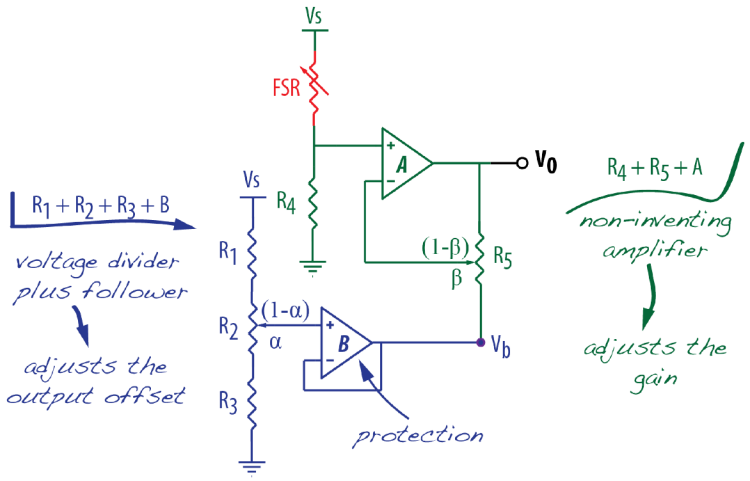

Fig. 2.8 Buffer with adjustable gain and offset: suggested circuit based on the circuit proposed by an FSR manufacturer [99]

Finally, if the FSR is intended to be used as a quantitative data source, the instrumentation amplifier might be the best option for signal conditioning (Figure 2.9). This amplifier topology is indicated for improving the SNR of low voltage signals. Its main advantages are very high input impedance, high Common-Mode Rejection (CMR), low DC (Direct

Current) offset and low offset voltage drift. The differential amplifier designed using three op-amps is not equivalent to the micro-machined instrumentation amplifier (in-amp) [43]. The reason for that resides in the fact that the differential amplifier must have matched resistors in order to achieve a high CMR, which is difficult to obtain in practice, whereas the in-amps have internal pre-trimmed resistors. The in-amp has a differential input and a single-ended output with respect to a reference [43] and it can be found with dual- and single-supply designs. Normally, the reference pin in single-supply in-amps is set to half power supply level and the output is rail-to-rail [44]. An ideal in-amp detects and amplifies only the difference in voltage between the two inputs, therefore any common-mode signal such as noise or supply voltage drops are rejected.

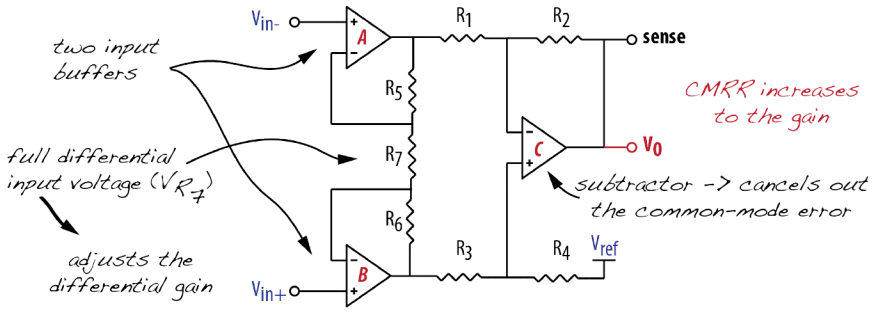

Fig. 2.9 Instrumentation amplifier [43].

Alternatively, one might want to detect a force threshold as the sensor is recommended for qualitative purposes. For this, a voltage comparator using an op-amp can be used. The circuit compares the non-inverting input voltage—determined by the voltage divider including the sensor—with the inverting input voltage. The threshold from which the voltage output will switch from low to high is determined by the reference voltage connected to the inverting input. This comparator presents an issue: the output fluctuates in the vicinity of the threshold, especially for slow moving input signals. In order to overcome this drawback, one can use the Schmitt Trigger (ST) comparator. The ST comparator has

stable switching between low and high states, which occurs at different levels according to the current output state. The reference inputs depend on the current output state: one for when output is low (V_l), and another for when output is high (V_h).

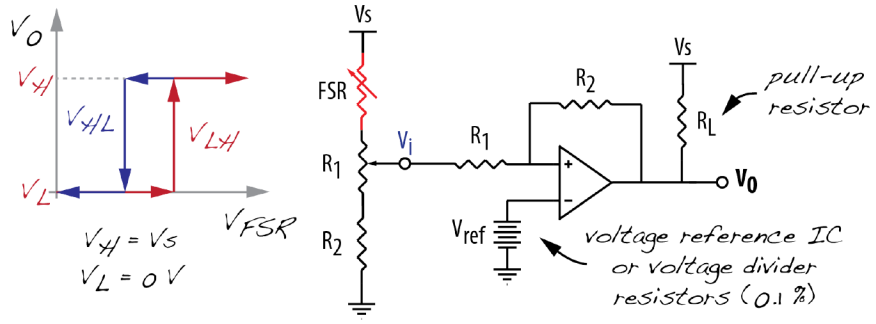

Fig. 2.10 Comparator with hysteresis based on IC manufacturer [102].

Figure 2.10 shows the schematics and the response curve of this qualitative conditioning circuit. Figure 2.10 shows the sensor attached to the inverting input. This way, the output voltage increases with increasing force. Alternatively, this can be easily changed by swapping the sensor and its series resistor. In addition, in order to guarantee complete integration of the output with digital circuits, diodes attached to the output could be used to regulate the voltage levels.

2.3.3 Strain Gage (SG)

These reliable sensors are widely used in industry—usually for maintenance and safety—and in research—usually for solid mechanic analysis of materials and mechanical structures. They have also been used in a few DMI applications [1, 20]. As the name states, strain gages measure strain caused by stress in a given material. The stress source can be normal, shear, residual, thermal, etc. The most common types of strain gages are piezoresistive (i.e., metal and semiconductor) and piezoelectric. The sensitivity—Gage Factor (GF)—is usually 2 for metallic strain gages, and ranges from 80 to 130 for semiconductor strain gages [41].

Our focus is on metallic ones, whose sensitivity reflects the ratio between relative resistance variation and strain. The operating principle of strain gages is based on a clean and thin bond between sensor and surface. This guarantees that the sensor will suffer the same strain as the Device Under Test (DUT).

Metallic strain gages rely on the principle of electrical conductors, whose resistance changes with mechanical stress. The resistance change is due to two factors: the change in the resistivity and the deformation of the conductive material. According to Pallás-Areny and Webster [29], for a circular isotropic conductor in the elastic mode, the resistance variation is expressed by the following equation:

$$\frac{dR}{R_0} = \left[1 + 2\,\nu + C\,(1 - 2\,\nu)\right] \frac{dl}{l} = GF\,\frac{dl}{l} = GF\,\epsilon \tag{2.5}$$

where R_0 is the resistance without any stress, ν is the Poisson ratio, C is the Bridgman constant, GF is the sensitivity and ϵ is the strain. Both ν and C are intrinsic to the material: ν is the transverse to axial ratio whereas C is the ratio between resistivity variation and volume variation. Strain and consequently resistance variation are very small, which makes strain hard to be measured. It is important to note that the absolute value of the resistance does not carry information about the strain. Instead, the resistance variation is the variable to be analyzed.

Balance conditioning circuits like the Wheatstone bridge can be deployed to measure small resistance variation [103]. The bridge is intended for common-mode rejection, in this case, rejecting the common nominal resistance of two resistances and/or strain gages. The bridge loses its balance when the sensor resistance varies due to a strain. For low SNR bridge output voltage, specialized conditioning solutions are required, which are reviewed further in Section 3.3.2.

Temperature Effect

Temperature is the main interference quantity when using strain gages, that is, temperature and its variations have effects on DUT and sensors. Given a perfect bond between the sensors and a DUT, not only is the mechanical strain transferred from DUT to strain gage, but the thermal strain is also transferred.

The main effect of temperature variation on the DUT is the change of its dimensions (visible or not). This occurs because of the thermal expansion coefficient of the DUT's material. The thermal longitudinal expansion has an effect on the strain measurement. It is impossible to distinguish the cause of strain: mechanical or thermal. One solution for that is in the sensor manufacturing. Some sensors are designed in such a way that they have the same thermal expansion coefficient of the material that they are intended to be applied to. This way, both the DUT and the sensors change their dimensions at the same rate, partially compensating for thermal stress in the sensor. Strain gages endowed with thermal treatment are called strain gages with matched temperature coefficient [41]. In order to take advantage of this method, the DUT's material and the sensor should have similar thermal coefficients.

Another source of thermal error while measuring strain occurs in the sensor itself. The sensor grid also changes its dimension in accordance with temperature changes. This effect can be compensated for using the balance principle of a Wheatstone bridge and an additional sensor. The second sensor, identical to the first one, is not submitted to mechanical strain and should be installed in the same material as the DUT and in such a way be exposed to the same temperature. This second sensor, submitted to thermal strain only, is then properly placed in the Wheatstone bridge in order to subtract the thermal effect in the overall voltage output [104].

Although these are the main effects of temperature on strain measurement, temperature of lead wires and power dissipation in the sensor can also be sources of artifacts.

Selecting Strain Gages

The selection of a strain gage for a certain application is one of the most important tasks in the whole procedure. The designer should take into account the material of the DUT, the type of stress to which the DUT will be submitted (axial, shear, residual, etc.), the expected strain magnitude, the stress state (uniaxial, biaxial or triaxial) and the possible sources of artifacts.

2.4 Sensing Recommendations for DMIs

In this section, we aim to offer suggestions for DMI designers. As mentioned earlier, the use of specialized sensors and conditioning circuits, as well as the use of sensor fusion, can improve the accuracy of DMI sensing. Previous work has shown that the use of specialized sensors can be a significant determinant of classifying musical gestures, allowing for different mapping according to the gesture being performed [59]. In that particular case, the strain gages in the DMI (The Rulers) were capable of determining the instants when the user was interfering in the inertia of the instrument. That is, using an analogy of a plucked string, the strain gages have a different response—transfer function—during intervals where the user is acting upon the string by displacing it, and during intervals where the string is vibrating according to its own physical properties [59]. This quality of the strain gages cannot be found in any of the other ordinary sensors previously used for the same instrument: infrared and Hall effector sensors [105].

2.4.1 Use of Specialized Sensor Technologies

In order to suggest improvements, we have selected some DMI examples and will review their reported measuring techniques.

Measuring Trumpet Valve Position

The challenge of measuring the valve position on a trumpet was approached with the use of potentiometers and buttons [106], and later by digital infrared proximity sensors [107]. The clarity of the latter paper allowed for the identification of the sensor as a VCNL4000 [108]. According to this sensor's datasheet, the infrared sensor is not linear and does not have a monotonic response. Nonlinear sensors require high order fitting curves that can be computationally expensive for ubiquitous microcontrollers. In addition, nonlinear responses present variation in sensitivity along the measurement range that must be accounted for while calibrating the system. The worst possible choice would be to fit the infrared response to a linear curve, yielding to errors along most of the measurement range [105]. A non-monotonic response occurs when a sensor presents the same output in response to multiple different inputs (proximity, in this case). A partial solution for this ambiguity would be to evaluate the previous measurement in order to obtain the instantaneous derivative of the signal. The sign of the derivative would partially solve the singularity issue. However, the sensitivity closer to the point of zero-derivative tends to zero, which is not at all desirable. Finally, the solution for nonlinear, non-monotonic sensor responses starts with good placement, calibration and coherent curve fitting (polynomial order higher or equal to 2) [105]. Another common issue using infrared sensors is saturation. The remedies described above can account for that as well.

Some developers mentioned that the sensor has a high sensitivity and that its placement

is a critical concern [107]. Then they built a series of tests to find an optimal placement that would provide the highest linearity, highest dynamic (measurement) range and robustness. These efforts are a good example of engineering development and evaluation.

Some suggestions could further help designers in selecting the best placement. One of them would be to evaluate monotonicity, linearity, saturation, sensitivity and dynamic measurement range along the valve operation range. Another recommendation would be to perform a calibration where the measurements provided by the sensors are compared with a reference. Calibration implies comparison with a truth value [3] and should not be misinterpreted as a measurement range adjustment. Therefore, the concept of "self-calibration" is flawed. In terms of linearization, if higher polynomial orders cannot be applied due to processing capability, a lookup table or conditional multiple linear measurement range can be alternatives [101].

Yet another possibility for this case would be the use of linear specialized sensors. Thibodeau and Wanderley have compared slide potentiometers, Hall effect sensors, non-infrared LED to LVDT—Linear Variable Differential Transformer—sensors, for the specific issue of measuring position of trumpet valves [69]. The comparison of sensor responses was done through calibration along the valve operation range. LVDT sensors are linear and monotonic; therefore, all issues presented by the use of infrared sensors are eliminated [69].

Measuring Key Pressing on a Piano or Gamelan Instrument

A lot of NIME projects could make use of strain gages, especially those that aim to measure stress on metallic/plastic parts of piano or gamelan instruments [109, 110, 100, 111, 112]. The most used sensors in these references are infrared and FSR sensors. One study implemented actuation and sensing of an electromagnetically sustained piano [110, 113]. This interesting work makes use of piezoelectric discs and infrared sensors. The infrared sensors measure

the deflection of the cantilever beam. Other studies have used strain gages for this purpose [105, 59]. Another example that uses infrared sensors improves the output response through the use of coherent conditioning circuits [109]. Note that while using piezoelectric discs, protective buffers must be used for protection, as these disks can deliver voltages that might not be supported by other circuits.

As cited before, infrared sensors are nonlinear and non-monotonic. In addition to that, for a cantilever application, there are two other issues that can compromise the measurement quality. The first one is the deflection angle of the cantilever beam. Infrared sensors usually work by providing an infrared beam and reading the respective infrared reflection. The reflection reading depends on the flatness of the reflective surface, guaranteeing the symmetry of incident and reflective light beams. If the flatness cannot be guaranteed due to the angular cantilever deflection, errors might occur as this angle increases. The second issue comes from the use of shiny cantilever beams. Some coating surfaces can interfere with the infrared reflection.

The examples based on FSR might suffer from artifacts related to flatness of the surface, mechanical robustness, latency, nonlinear response and deficient conditioning circuitry [112, 100]. For these examples, we recommend the use of strain gages and sensor fusion techniques. The strain gages' main advantages for this particular application are linearity, high SNR (provided by coherent conditioning circuits), and no electromagnetic interference. Finally, strain gages could potentially distinguish between touch and after-touch intervals, serving as a reference for the adaptive gain desired by the instrument designers. Furthermore, sensor fusion techniques could be deployed to improve sensing and control. Based on our previous work, instrument designers could take advantage of the known physical model of the cantilever beam and also eliminate high frequency harmonic vibration responses by limiting the physical model of the cantilever to a low order system [59].

Measurements on Violin and Cello: Distance, Force, Position, Fingering

Some interesting studies in NIME are dedicated to measuring bow hair deflection for tracking and force assessment [114, 115]. One of them presents an interesting triangulation method to track the bow, using infrared sensors [114]. The other work is based on tracking using Polhemus© motion capture [115]. The force information is a result of calibration using a load cell with applied strain gages [116]. The drawback of this approach is the magnetic artifacts on the tracking data. Yet another work on string instruments uses FSRs to measure finger position and pressure [112]. The main artifact of the chosen design is the application of the sensor in a curved surface [112, 117], as the contraction and extension created by a curved surface can be interpreted as pressure by the sensor. Another issue is the conditioning circuit. The author's design is a voltage divider followed by a zero-gain amplifier (buffer). This voltage divider configuration can lead to a short circuit in the power supply when a critical, however possible, situation occurs: high values of pressure on the sensor while the potentiometer set to a low resistance. According to Section 2.3.2, we recommend the circuit in Figure 2.7d as a voltage divider for FSR applications.

In contrast to artifacts in infrared sensors, FSRs and magnetic tracking systems, a solution using fiber optics proved to be successful for measuring fingering, bow speed, and bow pressure in an fMRI-compatible cello [118, 119]. The authors of the cited study had shown that the use of specialized sensor and sensor conditioning circuits can provide satisfactory reproducibility and accuracy, besides offering further possibilities to the DMI design. However, these features are obtained with the cost of creating dedicated hardware and software solutions [120]. A more simple but effective solution is the use of capacitive sensing for bow pressure and position [121]. Yet another alternative for measuring pressure on the fingerboard is the use of paper-based force sensors or printed capacitive sensing

[72, 71, 122].

2.4.2 Sensor Fusion

From the review presented in Section 2.1, forty percent of the NIME publications in recent years use more than one sensing technology. This considerable percentage allows for sensor fusion application. In this section, we briefly describe the sensor fusion domain and introduce two algorithms: complementary filtering and Kalman filter. Firstly, it is interesting to note the difference between multisensor integration and sensor fusion. The former means the synergistic use of multiple sensor data directly processed by the control application, that is, a direct mapping topology for multivariable systems. The latter uses multiple sensor data to generate another layer of sensor data that will then be mapped to a control process [123]. A common concept among several authors is that the product of a sensor fusion implementation is an information set that is better than the information gleaned from individual sources [123, 124, 125, 46, 126]. Some add that it provides an error improvement proportional to $N^{1/2}$, where N is the number of independent observations [46]. The human being's capacity to fuse information in order to convey meaning is often used as a reference for the information fusion community. Technology systems try to imitate this faculty as well as its connection to decision making. According to Raol [124] and Elmenreich [123], common limitations in most measurement systems justify the use of sensor fusion techniques, such as:

Sensor deprivation: breakdown of a sensor, causing information loss at a range, device or quantity;

Limited spatial coverage: range limitation of sensors, such as measurement scale and placement position;

Limited temporal coverage: the required time to perform a measurement and a transmission operation, thereby defining the sampling frequency;

Metrology limitations: metrology characteristics of sensors, such as resolution and errors;

Susceptibility to the environment: susceptibility of the system to interference that may degrade performance.

Techniques for sensor fusion make use of observations made by sensors to estimate a process state vector. Fusion techniques are usually used for smoothing, filtering and/or predicting. According to Raol, some potential advantages of sensor fusion systems are [124]:

Redundancy: the property of providing information even in case of partial fault or data loss from one or multiple sensors;

Enhanced spatial or geometrical coverage: overall better coverage obtained by using complementary sensors;

Enhanced confidence: measurements of one sensor confirm data from another sensor, hence overall statistical indicators may experience improvement;

Ambiguity reduction: controversial measurement scenarios can be solved by analyzing multi-sensor data;

Enhanced robustness: different sensors can present diverse robustness against a significant interference quantity. Using redundant fusion where at least one sensor is robust against that interference quantity improves the overall robustness of the system.

However, Waltz and Llinas [127] point to some limitation of sensor fusion, such as:

Requirement of good measurement sources: there is no general improvement based on bad input data. Additionally, sensor fusion techniques applied over bad input

data might reduce the overall performance by introducing time delays or unwarranted confidence [128];

High processing and communication power: the implementation of sensor fusion procedures in embedded and real-time applications can be unviable or limited;

Tools' selection: the selection of inappropriate filter topologies, process and measurement models for a certain problem might degrade the original error covariance;

Requirement of process model knowledge: some sensor fusion algorithms, such as the Linear Kalman Filter (LKF), strongly rely on the knowledge of the system process model description. An inaccurate physical modeling of the system and its measurements can lead to instability and inaccuracy [48].

The section below presents a brief review on the complementary and Kalman filter, two of the most commonly used techniques [28, 127].

The Complementary Filter

The complementary filter is a filter topology that can be applied alone or as a preprocessing technique for Extended Kalman Filters (EKF), for instance [58]. It is reasonable to explain its implementation by using frequency domain formulations. As an example, one can assume a system based on two measurement devices whose outputs are $y_1(t)$ and $y_2(t)$ and are represented by:

$$y_1(t) = c(t) + n_1(t) \tag{2.6}$$

$$y_2(t) = c(t) + n_2(t) \tag{2.7}$$

where n_1 and n_2 are measurement noises and c is the unknown signal to be determined. The noises $n_1(t)$ and $n_2(t)$ are considered stationary random process with known power

spectral densities. The signal $c(t)$ is unknown and can be deterministic or non-stationary [58]. The aim of a filter is to optimally produce an estimate $\hat{c}(t)$ of the unknown signal $c(t)$, assigning weights for the noisy measurements such as described in the following equations, as reported by Farell [58]:

$$\hat{c}(t) = g_1(t)\, y_1(t) + g_2(t)\, y_2(t) \tag{2.8}$$

$$\hat{C}(s) = (G_1(s) + G_2(s))\, C(s) + G_1(s)N_1(s) + G_2(s)N_2(s) \tag{2.9}$$

Equations ((2.8) and (2.9)) are respectively the time and frequency representations for the complementary filter. g_1 and g_2 are the transfer function of the filters whose input are respectively y_1 and y_2.

In order to avoid distortion, the following constraint must hold for all $c(t)$:

$$G_1(s) + G_2(s) = 1 \tag{2.10}$$

The complementary filter is considered to be a "safe" solution when no assumption is made about the signal structure, as it is particularly suggested for cases where the filter might need to cope with statistically unusual situations without resulting in large errors [45]. Complementary filters are usually applied for systems containing sensors with complementary spectral characteristics, as it is the classical example of inertial sensors. G_1 and G_2 can be chosen by running a Monte Carlo optimizer along with the knowledge of the true value for the estimate. Also, if the noises n_1 and n_2 have known complementary spectral characteristics, a low- or high-pass filter can be designed taking these spectra into account.

Kalman Filter

Essentially, the Kalman filter combines different measurement outputs in a systematic and optimal manner, given the prior knowledge about the system and measuring functions. The filter's goal is to provide an estimate of desired quantities, whose errors are improved in comparison with the original data sources. By carrying this out, Kalman filters can minimize the estimated error covariance and compensate for limitations of the sensing system such as lag and drift.

Some authors argue that the average results of the Kalman filter are better than the average results of any other filters used for sensor fusion [28, 129]. The filter has been widely used for tracking purposes [48], motion prediction and orientation estimate (mostly with MARG sensors) [28, 28, 130], navigation and process control [131]. Additionally, Kalman filters have a good real-time and online application potential [124]. They are said to be optimal as they use the maximum number of statistical descriptors to evaluate a system-measurement problem. Comparatively, other filter algorithms provide approximated results for the estimate covariance, since they do not require complete and accurate knowledge about the system, measurements and their statistical descriptors.

The description of system, measurements and their statistical descriptors is not always possible or fully definable. For these cases, other filter topologies such as particle filters can be deployed [132, 133].

The standard version of the Kalman filter provides the exact error covariance of the estimate, instead of an estimate of its value, with the cost of restricted requirements: zero-mean Gaussian noise, linear stochastic models for system and measurements, and correct description of measurement/model functions and errors. Based on the levels of confidence in measurements and system, the Kalman filter delivers the estimates of the system variables

and the covariance of those estimates. In a successful LKF implementation, the covariance of the estimate is smaller than any of the elements of the measurement covariance matrix main diagonal.

However, the application of these techniques to gesture analysis is not straightforward as there is no clear physical model describing the gestures used to control DMIs. Some research circumvents this problem by setting an enclosed gesture vocabulary for which the physical models can be accurately defined [50, 51]. This approach is not reasonable for musical gestures as it would excessively limit playing techniques.

Therefore, regarding skilled motor performance, it is impossible to define rules, patterns, probability or sequences for the human input that could well describe the process model of the system. In order to overcome that, previous work has developed a framework to apply sensor fusion to DMIs and other unpredictable signal devices [59]. The solution was based on a multiple-model LKF in combination with gesture/motion segmentation. The motion segmentation discriminates gestures according to the knowledge of their process model. This allows a more predictive estimation during periods of free motion, while relying on a less predictive approach for unknown user-driven signals [59]. Results reveal that the proposed method improves the error covariance of the estimate for driven and non-driven motions in comparison with single-sensor filter design and in comparison with single-model filter design. The method will be discussed throughly in Chapter 4.

The structure for this framework is presented as follows [59]:

- Offline tasks are performed in a heuristic manner:

  Motion segmentation: identification of distinct gestures with distinguishable physical model or measuring models;

  Regression: different slopes and intersections regression for each of the identified

gestures;

Evaluation: evaluation of optimal physical modeling for processes and measurement functions, for each identified gesture.

- Online tasks performed for each valid sample:

  Data acquisition: synchronization and alignment of multiple sensor data must be guaranteed;

  Classifier: classification of the gesture being performed and activation of the corresponding filter;

  Measurement function: computation of measurement output using the corresponding regression for the gesture being performed;

  Kalman filter loop: use of physical modeling, system and measurement error covariance matrices correspondent to the gesture being performed.

Sensor Fusion for MARG Sensing

Interesting examples of sensor fusion for human application using MARG sensing range from complementary filters to Kalman filter [134, 63, 50]. Complementary filtering fuses accelerometer and magnetometer data through the use of low- and high-pass filters, whereas the Kalman filter can potentially correct for noise in the yaw angle [58]. A framework for the application of Kalman filters for orientation purposes using MARG sensors is introduced as follows:

- Ensure alignment of all MARG sensors in case they are not packed together;
- Calibrate inertial sensors;
- Calibrate magnetometers and compensate for soft- and hard-iron artifacts [62, 135];

- Obtain systematic and random errors of all sensors. This information is necessary for defining the measurement covariance matrix in the Kalman filter;
- Know your process: design the physical model of your process. For free motions, that is, motions with dynamics which are steady and depend only on the structural mechanical features, the physical models can be well described. For human input processes or driven motions, it is hard to define the process without imposing constrains on the performer. The previous study's goal was to improve sensing design without restricting improvisation to an enclosed set of gestures or rules, resulting in an accurate sensing design that does not interfere in the exploration process of finding news ways to play. Under the proposed framework, these news ways are considered as unpredictable signals instead of a violation of arbitrary probabilities or rules. The mentioned work shows that it is possible to improve the accuracy of sensing using sensor fusion without restricting gestures to a set of probabilities, rules, or sequences [59];
- Apply the Kalman set of equations.

2.5 Conclusions

We have presented an overview of sensor use manifested in the NIME Conference proceedings from 2009 to 2013. The survey included total sensor use, use trends, use of motion capture tools and portable consumer electronic devices, concomitant use of sensors within the same application and embedded use of MARG sensors in portable consumer electronic devices. Then, we presented a brief overview on human motion analysis, discussing its kinematic and kinetic measuring methods. We showed that the most used sensors in DMIs provide force-related variables: accelerometer and FSR.

We then presented an overview of accelerometer and FSR use concerning techniques

of conditioning circuit and signal processing. We pointed to some limitations of recurrent designer choices, offering alternatives for a more advanced instrumentation design. We also proposed the use of strain gages as an alternative for force acquisition, a progressive and versatile choice with linear and reproducible response.

Then, we commented on interesting examples of sensing applications in NIME publications, once again proposing improvements for the instrumentation design and sensor signal processing through the use of specialized sensors, advanced electronic conditioning circuits and advanced sensor signal processing. Regarding the advanced sensor signal processing, we focused on sensor fusion. We remarked that for human input signals, as is the case for DMIs, most of the sensor fusion techniques are not straightforward, because human input signals are not trivially modeled. Therefore, despite the improvements brought by sensor fusion techniques, this method alone is not sufficient to obtain accurate signals.

Overall, we concluded that there is an urgent need to improve instrumentation techniques for DMIs and other human input devices, in order to design reliable instruments that are also robust, reproducible, responsive and accurate. We believe that efforts to improve sensing design—through the use of state-of-the-art engineering techniques—of DMIs can bring improvements concerning explorability and feature controllability [34]. Finally, as shown by the review of sensor use, there is an expansion in the use of MARG sensors for motion analysis. The current challenge is to fuse kinetics and kinematics for better analysis of human motion. Our future work is devoted to algorithms for biomechanical analyses that fuse positional data with sensor data—especially MARG sensors.

Chapter 3

Evaluation of Sensing Design for DMIs

Designing sensing for human-computer interfaces, particularly DMIs, is not a trivial task. A sensing design must satisfy not only common engineering requirements for reliable measuring, but also the requirements imposed by an exploratory context. In this chapter, we evaluate sensing designs for a DMI called The Rulers. The Rulers is a Kalimba-like instrument, whose mechanical design presents seven cantilever beams that can be bent or plucked individually or simultaneously. A previous design made use of infrared and Hall effect sensors. We introduce the use of strain gages as a sensing alternative. Strain gages are widely applied for solid mechanical analysis and present interesting features when applied to human-computer interfaces. We evaluate these three sensing technologies according to their metrology specifications—measurement function, linearity, resolution, sensitivity, resolution and hysteresis, according to environmental qualitative descriptors—mechanical robustness, installation and circuitry difficulty, and according to secondary sensitivities: force, stage light and temperature. Results indicate several advantages of the strain gages over the

infrared and Hall effect sensors, however their application requirements might be an obstacle for novice designers.

3.1 Introduction

As discussed in Chapter 2, we claim that stability, robustness, accuracy, reproducibility, and fast response are essential features for DMIs. Consequently, these requirements apply to the DMIs' sensing design. In most cases, these requirements differ from those in a laboratory environment, as interference quantities and operational conditions might differ. Often, DMIs require some adaptation after performers' practice sessions.

In order to evaluate sensing systems for DMIs, we used The Rulers as a testbed. Figure 3.1 shows The Rulers being played. This instrument, developed in 2004 by David Birnbaum [136, 137], has undergone two versions and has been played in numerous performances. However neither of these versions have produced a stable instrument, that is, neither were considered satisfactory to the point that further improvements would be dismissed.

Fig. 3.1 Archival photo (IDMIL Laboratory Library) of The Rulers being played by Fernando Rocha. Photo by David Birnbaum. Reproduced with permission.

The first version used infrared sensors to measure the distance between sensor and cantilever beam. The second version used Hall effect sensors to measure the distance

between sensor and a magnet firmly attached to the bottom of the beam. Using these sensor technologies, several issues of musical performance were identified such as sensitivity to stage light and timing issues due to hysteresis. These sensors are relatively easy to use and highly available, which makes them popular among researchers and makers [18]. As we intend to evaluate The Rulers' sensing as it was used in stage performance, no improvement on the sensor signal conditioning circuits or sensor placement was performed. The improvements are recommended in the end of this chapter, and executed in Chapter 4.

As a sensing alternative, we introduce the use of strain gages. As opposed to IR and Hall effect sensors, strain gages have not been widely employed in DMIs, possibly due to their relative complexity when compared to more popular sensors for measuring force and pressure, such as FSRs [19, 20, 1, 18]. SGs are widely used in solid mechanical analysis. The simplest application of these sensors is the measurement of strain in a clamped cantilever beam. We are interested in comparing the performance of specialized sensors—such as strain gages— and ordinary sensors—such as infrared and Hall effect sensors— using The Rulers as a testbed. For this purpose, we perform an in-depth review of SG application for bending strain.

The sensors are submitted to the same evaluation, as well as calibrated using the same reference measuring system and process. The evaluation method includes metrology descriptors and environmental qualitative factors.

3.1.1 The Rulers

The instrument was designed to induce the gestures of plucking or bending the free edge of seven beams [137]. The aluminum beams have different lengths, therefore, each beam oscillates at a different frequency when plucked. This provides visual and passive haptic feedback to the performer. However, free and driven motions are not meant for acoustic

output. The motion of each beam is measured by sensors, whose signals—after conditioning and processing—are mapped to a computer-based synthesizer. Figure 3.1 depicts The Rulers being played.

Ideally, the mechanical system is formed by beams clamped at one edge, and free at the other edge. The beams' thickness does not allow torsion, but allows bending. The beams' bending motions can be described by the Euler-Bernoulli beam equations [138]. These equations describe the deflection and the strain at any beam point. In practice, the instrument's clamps are not perfect, allowing degrees of freedom that compromise the sensing accuracy, as discussed further in this text.

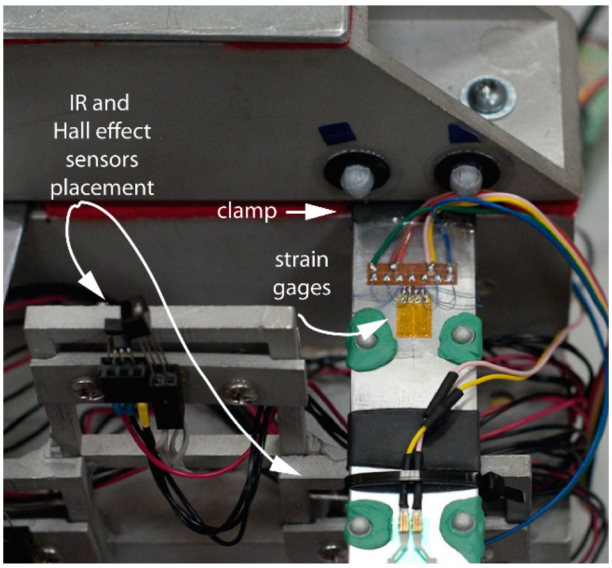

Fig. 3.2 Sensors placement and clamp.

This chapter is organized as follows. In Sections 3.2, we present the sensors and their signal conditioning circuits for the previous versions of the instrument. Section 3.3 presents strain gage technology and its application to The Rulers. Section 3.4 introduces the calibration protocol. Section 3.5 presents quantitative and qualitative evaluation. Section 3.6 discusses the results. Section 3.7 shows the future directions, and Section 3.8 presents

the conclusions.

3.2 Sensor Technologies for The Rulers

This section presents the considerations for sensor specifications, placement and signal conditioning for SG, IR and Hall effect sensors.

3.2.1 Infrared Sensor

The QRD1113 Fairchild^{TM} consists of an infrared emitting diode and a photosensitive transistor [139]. The process of measuring a distance between sensor and object, surface, or body using this sensor happens as follows. The diode constantly emits infrared light, which is reflected given the presence of an obstacle in the sensor active range. The sensor-obstacle distance determines the reflected infrared light, which consequently determines the polarization of the transistor's p–n junction(s). The polarization defines the transistor's collector current (I_F). The IR polarization circuit for this specific sensor is presented in Figure 3.3. The infrared sensor is placed underneath the beam, close to the clamp, as shown in Figure 3.11. Placement and polarization resistors for diode and transistor determine the sensor's operation range, which defines its sensitivity. Even a careful choice of resistors and placement can lead to non-monotonic ranges.

The deflection at the free edge is assessed by measuring the distance between sensor and beam. However, the flawed clamp does not guarantee a linear relation between measured distance and quantity of interest. The relation between the two quantities needs to be considered in the measurement function, which can also be obtained by calibration.

This sensor requires polarizing resistors as external components, as shown in Figure 3.3. A good practice is to use two resistors (R_{D1} and R_{D2}) in series with the diode. One

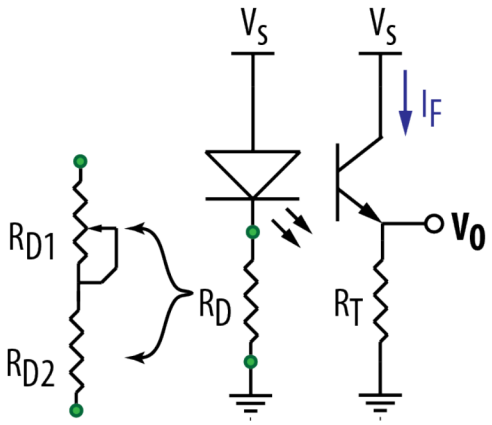

Fig. 3.3 QRD1113 polarizing circuit

resistor should account for the maximum current through the diode (R_{D2}), and the other should be a potentiometer, set from zero to nominal value, in order to control the incident infrared light R_{D1}. Therefore, the complexity in connecting this sensor is relatively low. However, the intricate adjustment of several dependent variables is necessary to obtain monotonic and high sensitivity measurement ranges: polarizing resistance, reflective surface and sensor placement. In terms of secondary sensitivities for the instrument context, the most substantial interference quantity is stage light, as it radiates infrared light.

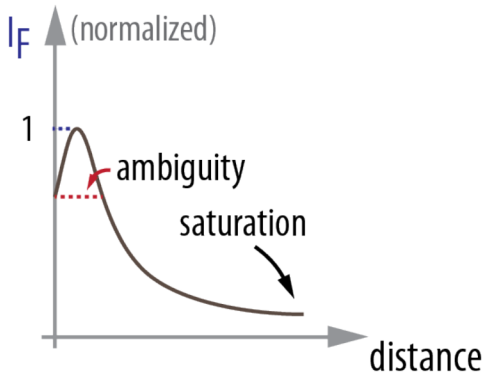

Fig. 3.4 Most common infrared-based proximity sensor response versus distance.

Other infrared-based proximity sensors adopt a triangulation method for reducing the sensitivity to "the reflectivity of the object and the environmental temperature" [140].

The features of almost all types of non-contact infrared proximity sensors follows the response curve presented in Figure 3.4. Common features to their response is the non-linearity and two diverse monotonic measurement ranges.

3.2.2 Hall Effect Sensor

Hall effect sensing was chosen as a proximity measurement technology for the second version of The Rulers, due to insusceptibility to stage light infrared spectrum, as opposed to the previous version of the instrument based on IR sensing. In this version of the DMI, a Honeywell ^{TM} SS39ET was used. It is a transistor that presents voltage in its edges in the presence of a magnetic field [141]. A magnet, firmly attached to the bottom of the cantilever beam, changes the magnetic field in the surroundings of the sensor. Due to the Hall effect, the voltage V_E is directly proportional to the strength of the magnetic field. The datasheet illustrates a linear sensor response in respect to the magnetic field [141]. However, the relation between sensor voltage output and distance is not linear. Figure 3.5 shows a common equivalent circuit for the Hall effect sensor, along with its response in respect to magnetic field and distance.

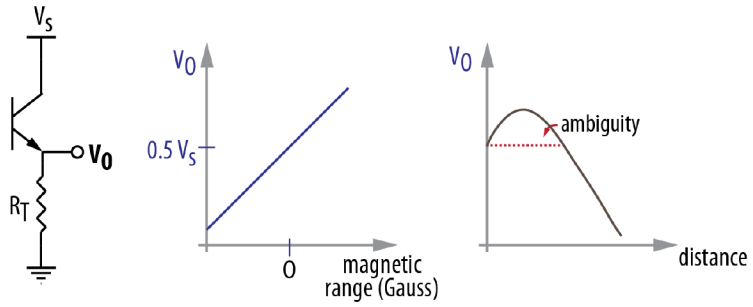

Fig. 3.5 Common Hall effect sensor equivalent circuit and voltage outputs: versus magnetic field and versus distance.

In its unipolar configuration, using only one magnet as magnetic field generator, the relation between magnetic field and distance is quadratic [142]. Furthermore, as expected from a magnetic sensing technology, Hall effect sensors present hysteresis. Besides non-linearity and hysteresis, another drawback of using the Hall sensor for The Rulers is related to the instrument's mechanical features, which allow rotation of the beams around their vertical axes, resulting in misalignment between sensor and magnet. Also, non-linearity due to the relation between quantity of interest and measured quantity can be expected. A possible source of interference for this sensor is any external magnetic field, created by other magnetic sources.

3.2.3 IR and Hall Effect Sensor Solutions

As presented above, IR and Hall effect sensors measure the distance between the sensor and the beam. The measurements are taken near the clamp in order to leave free space for the musical gestures. Therefore, as the measured quantities are smaller than the deflection at the free edge, adjustment of placement and polarization resistors should be performed, establishing a better measurement range and improving the SNR.

In addition, two layers of non-linearity are reported in this study. The first one is the non-linear relation between measured quantity and quantity of interest. The second one is the non-linear voltage sensor response in respect to distance.

The drawback of non-linearity can be dealt with by coherent calibration and regression, and signal processing techniques [143]. Also, linearization methods can be applied both in hardware and in software [144, 145, 146], and computational methods can be used for offline applications. However, for embedded real-time application—as is the case of most DMIs—the requirements of low computational cost and processing time limit the number of possible solutions. For instance, considering the popular Arduino platform, the possible

techniques for embedded processing of non-linear data are costly in time, and might produce only a few discrete measurement levels [101].

Ambiguity ranges are a consequence of non-monotonic functions, which usually present a certain measurement interval where the sensitivity is close to zero, compromising the responsiveness of the system. This is another issue of using infrared and Hall effect sensors. If a monotonic response is not achieved by careful selection of placement and polarizing resistors, possible solutions include advanced instrumentation design and sensor signal processing [101].

3.3 Strain Gage Technology

From physics, it is known that a force applied to a certain area result in stress given by $\tau = F/A$, where τ is the stress, F is the applied force and A is the area [104]. Strain is the relative deflection of rigid body particles, which can be described in its engineering normal form as: $\epsilon = \Delta L/L$, where ϵ is the engineering normal strain and L is the original length of the Device Under Test.

Materials can react to the stress elastically or plastically, depending on their own characteristics and on the load. In the elastic regime, the relation between stress and strain is linear, and there is no residual deflection when the force is released [147]. Materials in their plastic regime do not have a linear relation between stress and strain, and residual deformation might remain when the load is released [147]. Under elastic condition, the linear relation between stress and strain is given by the Young Modulus or Elastic Modulus (E): $E = \tau/\epsilon$. This chapter discusses strain and strain gage technology, relying on the hypothesis that the materials are operating in their elastic mode.

Besides mechanical stress, the other stress type common in rigid body materials is the

thermal stress [41]. Thermal stress results in strain, and respects the thermal expansion coefficient (α). A body with initial length of L changes its dimensions due to temperature changes, in respect to the following equation: $\Delta L = L\,\alpha\,\Delta T$, where T is the temperature.

Strain gages measure these strains indistinguishably: strain due to mechanical stress and strain due to temperature. For bending strain, given the mechanical structure of the beam, the mechanical strain is inversely proportional to the distance between measuring point and clamped edge. The equations that govern the beam's deflection at the free edge and strain at a given measurement point are [148]:

$$\delta(a) = \frac{2\,\mathbf{F}\,a^2}{E\,B\,H^3}\,(3\,L - a) \tag{3.1}$$

$$|\epsilon|(x) = \frac{6\,\mathbf{F}\,(L - x)}{E\,B\,H^2} \tag{3.2}$$

where $\delta(a)$ is the deflection at the free edge, given a force $\mathbf{F}$, applied at a longitudinal distance a from the clamped edge, E is the Modulus of Elasticity intrinsic to the material, x is the longitudinal distance between the measurement point and the clamped edge, L is the beam longitudinal length, B is the beam width and H is the beam thickness.

The most common strain gage types are piezoresistive and piezoelectric [41]. Among the piezoresistive strain gages, a variety of designs, purpose, temperature compensations and measurement ranges can be found commercially. Piezoresistive SGs can be classified as metallic or semiconductors. The popular metallic strain gage grid design defines which type of strain the sensors are be sensitive to. For instance, the strain gage in Figure 3.7, is mostly sensitive to strain in its longitudinal axis. Therefore, this sensor experiences changes in its nominal resistance in respect to strain in the longitudinal axis. Figure 3.6 shows metallic and semiconductor strain gages applied to a specimen for tensile testing.

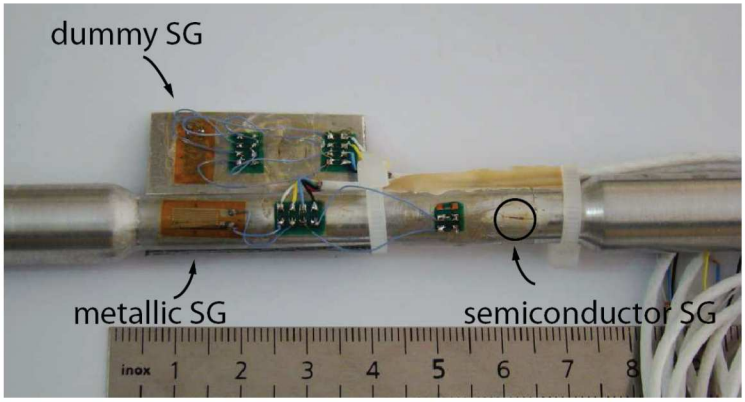

Fig. 3.6 Metallic and semiconductor strain gages. The reference ruler has 1 mm resolution. Photo by Edison da Rosa. Reproduced with permission.

3.3.1 Metallic Strain Gage

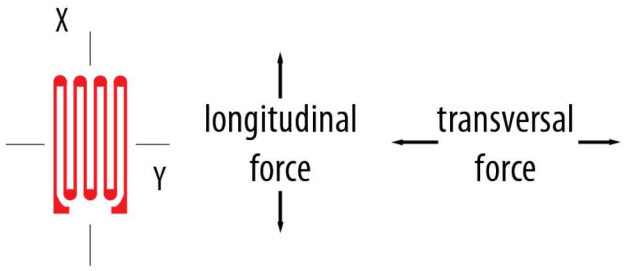

Fig. 3.7 Bonded metallic strain gage grid: design maximizes sensitivity to longitudinal strain—measurement of interest—and minimizes sensitivity to transversal strain. Transversal sensitivity is the sensitivity to strain in the sensor's transversal dimension.

Based on Areny and Webster's derivation for circular conductors [29], we have derived the equations for a square cross-section area conductor. For a rectangular conductor of length l, with a square cross sectional area of side b, the resistance is:

$$R = \frac{\rho\, l}{A} = \frac{\rho\, l}{b^2} \tag{3.3}$$

where R is the resistance, ρ the resistivity and A the cross sectional area. If the wire experiences a longitudinal load, both its dimensions and resistivity ρ will change at different

ratios [29]:

$$\frac{dR}{R} = \frac{d\rho}{\rho} + \frac{dl}{l} - \frac{dA}{A} \tag{3.4}$$

The longitudinal variation, within the elastic limit obeys Hooke's Law ($\tau = E\,\epsilon$) [147]:

$$\tau = \frac{F}{A} = E\,\epsilon = E\,\frac{dl}{l} \tag{3.5}$$

where τ is the mechanical stress, E the Young's Modulus and ϵ the strain. Also, according to Poisson, the transversal dimension b varies in respect to a longitudinal load:

$$\nu = -\frac{db/b}{dl/l} \tag{3.6}$$

In practice, the grid design of a longitudinal SG reduces its transversal sensitivity. This is obtained by thin grid lines and by thick end loops. That is, maximizing the end loop areas minimizes their equivalent resistance. These fabrication choices are illustrated in Figure 3.7, which displays a common metallic SG design.

From the previous equation, the area variation for a rectangular cross section is:

$$\frac{dA}{A} = 2\,\frac{db}{b} = -2\,\nu\,\frac{dl}{l} \tag{3.7}$$

Also, the applied force causes variation of the vibration intensity of the metal lattice, which reduces electron mobility [29]. Bridgmann's constant (C) relates the amount of variation of resistivity to the amount of variation of the volume.

$$\frac{d\rho}{\rho} = C\,\frac{dV}{V} = C\,\left[\frac{dl}{l} + 2\,\frac{db}{b}\right] = C\,\left[(1-2\nu)\,\frac{dl}{l}\right] \tag{3.8}$$

Finally, for an isotropic rectangular conductor, within the elastic limit, the amount of resistance variation due to mechanical strain is:

$$\frac{dR}{R} = \frac{dl}{l}\left[1 + 2\nu + C\left(1 - 2\nu\right)\right] = GF\,\frac{dl}{l} = GF\,\epsilon \tag{3.9}$$

As reviewed in Section 2.3.3, temperature affects the strain measurements in several ways. Usually, the main effects observed are [29, 41]:

- metallic DUT and sensor suffer dimensional changes governed by the thermal expansion coefficient;
- temperature variations alter the Gage Factor of the unstrained grid wire.

Some procedures can be taken to compensate for that:

- selection of material-alike compensated SGs, that is, sensors that have thermal expansion coefficient similar to the DUT;
- include dummy SGs in the balancing circuit. Dummy sensors are exposed to the same temperature but not submitted to mechanical strain (Figure 3.6);
- test DUT under temperature-controlled environment, which is not practical in most applications;
- limit the excitation voltage in order to reduce the power dissipated by area. This consists a hard design question as it involves SNR, sensor dimensions and sensor nominal value. An unloaded drift study can define temperature variations due to power dissipation effects [149];
- use bridge topologies where the temperature effect is canceled out. This will be further discussed in the next section.

3.3.2 Conditioning Circuit

A signal conditioning circuit for strain gages should include the following conditioning techniques and circuits: balancing conditioning circuit according to the stress profile, temperature compensation, zeroing circuit, lead wire compensation, amplification, and filtering (if necessary).

Following that, a calibration using a reference measuring system should be used. A conservative protocol for strain gage measurement and data analysis is given by the Unified Approach to the Engineering of Measurement System for Test and Evaluation [5]. This method synthesizes calibration, control, test and evaluation of measuring systems. One of its main contributions is the discussion of interference quantities and tests to detect their influences.

As reviewed previously, strain gages vary their resistance with respect to strain. However, this resistance variation can be as small as less than 1% of their nominal value [6]. In order to be able to measure this small variation on resistance, balancing conditioning circuits need to be used. The most common balancing circuit is the Wheatstone bridge. The bridge can be analyzed as two voltage dividers: one formed by sensors SG_1 and SG_2, and other formed by sensors SG_3 and SG_4 (Figure 3.8). The balance occurs when all four elements of the circuit have the same resistance. As far as one resistor changes its resistance, a non-zero voltage can be read in the bridge output V_O. However if two adjacent resistors present equal resistance variation, the bridge keeps its balance. This allows for temperature compensation through dummy sensors. Considering the sensor distribution in Figure 3.8, pairs of sensors facing each other (SG_1/SG_3 and SG_2/SG_4) have their variation summed, whereas adjacent resistors pairs (SG_1/SG_2 and SG_3/SG_4) have their variation subtracted.

The bridge is followed by circuits for offset-nulling compensating for lead wire resistances,

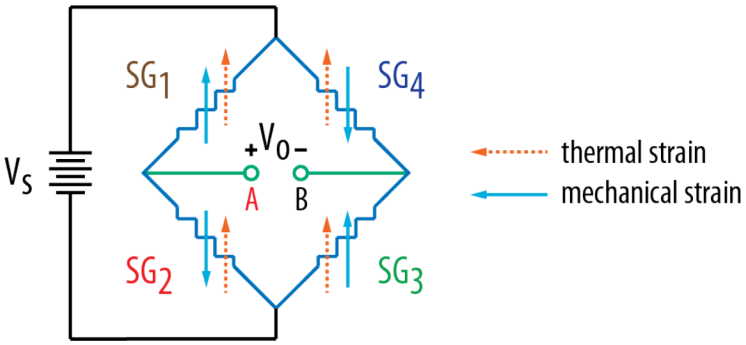

Fig. 3.8 Example of Wheatstone bridge for being strain measurement with temperature compensation.

and for amplifying the signal. First, an analog zeroing process is implemented by using three fixed resistors (tolerance 0.1%) and two trimpots (tolerance 1%), as shown in the schematics of Figure 3.9. By adjusting R_2 and R_4 resistors—course and fine adjustment respectively—it is possible to balance the bridge to zero output voltage when the sensors are unstrained. The zeroing process by hardware can also be used for fault detection, and cannot be substituted by zeroing by software.

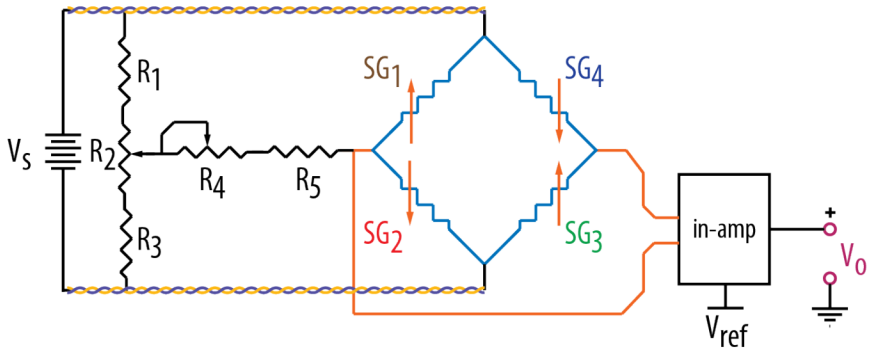

Fig. 3.9 Conditioning circuit: full bridge with zero nulling adjustment. in-amp circuit is shown in Figure 2.9. Arrows illustrate sign of strain when force is applied downward in the beam showed in Figure 3.10.

Lead wire resistances may be compensated, especially for remote measurements and for configurations with less than 4 gages. In full bridge configuration, the leading wires do not have significant contribution to the bridge unbalance, since all sensors can be connected

by wires of equal length and specifications. Even so, the resistance of the power source wires can be reduced by half using the 6-wire configuration. In this method, two wires are used to connect each of the supply voltage terminals. This enhancement is particularly interesting for remote measurements. The use of twisted pair cabling—shown in Figure 3.9—reduces the electromagnetic susceptibility of remote connections. For amplification reasons, an in-amp is used with reference voltage of $V_S/2$ in order to operate rail-to-rail in a single supplied circuit. The in-amp gain has to be adjusted in order to provide SNR enhancement, without compromising the measurement range.

An alternative conditioning circuit to the Wheatstone bridge is the circuit called Anderson Loop. The loop current remains constant with the sensor resistance variation, therefore, it eliminates possible non-linearities in unbalanced bridge topologies [150].

Wheatstone Bridge Topologies

The types of Wheatstone bridge are defined by the number of active elements, that is, sensors. This way, a quarter-bridge has one sensor and three fixed resistors, whereas a half-bridge has two sensors and two fixed resistors. Finally, in a full bridge configuration, all the elements are active. As The Rulers define a bending strain problem, a uniaxial measurement of strain was chosen. For this, double longitudinal SGs, also called XX, were applied to the bottom and the top of the beam. In order to maximize overall sensitivity, a full bridge was implemented. The temperature compensation is obtained by using self-compensated SGs and by coherent full bridge connection. This topology is depicted in Figure 3.8. Sensors SG_1 and SG_3 are applied to the top of the beam, whereas sensors SG_2 and SG_4 are applied to the bottom of the beam, as shown in Figure 3.10.

The summary of the effects of each sensor when the beam is bent downwards are:

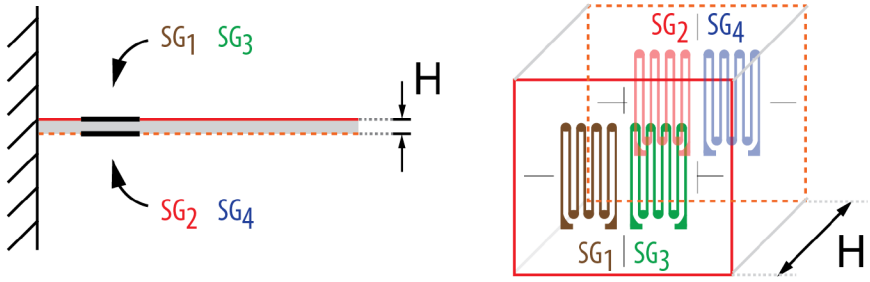

Fig. 3.10 SGs placement onto the beam: SG_1 and SG_3 onto the top, SG_2 and SG_4 onto the bottom.

SG_1 : tension or positive mechanical strain $+\epsilon_{mec}$, temperature strain ϵ_{temp};

SG_2 : compression or negative mechanical strain $-\epsilon_{mec}$, temperature strain ϵ_{temp};

SG_3 : tension or positive mechanical strain $+\epsilon_{mec}$, temperature strain ϵ_{temp};

SG_4 : compression or negative mechanical strain $-\epsilon_{mec}$, temperature strain ϵ_{temp};

$$V_A = V_s \frac{R_2^{SG} - \Delta R_{2M}^{SG} + \Delta R_{2T}^{SG}}{(R_1^{SG} + \Delta R_{1M}^{SG} + \Delta R_{1T}^{SG}) + (R_2^{SG} - \Delta R_{2M}^{SG} + \Delta R_{2T}^{SG})} \tag{3.10}$$

$$V_B = V_s \frac{R_3^{SG} + \Delta R_{3M}^{SG} + \Delta R_{3T}^{SG}}{(R_4^{SG} - \Delta R_{4M}^{SG} + \Delta R_{4T}^{SG}) + (R_3^{SG} + \Delta R_{3M}^{SG} + \Delta R_{3T}^{SG})} \tag{3.11}$$

$$V_O = V_A - V_B \tag{3.12}$$

where R_i^{SG} represents the resistance of SG_i, for $1 \leq i \geq 4$, ΔR_{iT}^{SG} represents the resistance variation due to temperature for all i, and ΔR_{iM}^{SG} represents the resistance variation due to stress for all i. Some assumptions simplify the problem. The first is that the beam does not experience torsion during operation. The second is that a perfect alignment between top and bottom applications of the strain gages is guaranteed. Ideally, these criteria result in equal mechanical strain in all sensors. Also, considering that the temperature experienced by all sensors is the same, the temperature effects can be compensated for. Finally, considering that all sensors have equal specifications—nominal resistance R, GF, self-compensation

for temperature, and that they are submitted to equal absolute mechanical and thermal strains—the total output voltage is:

$$V_A = V_S \frac{R - \Delta R_M + \Delta R_T}{2\,R + 2\,\Delta R_T} \tag{3.13}$$

$$V_B = V_S \frac{R + \Delta R_M + \Delta R_T}{2\,R + 2\,\Delta R_T} \tag{3.14}$$

The output is the difference between V_A and V_B:

$$V_o = V_A - V_B = V_S \frac{R - \Delta R_M + \Delta R_T - (R + \Delta R_M + \Delta R_T)}{2\,R + 2\,\Delta R_T} \tag{3.15}$$

$$= V_S \frac{-2\,\Delta R_M}{2\,R + 2\,\Delta R_T} = V_S \frac{\Delta R_M}{R + \Delta R_T} \tag{3.16}$$

however $R \gg \Delta R_T$ and $\Delta R/R = GF\,\epsilon$, therefore

$$V_o = V_S \frac{\Delta R_M}{R + \Delta R_T} = V_S \frac{\Delta R_M}{R} = V_S\, GF\, \epsilon_{mec} \tag{3.17}$$

The final bridge output is four times more sensitive to strain than the quarter-bridge topology using only one active gage.

3.3.3 Sensor Application to the Specimen

Applying the strain gages to the specimen requires special attention, due to the delicate structure of the strain gage. Also, the installation process requires a dirt-free environment and tools, because any impurity might degrade the strain gage grid and pads, or affect the strain transfer from specimen to sensor.

Once the specimen and sensor are clean and dry, the application point is selected. The selection of the measurement point is a compromise between maximizing SNR and maximum strain damage prevention. After selecting the point, signs are drawn to indicate the correct position to apply. A misalignment between the axial axes of bottom and top applications is acceptable if it does not exceed 4° [41].

The bond between SG and beams can be made by cold-cured cyanoacrylate adhesive [151]. The sensors must receive a protection given by dedicated coating material. Finally, the bridge and lead wires from the bridge to the remaining conditioning circuits must be installed with care. Unbalanced wiring can lead to apparent strain measurements. Last, a resistance measurement test can verify the correct installation of the sensors.

3.4 Calibration Setup

3.4.1 Sensors

The conditioning circuits for the IR, Hall effect, and strain gage sensors are respectively displayed in Figures 3.3, 3.5, and 3.9.

3.4.2 Acquisition System

The analog acquisition card is a National Instruments NI PCI-4472 ©, with the following specifications: 8 channels, 24 bits/sample, and up to 100 kHz. Five channels were used:

- power supply voltage;
- power supply at the sensors end;
- strain gage conditioning circuit output;
- Hall effect sensor output; and
- IR circuit output.

A .vi code (Labview©) was implemented for processing data from the acquisition board. The software incorporates the following blocks/functionalities:

- acquisition board settings;
- data manipulation settings (user);
- signal processing features such as filtering and zero-nulling by software;
- data visualization; and
- data logging.

Further processing such as filtering, regression and statistical analysis were performed with exported data from Labview© to Matlab©.

3.4.3 Measurement

The reference used for calibrating the sensors was the vertical distance between beam at rest position and discrete stoppers—using LEGO™ bricks as stoppers. LEGO™ bricks are a flexible, low cost, and dimension accurate option for designers that do not have a reference measuring system at their convenience—LEGO company reports a "machine tolerance" as small as 0.01 mm [152]. The measurement points were delimited by stoppers at a known distance from the rest position of the beam. The procedure diagram is shown in Figure 3.11.

A remark should be made about SG calibration. Given elastic behaviour of the beam, the applied force magnitude is linear with respect to the distance from the beam at rest position. Therefore, calibrating the SG using position reference or force reference results in equivalent transfer functions. If the material plastifies at any moment or if other forces besides bending exist, this equivalence might be compromised.

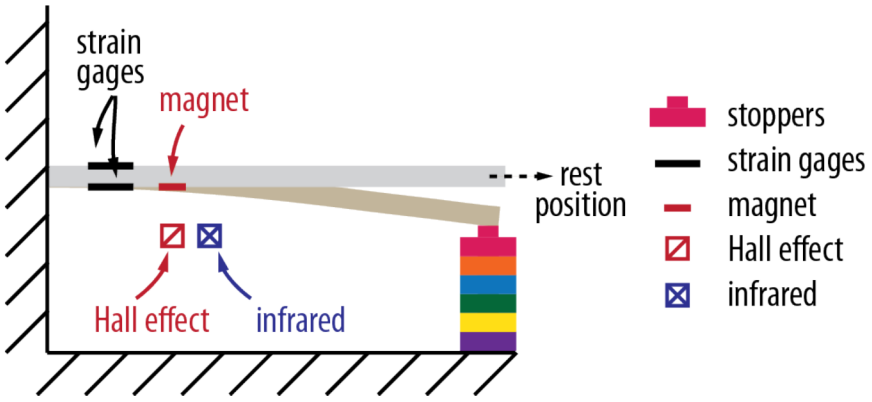

Fig. 3.11 Discrete calibration using as reference known distance between beam at rest position and stoppers.

Discrete calibration requires concomitant measurement of: 1) reference distance between beam at rest position and stopper; 2) sensor outputs of each calibration point. Also, several measurements should be taken for each of the calibration points. Finally, due to hysteresis effects, each calibration point should be measured for positive and negative position increments.

3.5 Evaluation

3.5.1 Quantitative Sensor Evaluation

The pairs of reference position and sensor voltage output for each sensor technology—SG, IR and Hall effect sensors—should be evaluated, in order to define the best measurement function for each sensor. This is obtained by least squares regression. The regression results for the given sensors and configuration are:

- **Strain Gage** — linear — $r^2 = 0.9987$

  $V_{SG} = 0.01524\,\delta + 2.507$;

- **Hall Sensor** — quadratic — $r^2 = 0.9670$

$$V_{HL} = -2.840\,10^{-5}\,\delta^2 - 2.131\,10^{-3}\,\delta + 0.2001;$$

- **Infrared** — quadratic — $r^2 = 0.9918$

  $$V_{IR} = -4.937\,10^{-4}\,\delta^2 + 1.505\,10^{-2}\,\delta + 4.538.$$

where V_{sensor} is the output of each of the sensors, δ is the deflection at the free edge given by the reference, and r^2 is the coefficient of determination, which indicates the quality of a fitting model.

It is notable that the Hall effect sensor has a low r^2 value, as compared to the other sensors. This is explained by the significant hysteresis presented by this sensor. This effect will be discussed later in this section. The regression curves for each sensor are presented in Figure 3.12.

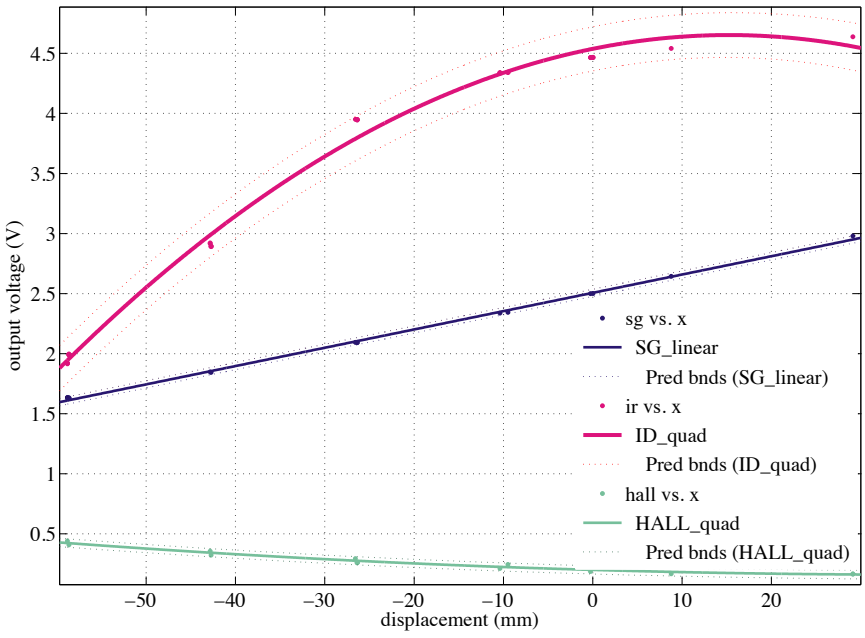

Fig. 3.12 Regression curves for each sensor

Clustering output voltage ranges, it is possible to better visualize the output response of each sensor (Figure 3.13). By analyzing this figure, it is clear that both IR and Hall

effect sensors are not monotonic, what leads to ambiguity ranges—highlighted in Figure 3.13. The ambiguity ranges are [0, 30] mm for the IR sensor, and [-60, -15] mm, for the Hall effect sensor. As stated in Section 2.4.1, non-monotonic ranges are not desirable even if the analysis of the instantaneous derivative can solve the ambiguity. This is due to the fact that non-monotonic ranges generally present regions with extremely low sensitivity.

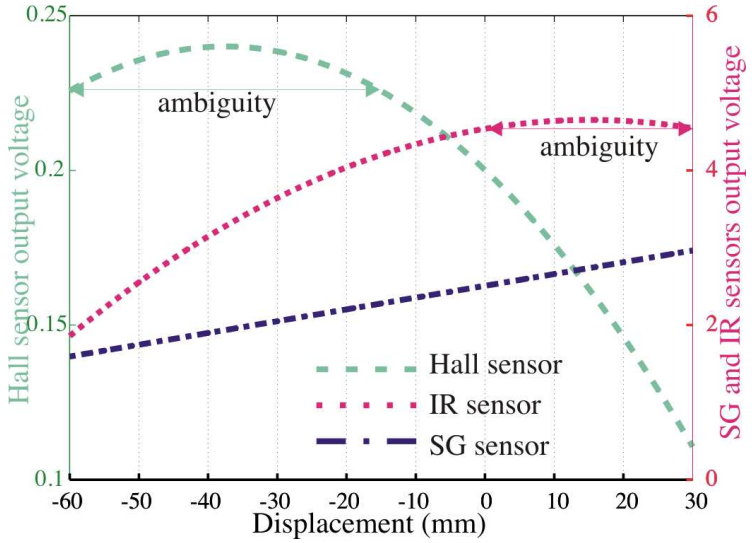

Fig. 3.13 Sensor responses for Hall effect sensor (left horizontal axis range) and SG and IR sensors (right horizontal axis range). Ambiguity ranges occurred due to non-monotonicity.

As shown in Figure 3.13, both IR and Hall effect sensors have non-linear quadratic responses. As mentioned earlier, for the most popular microcontrollers, there is little capability of processing non-linear polynomial or exponential measurement functions by firmware [101]. A possible solution is to process the measured data in more computationally powerful platforms that interface with the firmware. This workaround needs to be done, otherwise erroneous data mapping can degrade the overall performance of the DMI.

Given the measurement functions, it is possible to calculate the sensitivity for each sensor technology. Figure 3.14 presents the sensors' sensitivity, i.e., the amount of variation

observed in the output when a unitary variation of deflection occurs. As expected, IR and the Hall effect sensors have variable sensitivity across the measurement range.

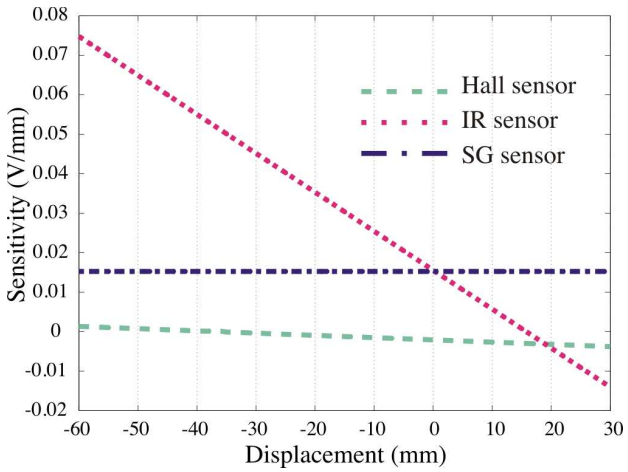

Fig. 3.14 Strain Gage, IR and Hall effect sensor sensitivities across the measurement range

Comparatively, the IR sensor presents good sensitivity within the range [-50, 0] mm, whereas the Hall effect sensor presents the poorest sensitivity across almost the entire measurement range.

The resolution indicates the "smallest change in a quantity being measured that causes a perceptible change in the corresponding indication" [3]. For instance, to date, most of the embedded analog-to-digital converters (ADC) in Arduino boards are 10 bits/sample [153]. Based on this ADC resolution and on the instantaneous sensitivity, the instantaneous resolution of each sensor measurement across the range is obtained. Figure 3.15 shows the sensor measurements resolution for a 10-bit ADC. For clarity purposes, the bottom graph in the Figure 3.15 is a scaled version of the upper one, where only resolutions lower than 5 mm are shown.

It was mentioned earlier that the Hall effect sensor response presents hysteresis. This is a common effect in magnetic devices. Aside from that, bending trajectories are not similar

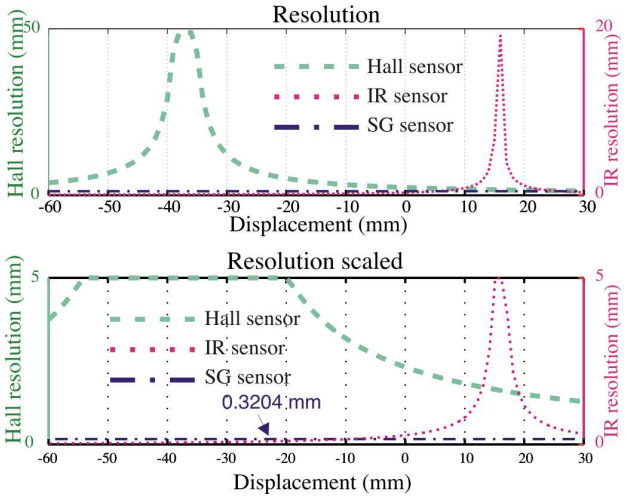

Fig. 3.15 Strain Gage, IR and Hall measurements resolution across the range. The bottom graph is a zoomed version of the top one, highlighting resolutions lower than 5 mm.

in ascending and descending motions, due to its imperfect clamp. For this experiment, the overall average hysteresis for each sensor is:

- **Strain Gage:** $\delta_{hyst} = 1.01$ mm ;
- **Hall Effect Sensor:** $\delta_{hyst} = 16.86$ mm ;
- **Infrared:** $\delta_{hyst} = 4.64$ mm ;

Figure 3.16 shows calibration curves for the Hall effect sensor, distinguishing ascending and descending bending.

3.5.2 Qualitative Sensor Evaluation

In the context of a DMI, some qualitative descriptors must be analyzed. Some of them are presented in Table 3.1 and described as:

linearity: although linearity can be defined quantitatively, it is also listed as qualitative

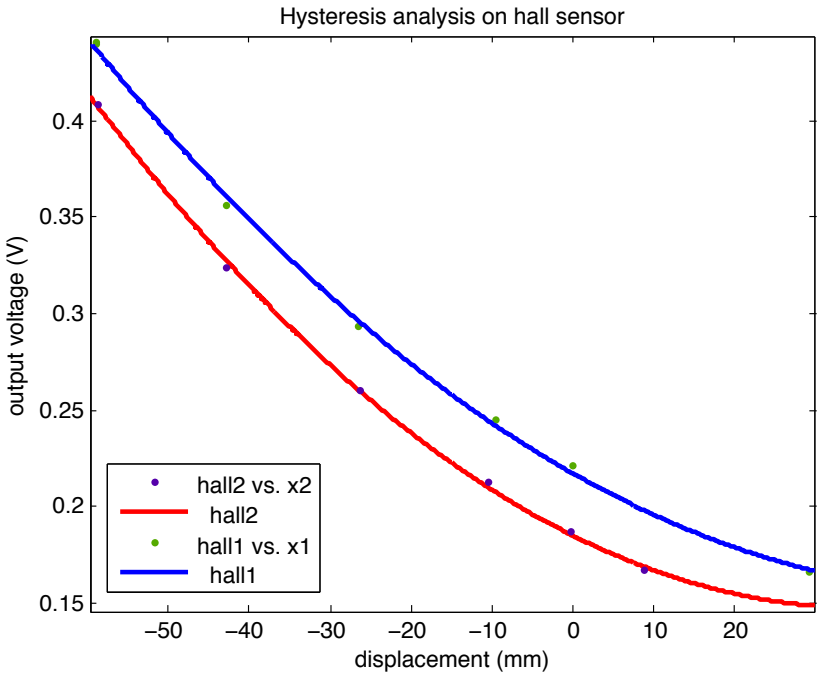

Fig. 3.16 Hall effect sensor hysteresis: a regression curve for each deflection direction.

descriptor because non-linear sensors require additional signal processing in order to be suitable for microcontroller operations;

force sensitivity: as opposed to IR and Hall effect sensors, SGs are directly sensitive to the applied force, which may be desirable. For instance, the forces acting in the cantilever beam during free oscillation and during driven motion are different. This can be used to determine the presence of external control;

stage light sensitivity: stage light has an infrared spectrum, which therefore interferes in the IR sensor response. Also, some stage lighting may be much warmer than ambient temperature. This thermal property might interfere in the SG response;

temperature sensitivity: Temperature, as an ubiquitous environmental quantity, might interfere in any measurement. Therefore, temperature interference should be observed in order to obtain reliable measurements [5]. Quality strain gages' datasheets include

Gage Factor response to temperature. The effect of temperature in IR and Hall effect sensors also affects their response according to their datasheets [139, 141]. However, it is hard to define and quantify the variation by examining the datasheet graphs. As a practical rule, a temperature sensitivity study should be run in order to define the effect of temperature on each of the sensors;

circuity complexity: represents how difficult it is to set up data acquisition for the three sensor types. In general, several IR and Hall effect sensors are commercialized with internal signal conditioning circuits. This was the case for the Hall effect sensor used in this work. IR and Hall effect sensors require simple conditioning signals, whereas strain gages require a more complex conditioning circuit and basic assessment of stress analysis;

installation complexity: strain gages require expertise in their manipulation and in their application onto the specimen, whereas IR and Hall effect sensor application is extremely simple. Despite this uncomplicated setup, it is hard to adjust sensor placement for obtaining a monotonic behaviour, that is, free of saturation.

mechanical robustness: mechanical robustness indicates the property of maintaining the functionality of the sensors through time and use. As strain gages are applied to moving parts, as well as their lead wires, this can imply fatigue or connection issues. The IR sensor does not have any moving parts, therefore it is mechanically robust. Finally, the Hall effect sensor was considered to exhibit a medium level of mechanical robustness, because the magnet is installed on moving parts, which can compromise the alignment between the Hall sensor and magnet.

Table 3.1 Qualitative descriptors for The Rulers

descriptors	SG	Hall	IR
linearity	linear	non-linear	non-linear
force sensitivity	yes	no	no
stage light sensitivity	negligible	no	yes
temperature sensitivity	yes	yes	yes
circuitry complexity	high	low	low
installation complexity	high	low	low
mechanical robustness	medium	medium	high

3.6 Discussion

After discussing the characteristics of the three sensors types and their evaluating descriptors, other overall parameters can be useful for sensor selection: responsiveness, robustness, price, availability, usability/complexity, and compatibility to real-time performance scenarios.

Concerning responsiveness, the main indicators are the sensitivity and linearity. The IR sensor presents the best sensitivity over 75% of the measurement range, however this value is range-variant and decays drastically for small deflections. This implies that small vibrations and the damped plucking oscillation are hardly sensed by this sensor. The strain gage has a constant sensitivity across the entire measurement range, as its output is linear. The Hall sensor has the smallest sensitivity across most of the measurement range. In terms of mapping sensor signals to control music, the non-linearity of IR and Hall effect sensors might be a drawback, as it requires algorithms to deal with high order regression functions and ambiguity.

The robustness of The Rulers in performance scenarios was the main motivation for evaluating the previous versions of this instrument—based on IR and Hall effect sensors—and to propose another version based on strain gages. Evaluation of the infrared version of the instrument under performance reported issues with stage light. The Hall version of

the instrument received several complaints about signal loss through misalignment, and delay through hysteresis. There were no performances with the strain gage version of the instrument yet.

IR and Hall effect sensors tend to be highly available at low cost. Furthermore, they are straightforward to set up, requiring simple tools and conditioning circuit components. For these reasons, they are popular in DIY design. In contrast, strain gages require a high initial investment as the tools and the products to install these sensors are expensive. Once this initial cost is invested, the sensor itself is not expensive. Also, the availability of strain gages may be more limited.

In terms of usability and complexity, strain gages are the most difficult to use, requiring special skills and materials in their application, whereas IR and Hall effect sensors are relatively easy to connect and apply. The complexity of handling IR and Hall effect sensors comes with dealing with their data, finding optimal placement, and optimizing polarizing resistances.

3.7 Future Directions

Future developments are essential to improve sensing in The Rulers. Some of them are:

- rebuild the mechanical structure of the instrument, guaranteeing a perfect clamp;
- improve sensor placement and sensor conditioning circuits for IR and Hall effect sensors, aiming for a monotonic measurement range;
- calibrate the sensors using a reference system with a continuous dynamic measurement range;
- incorporate other sensitivities to the mapping, such as force.

3.8 Conclusions

The evaluation above presented the features, advantages, and drawbacks of each sensor technology. It is important to remember that IR and Hall effect sensors' circuitry and placement could have been improved. However, intentionally, this task was not executed, in order to compare versions as used in performance with a new version based on strain gages.

Several improvements regarding the conditioning circuit and sensor placement could be done to improve the metrological properties of IR and Hall effect sensors. These changes were not done at this point in order to show, in the next chapter, the enhancements that can arise from using more careful engineering design including customized mechanical sensor fixture and conditioning circuit. The evaluations presented in this chapter used the instrumentation design already prepared for IR and Hall effect sensors, highlighting some limitations of a less careful approach. Therefore, in this context, the performance of IR and Hall effect sensing, compared to SG, might seem biased. Finally, it is expected that some drawbacks of IR and Hall effect sensors—such as non-linearity, non-monotonicity and hysteresis (Hall effect sensor only)—might persist in enhanced versions of their instrumentation design.

Strain gages proved to be a good alternative for The Rulers, due to their linear response. However, the complexity of their application and conditioning circuits might deter their use.

While the hysteresis of the Hall effect sensors could make their use prohibitive, this drawback could be used for identifying movement directions, which consequently could be used to solve ambiguity in the infrared sensor response. As for the analysis of Figure 3.13, excluding the ambiguity measurement ranges of IR and Hall effect sensors, they present complementary measurement ranges. This complementarity could be further explored with sensor fusion techniques.

Finally, taking into account all evaluations discussed throughout the chapter, it is hard

to identify a unique optimal sensor technology for the application. Even if strain gages appear to be an optimal sensing solution, their sensitivity to force might be further explored. Also, using strain gages as the sole sensing method might be risky, as their installation is delicate and fragile. Considering the performance context where the performer might not be aware of this drawback, we believe that at least another backup sensing method should be used in case of SG circuit failure. A working hypothesis suggests that, for a certain sensor placement, IR and Hall effect sensors might have complementary behaviours when it comes to sensitivity. Having said that, the natural direction towards combining positive features of several data sources is the use of sensor/data fusion.

Chapter 4

Multiple-model Linear Kalman Filter Framework for Unpredictable Signals

This chapter presents sensor fusion techniques for systems where the process model is a function of the human input and, therefore, unpredictable. The system consists of free and user-driven motion regimes. The free regime can be modeled as a damped sinusoidal waveform, while the driven regime and the transitions between regimes do not respect any sort of probability, pattern or sequence. The quantity of interest is the deflection of a clamped beam, measured using three sensor technologies: strain gages, infrared and Hall effect sensors. Experiments using infrared-based motion capture as a reference measuring system show that: 1) none of the sensors present optimal performance for both motion regimes; 2) measurement errors of each sensor differ significantly according to the motion regime. Our solution is based on a multiple-model linear Kalman filter in combination with motion segmentation. The motion segmentation discriminates gestures according to the knowledge of their process model. This allows a more predictive estimation during periods of free motion, while relying on a less predictive approach for unknown user-driven signals.

Additionally, we propose a framework for evaluation and selection of process models for unpredictable signals. The implementation was compared to single-sensor and single-model filter designs.

4.1 Introduction

The popularity of input devices for computer control has raised attention to gestures and sensors [1]. Typically, consumer electronics manufacturers introduce their own vocabulary of gestures to control their devices. These gestures are tracked by a number of sensors embedded in the devices. A predefined set of gestures, forming a vocabulary, facilitates the mapping between gestures and control, on account of expected patterns of sensor data. In these cases, sensor data should be accurate enough to allow for the gesture to be classified correctly within the predefined vocabulary. However, some devices do not have a predefined vocabulary of gestures, allowing freedom for the user to define his own gesture vocabulary, as is the case of Digital Musical Instruments.

Musicians are known to have refined motor control – they perform highly-developed body gestures while playing instruments – and proficient auditory perception. These qualities make them aware of the output of each gesture, allowing them to identify any incoherence in the mapping between gesture and sound produced. Also, on many occasions, musicians perform similar gestures with different qualities, extending their technique to something unique. In order to satisfy skilled users, the instrumentation design – sensor and signal conditioning – must meet several requirements. First, in order to empower musicians to control the instrument in an expressive way, a DMI must not restrict the user interaction to an enclosed vocabulary. Additionally, the instrumentation design should be accurate, reproducible, monotonic, with fast response in real-time and preferably embedded in the

device.

As shown in Chapter 2, most of the DMIs are based on one sensor technology. For these, operation is vulnerable to the limitations of the sensor technology used. Additionally, nowadays many DMIs are developed in a DIY manner, prioritizing ordinary sensors, that is, easily available sensors that require simple assembly and signal conditioning circuits. We believe that more robust designs can attain stability and full potential of sensing, as well as encourage greater dissemination and commercialization of DMIs.

In this work, we discuss instrumentation for a DMI based on three sensor technologies: strain gages, infrared and Hall effect (HL) sensors. Results demonstrate that each sensor has advantages and drawbacks. As seen in Chapter 3, it is not possible to determine an optimal single sensor solution that is advantageous in all common operations. It follows that the most favorable solution would be a combination of features of several sensors. This suggests the use of sensor fusion in order to design robust sensing for a DMI.

We then propose a linear Kalman filter in order to accomplish the fusion task. This filter is proven to be effective when the process and measurement models of the system are known [154]. For instance, there are numerous examples of Kalman filter application in navigation where the state variables are position, velocity and acceleration [52, 155, 124]. In the present case, user interaction with the DMI is unpredictable, and therefore the process model of the system is not entirely known. Model uncertainties deteriorate the optimality of the estimation or can even cause divergence [156]. The unpredictable nature of the DMI signals makes the implementation of a linear Kalman filter intricate due to the partial knowledge of the system model. The next section reviews other possible filter topologies used in similar problems.

4.2 Bayesian filter solution for unpredictable signals

The selection of a filter technique within the Bayesian realm is not only a technical decision but also a design choice. Some might say that a linear-Gaussian assumption is usually sufficient. Others may argue that nonlinear techniques can better account for nonlinearity and dynamic alternating behaviours. Some are interested in enumerating the exact error in their estimation, whereas others might disregard the approximation on the error determination. Some might prefer a less rigorous determination of process model and model error covariance, whereas others can assure the accuracy of the filter parameters.

Possible Bayesian methods include the following:

- **linear Kalman filter:** an optimal solution for linear-Gaussian signals and models;
- **Adaptive Kalman filter:** usually meant for tracking and not used for error covariance reduction;
- **Extended and Unscented Kalman filters:** suboptimal solution for Gaussian linearized signals and models. Suitable for weakly nonlinear and unimodal cases;
- **Interacting Multiple-Model:** distinct system behaviours are described by different models, usually selected according to their likelihood or sequence;
- **Particle filter:** a Monte Carlo sampling simulation using raw data points (particles). The particles' weights represent their quality as an estimated value.

The idea behind the adaptive Kalman filter is to modify the error covariance of the measurements, system or estimate according to some cues [157, 158, 159, 160]. This filter reduces the level of trust in uncertain process models. Consequently, in order to guarantee

coherent tracking, the level of trust in noisy sensor data is increased. This filter is usually meant for tracking and not for reducing noise in sensor data [160].

An Extended Kalman filter is a KF implementation using linearized models and measurements. The EKF is a common solution for problems where accurate knowledge of the process model is not available [161]. The disadvantage of the EKF in relation to its linear counterpart is the higher computation cost, which makes it non-viable for embedded real-time applications. Some works implement the EKF by setting the unknown parameters as state variables to be estimated, and therefore, estimating both states and process parameters [47, 162, 163]. For these cases, several factors contribute to the limitation of the EKF filter, most of them closely related to the linearization process [164, 165, 166, 167]. However, most of the DMIs offer low processing power, which prohibits all linearization-based and machine learning based solutions.

Other solutions implement multiple-model filter design in order to better describe distinct system behaviours. One previous work deals with sensor fusion for DMIs using Interacting Multiple Model Kalman filters where the likelihood of each of the models is tuned by weights producing a single output [168, 169]. Interesting implementations arise from the combination of multiple-model filters and computational intelligence tools. Some examples of these techniques are pattern recognition, machine learning, sequential rules, transition probabilities and statistical models or tools [170, 171, 172, 173, 174, 175, 176]. The combination of a multiple-model filter and these computational intelligence techniques is not suitable for our problem, as the transitions respect no probability, pattern or sequence. For the particular case of The Rulers, no statistical rule for multiple-model transitions is applicable as it is not possible to define duration, grip type or magnitude of gestures that will be performed by the musician.

Yet another alternative is the use of particle filters. Previous work used particle filters

for baton tracking [177]. In this study, rehearsal data is incorporated as a probabilistic model and the system relies on the fact that "conductors follow a set of rules (...)" [177]. That is, it includes a training stage where "adapted templates specific to the conductor and the piece of music are created" [177]. However, DMI performances are usually exploratory, implying little or no pre-established gesture repertoires.

Since its introduction in 1993, particle filtering has been used for estimation problems solved recursively and numerically [178]. One advantage of particle filtering over the popular Extended Kalman filter is that it does not rely on local linearizations [178]. The filter also offers a less stringent requirement for accurately describing process models, at the expense of computational cost [178]. The computational cost depends upon the number of particles. Therefore, the filter designer can specify a suitable number of particles in order to make his/her application suitable for real-time application. However, there exists a trade-off between optimal and reduced number of particles. Particle filtering methods are a set of powerful simulation-based techniques for estimation of nonlinear non-Gaussian problems [178]. The most common application is tracking, that is, the determination of the distribution of the state model at the current time, given available observations at the current time [178]. Several frameworks for particle filtering implementation have been presented, most of them a combination of two operations: sampling and resampling.

Sampling is the introduction of a set of particles to represent the posterior density, where a weight is set for each particle [179]. The weight is the evaluation of the particle quality with respect to the observations, followed by weight normalization [180]. Standard and Sequential Important Sampling suffer from a severe drawback: the variance of the estimates increases exponentially with the number of samples [178]. In order to partially solve this issue, resampling is introduced, which consists in removing the particles with low weight and multiplying particles with high weight [178]. An important factor that often

determines whether a particle filter algorithm works in practice is the presence of degeneracy. Degeneracy is the effect of having all but one – or a few – particles with negligible weight [180]. However, a good distribution of particle weights does not necessarily lead to good filter performance [178]. Several frameworks were presented to deal with degeneracy, such as resample-move [178], block sampling [181], and Rao-Blackwellised [178]. Another issue that can arise is the loss of diversity, that is, as the particles with high weights are statistically selected many times through resampling, the resultant sample will contain many repeated points [180].

Particle filter implementation requires the definition of the following parameters: the criteria for sampling, the importance distribution [182], and the number of successive resampling steps. Some evaluation descriptors are the effective sample size and the skewness of the distribution as measures of degeneracy [180]. To the best of our knowledge, there is no formal method for evaluating the performance of particle filters.

Probably the most common application of particle filters is tracking with single-sensor design. In order to perform fusion of multiple sensors, the global likelihood is the product of the individual likelihoods of the sensors [183]. These likelihoods are the probability of an estimate y at time t, given an observation at time t. This likelihood might not reflect the error properties of the sensors, given by calibration.

An "optimal" particle filter was presented by Doucet et al., though its application is rare in practice [184, 185]. This optimal particle filter is recommended for linear measurement models and additive Gaussian noises [184]. Opposed to the optimality of a linear Kalman filter, the practicle particle filter is an approximation technique. Therefore, its suboptimality leads to the fact that the standard deviation of the estimate is an estimate of the standard deviation, that is, it is not the measure of the standard deviation of the estimator [178].

4.2.1 Choice of a Bayesian method for estimation

As discussed in Chapter 3, we consider it essential to calibrate and evaluate sensing solutions. Therefore, systematic and random errors from each sensing technology in a given application are described by calibration using a reference measuring system. Given this premise, measurement functions and errors are well described. The accurate definition of these parameters is part of the requirements of a successful Kalman filter implementation. However, a Kalman filter implementation also requires accurate knowledge of the process model and the error in its determination. A particle filter becomes an alternative, as it presents a less stringent requirement to determine these parameters.

For both Kalman and particle filters, the definition of the model is complex, due to the unpredictability in human input signal. Selection of candidate models can benefit from filter evaluation. In an evaluation scheme, the resulting error covariance of the estimate for different candidate models could be compared to define the most suitable model for a system or gesture. This indicates the first advantage of a linear Kalman filter over the other suboptimal filter topologies: the linear Kalman filter is able to output a resulting error covariance of the estimate that reflects the real error, instead of providing an approximate error covariance of the estimate. Consequently, the error covariance given by the linear Kalman filter algorithm can be used to test how accurate the modeling of the system or gestures is.

The main interest in the linear Kalman filter is its optimality as our main goal is to improve the error covariance of the measured signals rather than predicting them. Optimality is obtained at the cost of rigorous knowledge of processes and signals. Therefore, throughout the thesis, we describe a sensor characterization method that provides robust knowledge of measurement models and errors, and we propose an evaluation method for determining the

most suitable model for unpredictable signals. Another advantage is the low computational cost and power requirements, as compared with the suboptimal filter solutions. Due to all these reasons, we have chosen the linear Kalman filter.

4.2.2 Implementation versus Framework

As discussed above, the determination of process models for a linear Kalman filter implementation is essential for its efficiency and convergence, and it is not straightforward for human input signals. As this thesis focuses on human input signals of DMIs, a remark must be made about considering these signals unpredictable. By experience, we know that few DMIs reach a stable design yielding extensive hours of practice and enclosed vocabulary of gestures. Instead, most of them engage through exploratory interaction, that is, composers and players experience the instrument and create new ways of playing it. The goal of this thesis is to improve sensing design in DMIs without restricting the player-instrument interaction by using pre-established gesture repertoires, restriction, or rules. Furthermore, sensing design must be suitable for DMI exploration, improvisation, and creation of original ways to play on-the-fly. Consequently, we aim to propose a solution for other problems whose signals and their possible models are hard to describe.

This indicates the need to define an evaluation method to select process models for the distinguishable behaviours. The use of multiple models requires the selection of a model for each sample. Due to the reasons discussed previously, we do not want to set rules or patterns for transitions between models, as occurs in interacting multiple-model Kalman filters [171]. Therefore, a method to determine the transitions between models should be created. Also, distinguishable gestures might yield different behaviours of sensor responses, and this should be evaluated and quantified. All these requirements and tasks cannot fit a linear Kalman filter implementation. Gesture segmentation, gesture classification, selection

of candidate models, filter evaluation, and sensor evaluation should be accounted for in a framework for linear Kalman filter implementation, which will be presented in this chapter.

An important remark is that we are focusing on improving the error covariance of the estimate, rather than on tracking. For this reason, using multiple sensors can provide not only error covariance reduction but redundancy in case of failure. For this, we examine three sensor technologies, two of them popular solutions in DMI design – IR and Hall effect sensors – and the other a specialized sensor technology – strain gages – rarely used in DMIs [1, 20]. In Chapter 3, we presented several advantages of the strain gages in relation to their counterparts. One of the disadvantages of strain gages, however, is the low mechanical robustness, which might not be suitable for the exploratory and expressive interaction duty of a DMI. The concomitant use of strain gages with two other sensing solutions not only potentially improves error covariance but also provides redundancy in case of fault. An experience of 12 years working with strain gages allows me to say that the most common fault is the delicate wiring and soldering. However, this drawback brings its own solution. These faults cause open circuits, resulting in easily identifiable voltage outputs. Therefore, the faults once detected could be solved by a multi-sensor system and a fusion filter.

4.3 Device and Instrumentation Description

In this chapter, we use David Birnbaum's The Rulers as a testbed for evaluating and validating a method for sensor fusion when the signals are unpredictable. The instrument—shown in Figure 4.1—evokes deflection gestures [136]. In this thesis, deflection refers to the distance between the vertical position at rest and the deflected vertical position at the free edge of the beam (see Figure 4.3).

The main categories of gestures used to play The Rulers are "bending" and "plucking".

Fig. 4.1 Archival photo (IDMIL Laboratory Library) of The Rulers: a Digital Musical Instrument, a set of seven cantilever beams designed to evoke deflection gestures. Photo and design by David Birnbaum.

Bending is described as a driven motion where the user grips the free edge of the beam, bending it up or down or stopping a motion (see Figure 4.2). When the grip is released and the beam is not at the equilibrium position, the beam deflects around its equilibrium position with respect to a damping ratio. This free oscillation is called "plucking" (see Figure 4.4). We must note that in order to have plucking motions, an initial driven deflection in relation to the equilibrium position must be carried out, which means that any plucking motion is initiated by a bending motion. In other words, bending happens whenever the user is controlling the beam deflection, and plucking happens whenever the user is not interacting with the beam.

Fig. 4.2 Performer executing **bending**: driven motion. Photo by Guillaume Pelletier. Reproduced with permission.

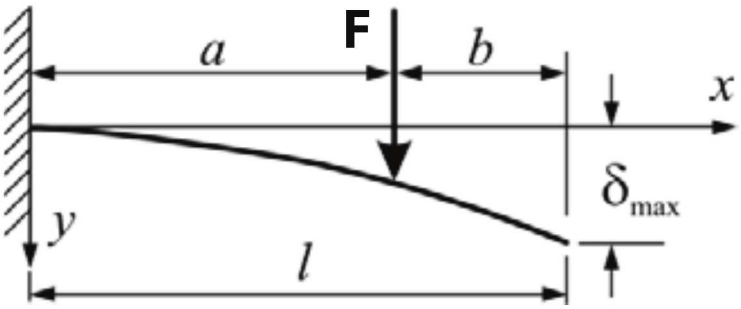

Fig. 4.3 A concentrated force **F** is applied at a given point. The distance between the load and the clamped edge is a and the distance between the load and the free edge is b. The deflection at the free edge δ_{max} depends on the beam material, beam geometry, force magnitude **F**, distance between load and clamped edge a and length of the beam l.

Bending gestures can be approximated as a deflection resulting from a concentrated load at the free edge. The deflection depends on the mechanical properties of the material, the beam geometry, the force magnitude and the distance between the clamp and the force application point. Figure 4.3 shows a diagram of a clamped beam being bent.

Given a concentrated force **F**, the deflection δ at a distance x from the clamp where $(a < x \leq l)$ is given by a reformulation of Equation 2.1:

$$\delta = \frac{\mathbf{F}\, a^2}{6\, E\, I}\,(3\, x - a) \tag{4.1}$$

where E is the Modulus of Elasticity, intrinsic to the material, and I is the area moment of inertia, defined by the beam geometry. Note that the force $\mathbf{F}$ and the distance a are not definable once they are determined by user input.

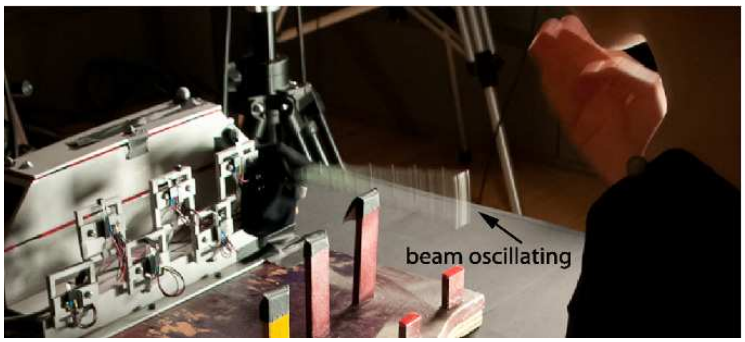

Fig. 4.4 Performer executing **plucking:** free beam oscillation originated by an initial driven deflection. Photo by Guillaume Pelletier. Reproduced with permission.

Plucking gestures can be approximated as an underdamped oscillation, and therefore, satisfy the second-order differential damped wave equation. The oscillation depends on the angular frequency, the damping ratio and on the deflection magnitude at the beam release.

4.3.1 Limitations of previous instrumentation strategies

The previous chapter evaluated and compared three sensor technologies to measure the deflection for The Rulers. Improvements of the mechanical design and sensor placement of the instrument were performed according to the mentioned recommendations. Concerning the mechanical design, a single beam, perfectly clamped, was built as a platform for testing sensors and as a prototype version for the DMI (Figure 4.6). Also, other components for infrared and Hall effect sensing were used, in order to suit the operation ranges of the new mechanical structure.

Infrared and Hall effect sensors are popular solutions for measuring proximity. Strain gages are the state-of-the-art solution to measure strain, deriving quantities such as stress,

pressure, deflection and flow. Operating and measurement ranges for the application were considered to specify the most suitable IR, Hall effect and strain gages sensors for the given application. This characterizes an improvement in relation to the previous chapter, where IR and Hall effect sensors from previous versions of the DMI were used.

The TCRT5000 infrared sensor has a phototransistor detector with peak operating distance at 2.5 mm and a daylight blocking filter. Its collector current varies with the distance to a reflecting surface [186]. The Hall effect sensor AD22151 has temperature compensation, adjustable gain and was set to bipolar operation. Magnets were attached to the beam, so that the Hall effect sensor could sense the proximity of the beam. Even if the manufacturer claims the sensor as a "Linear Output Magnetic Field Sensor", it is crucial to note that being linear to magnetic fields does not imply linearity to magnetic field variability that results from the beam deflection [187, 142]. The strain gages are connected in a full Wheatstone bridge: two submitted to compression and two submitted to tension, installed on the bottom and top of the beam. Considering that there is temperature gradient between top and bottom of the beam, temperature compensation is performed by the full bridge configuration.

It is important to note that none of the sensors are directly sensitive to distance, but rather to infrared light, magnetic field (Hall effect) and strain. Therefore, they indirectly measure the quantity of interest: deflection. As a consequence, these sensors might be vulnerable to environmental factors [4, 3], such as external magnetic fields, temperature, other stress sources, and stage lighting with considerable infrared spectrum.

We are interested in the deflection at the free edge, where the user input is most perceptible. Figure 4.5 presents the deflection at the free edge versus the sensor output for bending motions. Subsequently, some practical considerations for the sensors are presented, followed by a summary of their characteristics.

Infrared and Hall sensors measure the beam-sensor distance next to the clamped edge. The ratio r_s^{fe} between the deflection measured by the sensor and the deflection at the free edge was investigated. Tests using a Qualisys© 16-camera passive near-infrared motion capture system for measuring deflection reported that the ratio r_s^{fe} is constant along the full deflection range. In addition, for infrared and Hall effect sensors, the distance between sensors and beam varies with respect to an angle. This can be an issue especially dealing with infrared sensors whose operation is based on surface reflection. The solution for this potential artifact was to make sure that the surface area of the beam and magnet are larger than the focus area of the sensors.

Furthermore, infrared and Hall effect sensors might present measurement ranges that are not monotonic. Non-monotonic ranges require intense processing to map input to output and this is prohibitive in embedded real-time systems. In order to avoid these non-monotonic regions, a careful placement of these sensors is required. For instance, for a given sensor placement, the infrared transfer function in Figure 4.5 illustrates the sensor operating in a non-monotonic range (*Region 1*). An effort to place the Hall effect sensor in a manner that guarantees monotonicity led it to saturation as shown in *Region 2* in Figure 4.5. Another example of how problematic it is to tweak the placement of Hall effect and infrared sensors is shown in *Region 3* (Figure 4.5). This region is monotonic and is not under saturation, however the knee-shape region requires high order polynomial data regression functions to model its behaviour, therefore, increasing complexity and processing time. In short, extremely careful placement for infrared and Hall effect sensors should take place in order to avoid issues such as non-monotonicity, saturation and high order polynomial regression.

As shown in Figure 4.5, infrared and Hall effect responses are not linear in relation to the input quantity, deflection. Therefore, their sensitivity is not constant along the measurement range. In contrast, strain gages present a linear relationship between output,

voltage, and input deflection.

Strain gages measure the strain related to the stress at the measurement point. This stress derives from a force applied by the user or from the clamp reaction force. Therefore, strain gages present distinct responses between driven and free motions. The difference varies according to the properties of the clamp. For instance, adding a cushion layer in the clamp reduces the reaction forces, increasing the damping factor. The distinguishable response is a concern that needs to be further analyzed. Finally, this multi-modal response may be labeled as an advantage or as a drawback of using strain gages, depending on the application and signal processing applied. Fitting options will be discussed in the following section. Other important properties of IR, Hall effect, and strain gage sensors are presented in Table 3.1.

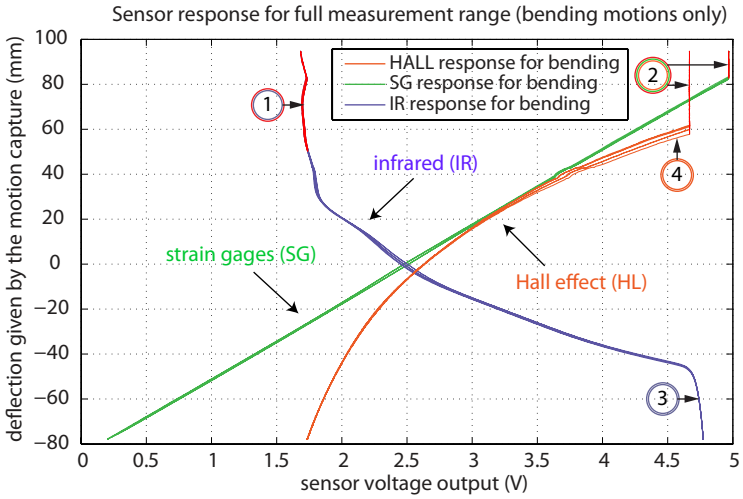

Fig. 4.5 Sensor response for bending motions (over multiple runs). Sensor placement is extremely important to avoid saturation, non-monotonic ranges and high order polynomial regression. **Region 1** indicates non-monotonic range; **Region 2** indicates saturation; **Region 3** requires high order polynomial regression; **Region 4** points to hysteresis in the Hall sensor response.

In the previous chapter, we have shown that none of the sensors were optimal under all motions. For this new experiment, better sensors and conditioning circuits were used in

order to make a fair comparison between sensor technologies. This way, the improvements brought by better conditioning circuits and enhanced sensor placement are highlighted. Additionally, for this new experiment, we use a dynamic reference measuring system. The sensor responses of this experiment are reported in the following section.

4.4 Sensor Signal Processing

In order to design an improved instrumentation strategy, we evaluated each sensor according to the gesture performed: bending or plucking. The evaluation is based on deflection given by the sensors and on the deflection given by a reference measuring system. Sensor data and the reference system are synchronized to each other. The deflection reference measuring system is a 16-camera passive infrared motion capture system operating at 448 Hz. The system has a resolution of 0.01 mm with a standard deviation given by calibration of 0.31 mm. The tracking system acquired the 3D position of reflective markers placed along the beam, with an analog acquisition system registering the sensor outputs at 6720 Hz, 16 bits/sample. The sensors are installed next to the clamp: on, below and above the beam, as shown in Figure 4.6, indirectly measuring the deflection at the free edge of the beam.

As discussed in the previous section, sensor placement is an issue for infrared and Hall sensors. In order to solve that, we designed an apparatus to optimize the placement of infrared and Hall effect sensors, limiting their measurement range to a monotonic range, free of saturation. The apparatus was built using parts manufactured by a 3D printer and LEGO© bricks as partially shown in Figure 4.6. The measurement range for the strain gages was scaled to be similar to the other sensors. The curves in Figure 4.7 reflect the results achieved using the apparatus for sensor placement. Appendix A discusses our view of the use of LEGO© on sensing design.

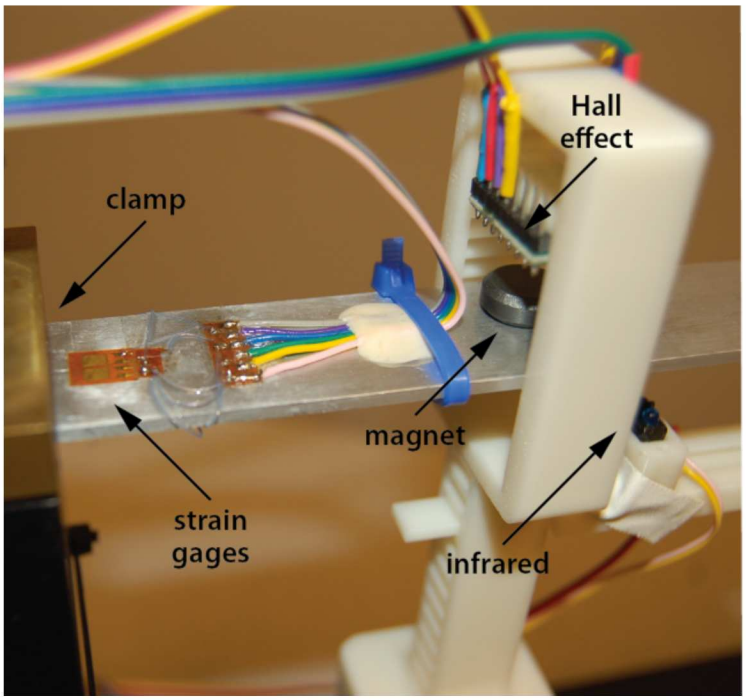

Fig. 4.6 Apparatus for sensor placement allows 2D positioning for infrared and Hall effect sensors: discrete positioning for vertical position and continuous positioning for horizontal position. Photo by Vanessa Yaremchuk. Reproduced with permission.

4.4.1 Measurement Functions and Measurement Errors

The measurement functions are those describing the measured output quantity value as a function of the known input quantity value [3, 4]. In order to obtain them, polynomial regression is applied to the following datasets of data. The first n-length dataset, $\mathbf{X}_1$, contains samples with deflection driven by the user. The samples are equally distributed in positive and negative deflections. The second n-length dataset, $\mathbf{X}_2$, contains samples with free deflection. This dataset excluded samples with SNR lower than 2, since lower SNR signals in the end of the oscillation tend to bring the bias to zero-mean, even if this is not accurate along most of the measurement range. The third n-length dataset, $\mathbf{X}_3$, contains both motions: $n/2$ samples of $\mathbf{X}_1$ and $n/2$ samples of $\mathbf{X}_2$.

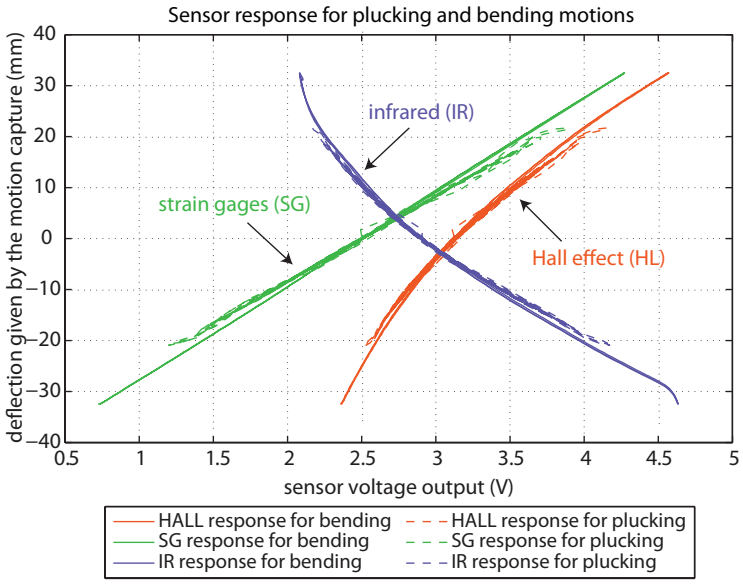

Fig. 4.7 Sensor response for bending and plucking motions: deflection given by the reference measuring system, in mm, versus the sensor output, in Volts. The use of the apparatus limits the measurement range to a monotonic range, free of saturation.

There are two approaches for linear regression. The first approach uses Different Slopes and Intercepts (DSI) regression for each motion. Therefore, for each motion and its respective dataset $\mathbf{X}_1$ and $\mathbf{X}_2$, there will be response variables $\mathbf{Y}_1$ and $\mathbf{Y}_2$, respectively. The linear regression equations for this approach have the form:

$$\mathbf{Y}_1 = \mathbf{X}_1 \beta_1 + \alpha_1 + \epsilon_1 \tag{4.2}$$

$$\mathbf{Y}_2 = \mathbf{X}_2 \beta_2 + \alpha_2 + \epsilon_2 \tag{4.3}$$

where $\mathbf{Y}_1$ and $\mathbf{Y}_2$ are the response variables for bending and plucking respectively, $\mathbf{X}_1$ and $\mathbf{X}_2$ are the datasets for bending and plucking respectively, β_1 and β_2 are the slopes, α_1 and α_2 are the intercepts and ϵ_1 and ϵ_2 are the error terms.

The second approach finds a Common Slope and Intercept (CSI) for all motions, using

the dataset $\mathbf{X}_3$. The equation for this approach is presented in the form:

$$\mathbf{Y}_3 = \mathbf{X}_3\,\beta_3 + \alpha_3 + \epsilon_3 \tag{4.4}$$

where $\mathbf{Y}_3$ is the response variable for all motions, $\mathbf{X}_3$ is the dataset containing bending and plucking samples, β_3 is the common slope, α_3 is the common intercept and ϵ_3 is the error term.

The regression techniques result in measurement functions $\mathbf{Y}_i \approx f(\mathbf{X}_i)$. Once slopes, intercepts and errors are determined by Least Square Estimation, the measurement functions provide the deflection in millimeters ($\mathbf{Y}_i$), given the sensor output in Volts ($\mathbf{X}_i$).

The measurement errors are defined by the measured quantity value ($\mathbf{Y}_i$) minus the reference quantity value. The reference is a motion capture system providing deflection measurements. The measurement errors consist of random and systematic errors. They are described by their error probability density function type, skewness and modality. The probability density function was assumed and fit to a Gaussian in order to use the measurement errors on a linear Kalman filter implementation later. The measurement errors for the following combinations of datasets and regression were analyzed (Figure 4.8):

- bending samples $\mathbf{X}_1$, DSI regression $(\beta_1, \alpha_1, \epsilon_1) \Longrightarrow$ measurement error b;
- plucking samples $\mathbf{X}_2$, DSI regression $(\beta_2, \alpha_2, \epsilon_2) \Longrightarrow$ measurement error p;
- bending samples $\mathbf{X}_1$, CSI regression $(\beta_3, \alpha_3, \epsilon_3) \Longrightarrow$ measurement error B;
- plucking samples $\mathbf{X}_2$, CSI regression $(\beta_3, \alpha_3, \epsilon_3) \Longrightarrow$ measurement error P.

The Gaussian measurement errors are presented in Figure 4.9. As expected, DSI regression outputs smaller measurement errors than the CSI regression. The improvement factors for the random errors range from 1.3 to 4, when using the DSI regression. Error reduction leads us to justify the use of DSI regression, and consequently, multiple measurement

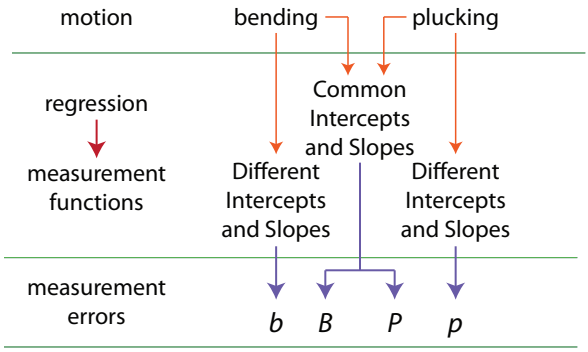

Fig. 4.8 Sensor evaluation method. *b, B, p, P* are the suffix letters to be assigned to the sensor name. Letter *b/B* represents bending samples; letter *p/P* represents plucking samples. Lower case letters represent Different Slopes and Intercepts regression results, whereas upper case letters represent Common Slopes and Intercepts regression results.

functions and error for each gesture, per sensor. The improvement factor on the error standard deviation is bigger for the strain gages: approximately 1.6 times greater than the difference reported for Hall effect and infrared sensors.

Additional conclusions regarding the measurement errors are summarized as follows:

- for plucking motions, the infrared sensor has the lowest random error, followed by the strain gages and then by the Hall sensor;
- for bending motions, the strain gage has the lowest random and systematic errors. The second lowest random error is from the Hall effect sensor followed by the infrared sensor;
- systematic errors of Hall effect and infrared sensors are correlated to the distribution of samples in the positive and negative deflection (confounding variables). As the dispersal of positive and negative deflection samples is impossible to estimate, these systematic errors are impossible to correct.

Furthermore, it is noticeable that all sensors differ according to the motion being performed, with respect to their error. This scenario can benefit from sensor fusion, where

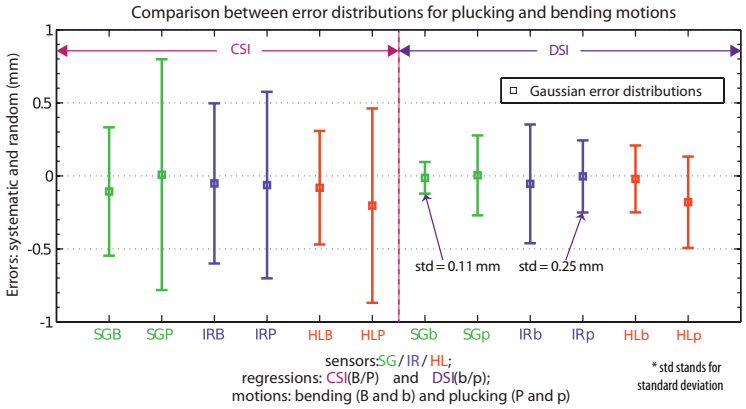

Fig. 4.9 Error distributions for CSI (left) and DSI (right) measurement functions, for plucking samples (P,p) and for bending samples (B,b). b and p denote errors for bending and plucking samples respectively, using DSI measurement functions. B and P denote errors for bending and plucking samples respectively, using CSI measurement functions. The term *std* stands for standard deviation, *CSI* stands for Common Slopes and Intercepts and *DSI* stands for Different Slopes and Intercepts. DSI measurement functions result in lower systematic and random errors.

the weights for each sensor technology are given according to their error covariance. Under a DSI regression, strain gages presented the lowest error covariance for bending motions, while infrared sensors slightly outperform strain gages, presenting the lowest error covariance for plucking motions.

4.5 Problem Statement

As previously discussed, the present case is suitable for a sensor fusion design. The embedded real-time employment of a DMI requires low processing cost for a sensor fusion design. Therefore, reasonable solution is the implementation of a linear Kalman filter. However, in Kalman filter designs, the knowledge of measurement and process parameters is essential. Poor description of these parameters might lead to inaccurate estimates or even divergence problems [188]. The user-driven bending motions are not predictable, and therefore, rule out

the use of physical modeling. Aside from that, these motions do not respect any probability, pattern or sequence. For these cases, the range of solutions for estimating states is reduced, particularly in real-time applications where processing time is an issue.

A solution for the problem should account for the definition of a process model for unknown signals and for the evaluation of the selected process, given the dangers of inaccuracy and divergence.

4.6 Proposed Solution

Not only the sensors but the system presents distinguishable physical behaviour under driven (bending) and free (plucking) motions. The driven motions are unpredictable whereas the free motion is a dampened sinusoidal waveform. We propose a framework that takes advantage of the discernible physical behaviour of the sensors and the system. Therefore, for any problem where the signals are partially unpredictable, we suggest the following:

1. **motion segmentation**: identification of all known and unknown motions. Known motions are the ones eligible for physical modeling;
2. **motion classification**: clustering of known and unknown motion process models according to the segmentation;
3. **regression**: determination of different slopes and intercepts for each distinct motion;
4. **multiple-model process model**:
    - physical modeling for known motions;
    - descriptor analyses for selecting process model for unpredictable signals;
5. **evaluation**.

To sum up, we propose the combination of motion segmentation and classification, DSI regression and multiple-model filter design. Ultimately, we predict the system behaviour using an appropriate process model during periods of free motion, while counting on a less predictive approach during the unknown user-driven regime. Additionally, we propose a method to determine and evaluate the process model for unpredictable signals based on descriptors. The evaluation of the process using various datasets is essential to guarantee the robustness of the filter implementation, given the process model uncertainty.

4.7 Filter Design

This section focuses on the design of a linear Kalman filter. A filter evaluation method is introduced based on qualitative and quantitative descriptors. Lastly, the descriptors values are used to determine the most advantageous process model for each motion.

4.7.1 Kalman Filter Design Basics

Kalman filters are based on the implementation of predictor-corrector estimators. The filter estimates the state $\mathbf{x}_k \in \mathfrak{R}^n$ given a controlled process governed by the linear stochastic difference equation [47],

$$\mathbf{x}_k = \mathbf{\Phi}_k \, \mathbf{x}_{k-1} + \mathbf{G} \, \boldsymbol{u}_k + \boldsymbol{\chi}_k, \tag{4.5}$$

where $\mathbf{x}_k$ is an n sized vector representing the state and its state variables; $\mathbf{u}_k$ is an l sized vector representing the inputs to the system. The $n \times n$ matrix $\mathbf{\Phi}_k$ represents the state-propagation matrix, when no driving function or process noise is considered. The $n \times l$ matrix $\mathbf{G}$ represents the optional control input $\mathbf{u}_k \in \mathfrak{R}^l$. The system state propagation is subjected to noise $\boldsymbol{\chi}_k$.

The system is observed by a set of measurement variables forming a measurement vector $\mathbf{z}_k \in \Re^m$

$$\mathbf{z}_k = \mathbf{H}_k \, \mathbf{x}_k + \boldsymbol{\nu}_k. \tag{4.6}$$

where the $m \times n$ matrix $\mathbf{H}_k$ is the measurement matrix; $\mathbf{x}_k$ is the states vector and $\mathbf{z}_k$ is the measurement vector. The observation of the true quantity value of the state ($\mathbf{x}_k$) includes noise $\boldsymbol{\nu}_k$.

The noises $\boldsymbol{\chi}_k$ and $\boldsymbol{\nu}_k$ represent the process and measurement noise vectors respectively. The noises are assumed to be independent from each other, white, Gaussian and bias-free, given by Equations 4.7 and 4.8,

$$p(\boldsymbol{\chi}_k) \sim N(0, \mathbf{Q}_k), \tag{4.7}$$

$$p(\boldsymbol{\nu}_k) \sim N(0, \mathbf{R}_k) \tag{4.8}$$

where $\mathbf{Q}_k$ and $\mathbf{R}_k$ are respectively the process error covariance and the measurement error covariance matrices. Equation 4.7 is read as the probability density function of $\boldsymbol{\chi}_k$ is a zero-mean Gaussian distribution whose error covariance equals $\mathbf{Q}_k$. Equation 4.8 is read analogously. It is important to recall that the determination of $\mathbf{Q}_k$ and $\mathbf{R}_k$ and other measurement and process parameters should agree with the actual physical behaviour of the system and the signals. If this statement cannot be guaranteed, divergence may occur [156].

We determine the measurement error covariance matrix $\mathbf{R}_k$ according to the measurement errors described in Section 4.4.

The lack of detailed knowledge about the statistical properties of the process model

prohibits a straight-forward determination of the process error covariance matrix $\mathbf{Q}_k$. First, considering a process model with two state variables defining a 2×2 state-propagation matrix $\mathbf{\Phi}_k$. Next, one should define which state variables are subject to noise. We define a matrix $\mathbf{Q}_k^e$ that specifies the presence of noise on each of the state variables (Equation 4.9),

$$\mathbf{Q}_k^e = \mathbf{\Phi}_k \begin{bmatrix} m_{1,1} & 0 \\ 0 & m_{2,2} \end{bmatrix} \tag{4.9}$$

where $m_{1,1}$ and $m_{2,2}$ are either 1 or 0, defining if each of the state variables is noisy. As an example, for the given $\mathbf{\Phi}_k$, considering that only the higher order state variable is noisy, $m_{1,1}$ would be 0 and $m_{2,2}$ would be 1.

The process error covariance matrix $\mathbf{Q}_k$ is given by Equation 4.10,

$$\mathbf{Q}_k = C_k^{mc} \int_0^{t_s} \mathbf{\Phi}_k(t)\ \mathbf{Q}_k^e\ \mathbf{\Phi}_k^T(t)\ dt \tag{4.10}$$

where C_k^{mc} is the tuning constant given by a Monte Carlo optimizer, t_s is the sampling time. The Kalman filter algorithm operates under a trade-off between process model trust and measurement trust. Given that the measurement trust is fixed and defined by the measurement errors, the process error covariance matrix expresses the trade-off between a more effective filter and a wider bandwidth filter that is able to outline disagreements of the model with the system behaviour.

4.7.2 Kalman Filter Algorithm

A standard Kalman filter algorithm comprises prediction and correction or update. The predicted variables are called *a priori* and are denoted by a minus sign ($^-$) superscript to the variable. The corrected or updated variables are called *a posteriori*. Predicted and

corrected/updated estimated variables are represented by the symbol (ˆ) superscript to the variable. The subscript indexes k and *k-1* define the current and previous steps respectively.

$$\hat{\mathbf{x}}_k^- = \mathbf{\Phi}_k \, \hat{\mathbf{x}}_{k-1}^- + \mathbf{G} \, \mathbf{u}_{k-1} \tag{4.11}$$

$$\mathbf{P_k}^- = \mathbf{\Phi}_k \, \mathbf{P}_{k-1} \, \mathbf{\Phi}_k^T + \mathbf{Q}_{k-1} \tag{4.12}$$

$$\mathbf{K}_k = \mathbf{P}_k^- \, \mathbf{H}_k^T \, (\mathbf{H}_k \, \mathbf{P}_k^- \, \mathbf{H}_k^T + \mathbf{R}_k)^{-1} \tag{4.13}$$

$$\mathbf{P}_k = (\mathbf{I} - \mathbf{K}_k \, \mathbf{H}_k) \, \mathbf{P}_k^- \, (\mathbf{I} - \mathbf{K}_k \, \mathbf{H}_k)^T + \mathbf{K}_k \, \mathbf{R}_k \, \mathbf{K}_k^T \tag{4.14}$$

$$\mathbf{P}_k = (\mathbf{I} - \mathbf{K}_k \, \mathbf{H}_k) \, \mathbf{P}_k^- \tag{4.15}$$

$$\hat{\mathbf{x}}_k = \hat{\mathbf{x}}_k^- + \mathbf{K}_k \, (\mathbf{z}_k - \mathbf{H}_k \, \hat{\mathbf{x}}_k^-) \tag{4.16}$$

The implemented algorithm loop is presented from Equation 4.11 to Equation 4.16 [155]. $\hat{\mathbf{x}}_k^- \in \mathfrak{R}^n$ is the *a priori* state estimate at step k, and it is the expected value of $\mathbf{x}_k$, given the previous measurement $\mathbf{z}_{k-1}$: $\hat{\mathbf{x}}_k^- = \mathrm{E}[\mathbf{x}_k \mid \mathbf{z}_{k-1}]$ or still $\hat{\mathbf{x}}_k^- \rightarrow \mathbf{x}_{k|k-1}$. $\hat{\mathbf{x}}_k \in \mathfrak{R}^n$ is the *a posteriori* state estimate at step k, and $\hat{\mathbf{x}}_{k-1} \in \mathfrak{R}^n$ is the *a posteriori* state estimate at step $k-1$.

$\mathbf{P}_k^-$ is the *a priori* error covariance matrix on the state at step k, $\mathbf{P}_k$ the *a posteriori* error covariance matrix at step k shown in two alternative formulations discussed further in the text, and $\mathbf{P}_{k-1}$ the *a posteriori* error covariance matrix at step $k-1$. $\mathbf{K}_k$ is the Kalman gain matrix and $\mathbf{I}$ denotes an identity matrix of order n. Finally, $\mathbf{z}_k$ is the measurement vector/matrix at step k.

The Kalman gain evolves according to the confidence in the process, the confidence in the measurements, and the initial error covariance ($\mathbf{P}_0$) [189]. In steady state, the Kalman

gain matrix becomes constant and depends only on the confidence in the process and measurements, if the system and the noises are stationary [189].

The error covariance matrix ($\mathbf{P}_k$) describes the variance of the estimate. There are several ways to calculate the error covariance matrix update, including Equation 4.14 and Equation 4.15 [155]. Equation 4.15 requires the least computation power and it is recommended when the number of measurement sources is significant less than the number of states [155]. Equation 4.14, referred to as *Joseph form*, has symmetric operations only and is recommended for numerical stability [155]. There is a tradeoff between lower computational cost and higher numerical stability. The designer should choose one of the formulations according to her/his requirements.

4.7.3 Filter Evaluation

A filter design depends on accurate knowledge about the measurement sources and the process model. The measurement sources were studied thoroughly in Section 4.4. The process model remains to be determined as it is partially unknown. The selection of a process model implies the setting of the process model state-propagation matrix ($\mathbf{\Phi}_k$) and the process error covariance matrix ($\mathbf{Q_k}$) (Equation 4.10). Our method to select a process model consists of testing process model candidates and verifying the corresponding filter design efficiency. The efficiency is described by a set of qualitative and quantitative variables, here called descriptors. Ultimately, a highly efficient filter simulation, measured according to the specifications of the descriptors, is indicative of a good selection for the process model. The descriptors for the filter evaluation are defined as follows:

Null Process Error Covariance Matrix ($\mathbf{Q_k}$)

A reasonable qualitative test to declare a process model suitable for a dataset is to analyze the estimate error while setting the process noise to zero. A process model that does not represent the physical behaviour to any extent produces a significant error if submitted to this test. This test is proposed by Zarchan and Musoff [48].

Steady-state (a posteriori) Error Covariance for Deflection Estimation

In order to obtain this descriptor, the error covariance matrix (Equation 4.14) in steady state regime is selected. Then, the first element of main diagonal of this matrix is isolated. It corresponds to the error covariance for estimating the deflection: the variable of interest. Its steady-state value is represented by $(\mathbf{P})^{ss}_{1,1}$ and determines the stability of the filter. A stable filter should reduce its error covariance matrix elements with time, converging to a minimum value in regime [48]. From the error covariance element $(\mathbf{P})^{ss}_{1,1}$, one can derive the error standard deviation of the deflection estimate. We call it algorithm standard deviation (e_A). This descriptor is well-cited by several authors as a standard or unique method to test filter efficiency and stability [190, 191, 129, 192]. This descriptor is sometimes called covariance performance analysis.

Confidence Bounds

This descriptor discusses how well the error covariance matrix describes the actual error between the estimate and true value given by the reference. The filter algorithm describes its accuracy through the estimate error covariance matrix $\mathbf{P}_k$. However, the filter processing can report satisfactory $\mathbf{P}_k$ even if the estimate is diverging from the true value [48]. To account for this, we define two error standard deviations. The first one is the algorithm

standard deviation (e_A) derived from the error covariance matrix of the estimate. The second one comes from the error between the estimate and the true value given by the reference measuring system. We call it experimental standard deviation (e_E). Then, for each sample, we verify if the experimental standard deviation is within the bounds of the algorithm standard deviation. Finally, we compute the percentage of samples where $e_E \leq e_A$. If this percentage is 68% or higher, the error covariance matrix accurately describes the estimate errors [48]. This descriptor is analogous to several other tests available in the literature. For instance, some authors compare the algorithm standard deviation for correct and incorrect implementation of process and models [190, 129, 192]. Other authors perform a visual comparison between the algorithm and the experimental standard deviations. This test is often referred to as a consistency check [154, 188]. Finally, some authors use the threshold of 68%, as is the case in this work [48].

Bandwidth

We have created a novel descriptor, bandwidth, which sets the maximum trust in the sensor data, given by the sum of the main diagonal elements of the Kalman gain matrix. If the process model is selected properly, the filter can rely on it, reducing the bandwidth for noisy sensor data. High levels of sensor trust, indicated by high Kalman gains, reflect weak confidence in the process model. In this case, the process model is not a good guess as to the physical behaviour of the system. In order to consider a process model a good candidate for describing the system, we define bandwidth as the sum of the trust of all sensors—the sum of the Kalman gains for each sensors—whose value should not exceed a certain threshold.

The bandwidth threshold is defined as follows. The Monte Carlo optimizer stores the bandwidth value for each of its multiple runs. For each motion, the bandwidth values are fit into a Gaussian probability density function. The threshold is defined to be the mean plus

one standard deviation of this distribution. For our application, the threshold for bending and plucking motions were approximate to 0.70. It can occur that the mean and standard deviation of the bandwidth value for the different motions are not similar. In this case, the filter designer should define a dedicated threshold for each motion, defined by the value of the mean plus one standard deviation.

Kalman Filter Evaluation Background

In this work, most of the references for Kalman filter evaluation used date from the 70s, especially by Gelb and Maybeck [190, 129, 192]. They suggest the implementation of sensitivity analysis, mostly for evaluating applications where the state dimensions were reduced in order to overcome computational constraints. The sensitivity analysis they present could not be applied to the current problem because of the unpredictable signals. The reason for that resides in the fact that their sensitivity analysis takes into account the correct description of the system dynamics, which are only partially known in our case. In addition to that, they use covariance performance analysis (analogous to our steady-state error covariance descriptor) and Monte Carlo runs for defining parameters values. Also, they compare the algorithm error covariance matrix with the true error covariance matrix obtained using the true model (no dimensionality reduction). This comparison is similar to our confidence bounds descriptor, which compares the algorithm standard deviation and the experimental standard deviation (defined by the difference between the estimate and the true value given by a reference measuring system).

Later in 2007, Jwo and Cho [154, 188] published works about Kalman filter evaluation. They analyze Kalman filter performance degradation due to uncertainties in process and measurement noise statistics. They use sensitivity analysis, covariance analysis, and consistency check. Their covariance analysis is similar to our steady-state error covariance

descriptor [190, 129, 192]. The consistency check evaluates the consistency between theoretical and simulation results for the error covariance matrix, performed through graphical interpretation. The difference between their consistency check and our confidence bounds descriptor is that, as described by Zarchan and Musoff [48], we define an acceptable maximum disagreement between simulation and theoretical/true value.

Finally, we base our evaluation method on Zarchan and Musoff's [48]. Three out of four descriptors are inspired by tests proposed by Zarchan and Musoff [48]. We then reintroduce them as part of a method for filter evaluation and for process method selection. Yet one more descriptor, introduced in this thesis, relates specifically to the selection of process models for signals whose physical modelling is hard to define.

The higher the trust in sensor data, the more corrective the filter is, indicating a poor prediction step, defined by the process model and its noise. From this, it is possible to infer that, in steady state, higher Kalman gains represent poor trust in the process description, and conclusively, the process candidate and its error description might not be the best representation of the physical behaviour of the system.

4.7.4 Process Model Determination

The variable we are interested in estimating is deflection at the free edge of the beam. So, the essential state variable is position. Considering that position is not constant in time, an estimate of velocity is needed. Also, an acceleration estimate might be used. Lower order filters have the advantage of converging to the steady-state error covariance faster than higher order filters. On the other hand, higher order filters tend to track higher order derivatives of the estimate better than lower order filters [48].

Firstly, good candidates for the process model should be hypothesized. For plucking motions, the best guess according to the physical behaviour of the beam and to the sensor

data is a damped sinusoidal model. This model is based on two parameters: the undamped angular frequency (ω) and the damping ratio (d). A simpler guess would be a sinusoidal model that depends on only one parameter: the undamped angular frequency (ω). These parameters are determined by physical modeling of sensor data. It seems reasonable to inquire if simpler state-space models — derived from i-order polynomial functions — would perform as well as the physical model described above.

The specification of a process model for bending motions is more complicated as there is no predictable physical behaviour, that is, duration, frequency, and magnitude of the deflection are totally unknown. First, we select between polynomial and non-polynomial models. For polynomial models, we tested first- and second-order polynomial functions. For non-polynomial models, we tested damped and undamped sinusoidal functions.

Therefore, four process models were studied for both motions: first- and second-order polynomial models and damped and undamped sinusoidal models. All candidate models were declared observable after attaining the observability rank condition [124].

All models are analyzed according to the descriptors for each of the motions. In order to fine-tune each of the 8 possible process model and motion pairs, we adapted the algorithm to run in a Monte Carlo optimizer. The optimizer consists of a uniformly distributed number of values for the tuning constant C_{mc} (Equation 4.10) and for the initial error covariance matrix $\mathbf{P}_0$. The initial error covariance matrix represents the confidence in the error covariance matrix in steady-state regime. Setting $\mathbf{P}_0$ as a null matrix is equivalent to expecting no errors on the estimate. Setting $\mathbf{P}_0$ with non-zero entries implies that some errors are expected in the estimate. Also, the main diagonal of $\mathbf{P}_0$ determines the settling time for the error covariance matrix $\mathbf{P_k}$ [48]. The optimization process registers the constants along with the resultant descriptors presented in Section 4.7.3.

4.8 System Integration

In order to clarify the description of the proposed solution, this section discusses the data flow and the integration between the steps of the framework. Offline tasks – those to be done before the actual fusion – and online tasks – those performed in real-time – are described as follows.

4.8.1 Offline Tasks

Some preliminary tasks are needed before the system can be put into operation. These initial tasks are: segmenting the motions; defining the measurement functions for each sensor and motion (regression); evaluating filters in order to select the best process model $\mathbf{\Phi}_k$, process error covariance matrix $\mathbf{Q}_k$, measurement matrix $\mathbf{H}_k$ and tuning parameter C_k^{mc}. Figure 4.10 shows the tasks and their inputs and outputs when applicable. The tasks were introduced in Section 4.6.

Motion segmentation aims to distinguish signals that have: different sensor responses, different durations or frequencies, different complexity levels, and different knowledge about the state variables with which they may be described. Prior knowledge of the nature of the underlying signals, direct observation of the signal, signal processing techniques (including frequency analysis, normalization, and derivative calculation) and machine learning tools for clustering are useful techniques to carry out motion segmentation.

The regression task uses one motion at a time to define a measurement function for each sensor through linear regression. One of the outcomes of the regression task is definition of the coefficients for the polynomial measurement functions per sensor and motion. The other outcome is the definition of the regression errors in comparison to the deflection reference. These errors are fitted to a Gaussian distribution and will form the measurement error

covariance matrix $\mathbf{R}_k$.

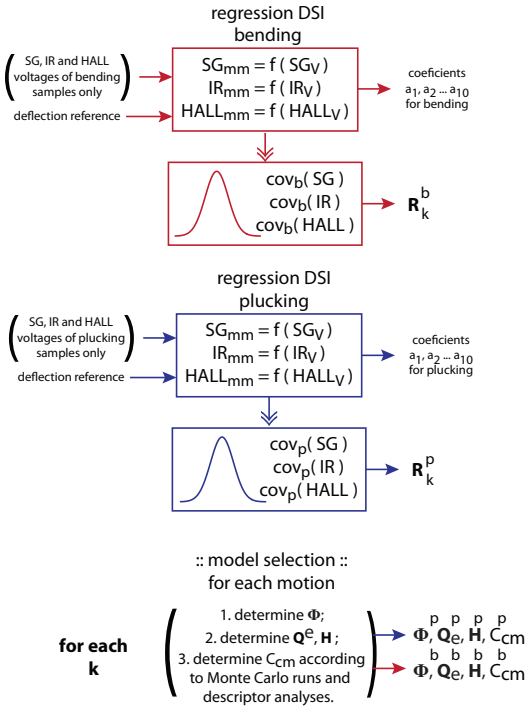

Fig. 4.10 Offline tasks: motion segmentation; DSI regression for each motion and process model selection for each motion. The iteration indexes were excluded for clarity.

The evaluation tasks are based on the selection of process model candidates. The candidates are defined by physical modelling of the signals when possible. Process model candidates $\mathbf{\Phi}_k$, the process error covariance matrix $\mathbf{Q}_k$, and the measurement matrix $\mathbf{H}_k$ are fed in Monte Carlo runs. The output of the Monte Carlo optimization are the descriptors' values (Section 4.7.3) and consequently, the tuning parameter C_k^{mc}.

4.8.2 Classifier

There are two possible topologies to integrate the gesture classification and the Kalman filter implementation (Figure 4.11). The first topology is based on setting a classifier immediately after gesture acquisition. The classification output activates either the Kalman filter for

bending or the Kalman filter for plucking. The classifier output also selects the measurement functions (coefficients $a_1, a_2, ..., a_{10}$), the measurement error covariance matrix $\mathbf{R}_k$, the state-propagation matrix $\mathbf{\Phi}_k$, the process error covariance matrix $\mathbf{Q}_k$, the measurement matrix $\mathbf{H}_k$ and the tuning constant C_k^{mc}. The sensor data, the a posteriori state estimate at step $k-1$ ($\hat{\mathbf{x}}_{k-1}$) and the a posteriori error covariance matrix at step $k-1$ ($\mathbf{P}_{k-1}$) are sent to the selected filter. We call this topology the online classifier. This classifier is designed using cross-zero detection, logic (operators such as AND, OR, etc), and first-derivative analysis. A simplified solution for classifying between the different motion models would be the use of an extra sensor detecting the grip to the beam. Although this is particularly possible when it comes to classifying motion for the The Rulers, we have chosen to offer a more general solution, applicable to a broader variety of problems.

The second topology runs the Kalman filters for bending and plucking in parallel, without any previous gesture classification. The outputs of both filters are compared to the sensor output presenting the lowest random error for each motion—given by the DSI regression (Figure 4.9): strain gages for bending motion and infrared for plucking motions. In summary, the residuals between the two filters and the two sensors are calculated. These residuals are used to train a layer recurrent network in Matlab with a single hidden layer of five units. A layer recurrent network has recurrent connections with associated tapped delays for each layer [193]. That is, given the residuals, the desired network output specified in training is 1 when the motion corresponds to bending and -1 when the motion corresponds to plucking. In this way, the network output indicates which of the two filters is appropriate for a given motion [194]. The affirmative output is the right match between motion and filter. We call this topology the machine learning classifier.

The online classifier is simpler and more straightforward, as the models are easily distinguishable. The machine learning classifier presents faster transition from one model

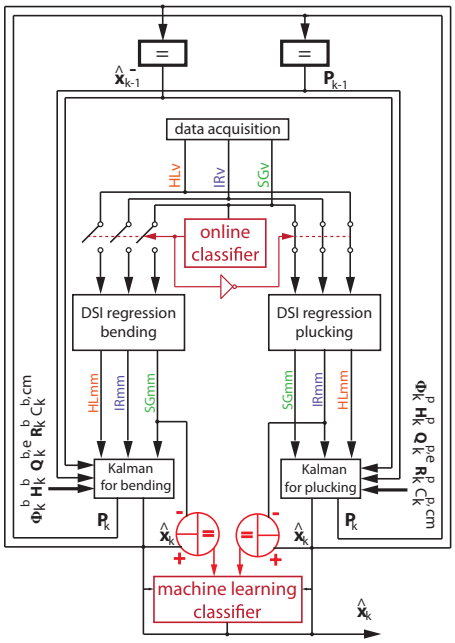

Fig. 4.11 Possible classifier applications: online classifier or machine learning classifier. $\hat{\mathbf{x}}_k$ is the *a posteriori* state estimate at step k, $\hat{\mathbf{x}}_{k-1}$ is the *a posteriori* state estimate at step $k-1$, $\mathbf{P}_k$ is the error covariance matrix at step k, $\mathbf{P}_{k-1}$ is the error covariance matrix at step $k-1$, $\mathbf{\Phi}$ is the state-propagation matrix, $\mathbf{Q}_k^e$ is the process error covariance matrix, $\mathbf{H}_k$ is the measurement matrix, $\mathbf{R}_k$ is the measurement error covariance matrix and C_k^{mc} is the tuning constant. *SGv, IRv, HLv* indicate the digitized sensor output in Volts, while *SGmm, IRmm, HALLmm* indicate the sensor data in millimeters. Indexes b refer to parameters or data for bending motions, while indexes p refer to parameters or data for plucking motions.

to another, however it requires learning. In this work, the online classifier was chosen due to simplicity. The integration filter-classifier for both approaches is shown in Figure 4.11.

Online Classifier Implementation

The online classifier simply consists of two tests that examine the frequency content of both types of motion. While plucking presents higher constant frequency, bending has variable lower frequency. The first test is to count the distance between the samples that cross zero. Exhaustive tests show that users do not bend the beam in opposite directions passing by

the rest position faster than the plucking oscillations. The second test involves calculating the derivative of the signal by subtracting the current from the previous sample values. This simplified derivative operates as a high pass filter, attenuating the slow rate of change in bending motions. For plucking motions, the derivative output is an attenuated version of the deflection oscillations, maintaining the same frequency content. The plucking derivative has a considerably higher magnitude than the bending derivative. The online classifier pseudocode is presented in Figure 4.12. *Cell A* arbitrarily classifies the first 20 samples as bending, due to classifier design constraints. *Cell B* evaluates the current (*SGv*) and previous (*SGant*) strain gage value and determines whether there is zero crossing. In case no zero crossing is detected, a counter is incremented (variable *numberOfNonZeros*). *Cell C* counts the number of samples since the last zero crossing. Due to the mechanical properties of the beam, plucking motions intercept zero approximately every 17-18 samples. Bending motions are slower than plucking, according to exhaustive testing. If two consecutive zero crossings are less than 20 samples apart, there is a strong belief that the current motion is plucking, otherwise it is bending.

The implementation of *Cells A,B and C* results in two artifacts. The first one is a delay in detecting the transition from bending to plucking motions. The second is an oscillation between classifier outputs during low amplitude plucking deflections. These artifacts are solved by *Cells E and F*. *Cell D* calculates the difference between the current and the previous strain gage value (variable *deriv*). The difference is then used in *Cell E* in order to detect the beam release, that is, the start of a plucking motion. In order to prevent alternating classifier outputs during low amplitude plucking deflections, when the classifier switches from plucking to bending, the variable *lockOnBending* is set to one, preventing the classifier output to return to plucking unless the derivative of the signal (variable *deriv*) is greater than the threshold (line 30).

▷ **Initialize with zeros:** crossedZero, numberOfNonZeros, lockOnBending, deriv
▷ **A:** classify first 20 samples as bending

```
if k < 21 then
    motion = bending
end if
```

▷ **B:** test zero crossing

```
if ((SG_V ≥ 0 & SG_ant < 0)||(SG_V ≤ 0 & SG_ant > 0)) then
    crossedZero = 1
else
    numberOfNonZeros + = 1
    crossedZero = 0
end if
```

▷ **C:** count number of samples since last zero crossing

```
if crossedZero = 1 then
    if numberOfNonZeros ≤ 20 & lockOnBending = 0 then
        motion = plucking
    else
        motion = bending
    end if
else if numberOfNonZeros > 20 then
    motion = bending
end if
```

▷ **D:** calculate derivative for SG data

```
deriv = SG_V − SG_ant
```

▷ **E:** corrects transition from bending to plucking

```
if motion = bending & deriv > 1 then
    motion = plucking
    lockOnBending = 0;
end if
```

▷ **F:** corrects transition from plucking to bending

```
if motion − motion_ant = −2 then
    lockOnBending = 1;
end if
```

▷ **Store:**

```
SG_ant = SG_V;
motion_ant = motion
```

Fig. 4.12 Code for the online classifier: cross zero detection, first derivative analysis and logic. The subscript $_{ant}$ denotes the value of a quantity in the previous iteration.

4.8.3 Online Tasks

The online tasks are performed in real-time and consist of data acquisition, classification and Kalman filter loop (Figure 4.13). Right after the data acquisition, the strain gage voltage output is used as input for the online classifier described in the previous section.

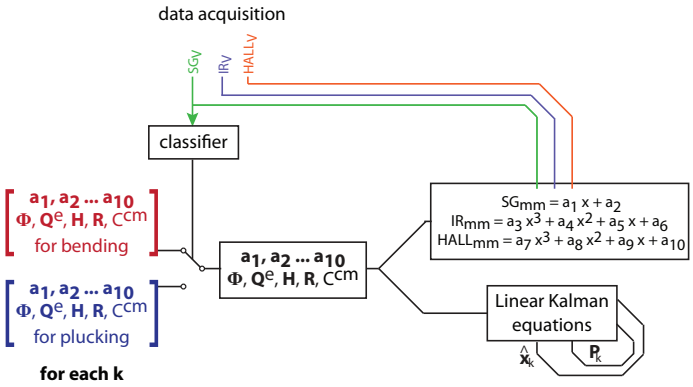

Fig. 4.13 Online tasks: classification; selection of parameters according to the classifier output; linear Kalman filter loop. The parameters to be selected according to the classifier output are: coefficients for the measurement functions, the state-propagation matrix $\mathbf{\Phi}_k$, the process error covariance matrix $\mathbf{Q}_k^e$, the measurement matrix $\mathbf{H}_k$, the measurement error covariance matrix $\mathbf{R}_k$ and the tuning constant C_k^{mc}. The iteration indexes were excluded for clarity.

The strain gages' values in Volts are used for the following reasons:

- as the transfer function between the strain value in Volts and in millimeters is linear, the value in Volts can be used for classification without requiring a CSI regression;
- the strain gage is the sensor type that presents greater difference between bending and plucking motions (Section 4.4.1), concerning the measurement errors.

The classifier output selects the parameters calculated during the offline tasks according to the motion. The coefficients $a_1, a_2, ..., a_{10}$ are used to define the measurement vector $\mathbf{z}$. The remaining parameters are used in the filter algorithm. The state estimate vector and the error covariance matrix are fed into the system at every new iteration.

4.9 Results

This section presents the descriptor values for each process model and motion pair, culminating in the selection of the best process model for both motions: bending and plucking. Some descriptors are used to disqualify non-efficient or incoherent simulation runs. Other descriptors are used to find the best tuning parameter for each process model and motion pair.

Next, we report the improvement in the sensing design using segmented gestures multiple-model sensor fusion as opposed to a single-sensor and single-model sensing approaches.

4.9.1 Process Model Selection

Firstly, we examine the qualitative descriptor where the process error covariance matrix is set to a null matrix. Figure 4.14 and Figure 4.15 show examples of process model comparison for bending and plucking motions, setting the process error covariance to zero.

Clearly, polynomial models are the better for bending motions, while non-polynomial models are better for plucking motions. For instance, Figure 4.14 shows that the damped sinusoidal model does not estimate any deflection for bending. For plucking motions, as shown in Figure 4.15, it is clear that the damped sinusoidal model is the most suitable process model for the motion, presenting small deflection estimate error (bottom graph), while the first-order polynomial model is not capable of tracking the deflection variation.

Additionally, we impose a minimum value of 68% for the confidence bounds descriptor, as mentioned in Section 4.7.3. It means that only optimizer trials that accomplish this goal are going to be evaluated. Lastly, we analyze the steady-state error covariance for deflection estimate $(\mathbf{P})^{ss}_{1,1}$ and the bandwidth.

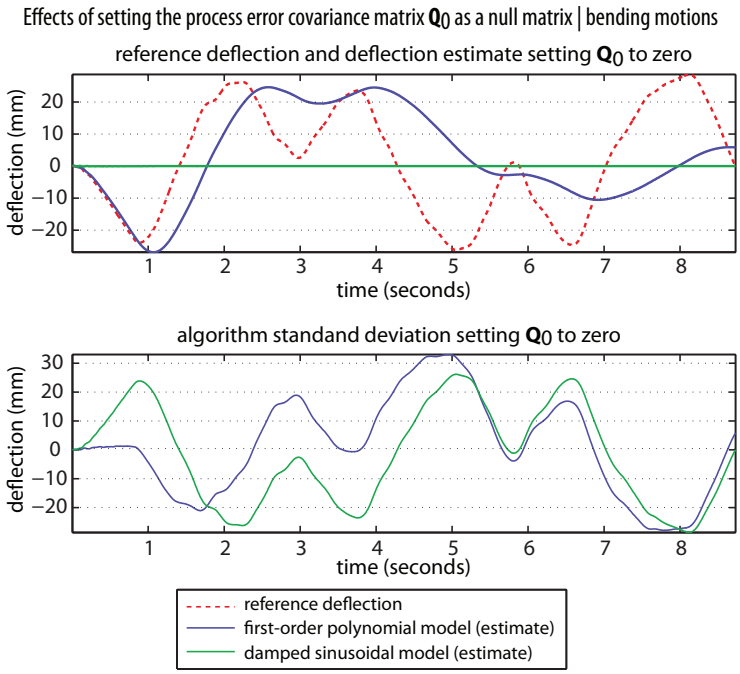

Fig. 4.14 Effects of setting the process error covariance matrix as a null matrix, for **bending** motions. The top graph displays the deflection given by the reference measuring system, the deflection estimate given by a first-order polynomial filter, and by a damped sinusoidal filter (which does not estimate any deflection). The bottom graph compares the algorithm standard deviation for both model settings.

Bending Motions

A comparison between process models for bending motions reports no significant difference between first- and second-order polynomial filters. As lower order filters are faster and as we are interested in position estimate and not in its derivatives, we selected the first-order filter. Two types of first-order filters were evaluated: one where only velocity is considered noisy (denoted by *noisy vel.*) and another where velocity and deflection are considered noisy (denoted by *noisy vel. pos.*). Refer to Table 4.1 for the descriptors' results on bending motions.

One might think that the non-polynomial filters are comparable to the polynomial ones

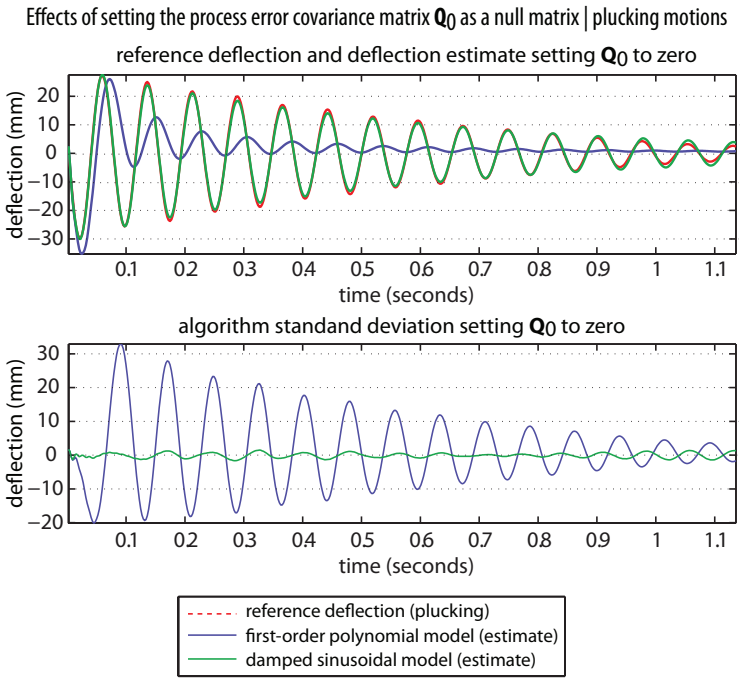

Fig. 4.15 Effects of setting the process error covariance matrix as a null matrix, for **plucking** motions. The top graph displays the deflection given by the reference measuring system, the deflection estimate given by a first-order polynomial filter and by a damped sinusoidal filter. The bottom graph compares the algorithm standard deviation for both model settings. The estimate given by the damped sinusoidal filter and the reference deflection are overlapped, reflecting a small random error in the bottom graph.

since their error covariance for deflection estimation $(\mathbf{P})^{ss}_{1,1}$ is similar. However, the non-polynomial filters make significant use of the sensor data, that is, have a higher bandwidth (Table 4.1), which reflects a low trust in the process model selected.

Plucking Motions

A comparison between process models for plucking motions (Table 4.2), reveals a significant difference in performance between polynomial and non-polynomial filters. The non-polynomial filters present the best performance not only concerning the steady-state covariance for deflection estimation but also the bandwidth.

Table 4.1 Comparison between candidate process models for bending motions. Bold font represents the best results.

$\mathbf{\Phi}_{BENDING}$		$(\mathbf{P})^{ss}_{1,1}$ $[10^{-3}\ mm^2]$	bandwidth
first-order	noisy vel.	**5.4**	**0.69**
	noisy vel. pos.	6.4	0.71
second-order		6.6	0.74
sinusoidal		8.7	*0.96*
damped sinusoidal		8.5	*0.95*

Two choices of process error covariance matrix $\mathbf{Q}_k$ (Equation 4.10) for the sinusoidal filters were tested. The first one is based on the actual state-propagation matrix $\mathbf{\Phi}_k$ for sinusoidal model. The alternative simplified $\mathbf{Q}_k$ is based on a first-order polynomial state-propagation equation. There were no significant advantages in using the simplified $\mathbf{Q}_k$ concerning any of the descriptors, except by its faster processing. Finally, the best option is the damped sinusoidal filter, matching the physical modeling of the signals.

Table 4.2 Comparison between candidate process models for plucking motions. Bold font represents the best results.

$\mathbf{\Phi}_{PLUCKING}$		$(\mathbf{P})^{ss}_{1,1}$ $[10^{-3}\ mm^2]$	bandwidth
first-order		17.6	0.70
second-order		15.1	0.60
sine	process model error	6.3	0.25
	process model as in 1^{st} order filter	6.2	0.25
damped sinusoidal		**4.8**	**0.19**

The bandwidth reduction obtained due to a better description of the process model is remarkable. It can be seen that the bandwidth value of 0.69 was obtained for the bending filter, whereas a bandwidth of 0.19 was obtained for the plucking filter. This strengthens the

idea that correct knowledge of the process model is essential. This work proposes that in the case of partial knowledge of the process model, motion segmentation and multiple-model filters should be implemented in order to reduce the bandwidth for noise whenever the process model is known accurately.

4.9.2 Selected Process Model and Motion Pairs

Given the results presented in Tables 4.1 and 4.2, we introduce the state-propagation matrices that best describe the system behaviour while in the bending or plucking regimes.

For bending motions, the best model is the first-order polynomial model. Its state-space representation ($\mathbf{\Phi}^b$) is presented in Equation 4.17:

$$\mathbf{\Phi}_k^b = \begin{bmatrix} 1 & t_s \\ 0 & 1 \end{bmatrix} \tag{4.17}$$

where t_s is the sampling time.

For plucking motions, the best model is the damped sinusoidal model described by its state-space representation (from Equation 4.18 to Equation 4.22):

$$\mathbf{\Phi}_{11}^p = e^{d\,w\,t_s}\,(-d\,w\;sin(b\,t_s) + b\;cos(b\,t_s)) \tag{4.18}$$

$$\mathbf{\Phi}_{12}^p = e^{d\,w\,t_s}\;sin(b\,t_s) \tag{4.19}$$

$$\mathbf{\Phi}_{21}^p = -w^2\,e^{d\,w\,t_s}\;sin(b\,t_s) \tag{4.20}$$

$$\mathbf{\Phi}_{22}^p = e^{d\,w\,t_s}\,(d\,w\;sin(b\,t_s) + b\;cos(b\,t_s)) \tag{4.21}$$

$$\mathbf{\Phi}^p = \frac{1}{b}\begin{bmatrix} \mathbf{\Phi}_{11}^p & \mathbf{\Phi}_{12}^p \\ \mathbf{\Phi}_{21}^p & \mathbf{\Phi}_{22}^p \end{bmatrix} \tag{4.22}$$

where w is the undamped angular frequency, d is the damping ratio and b is the underdamped angular frequency given by $b = w\sqrt{1-d^2}$. The iteration index 'k' was excluded for clarity.

4.9.3 Sensor Fusion Contribution

In order to make clear the advantages of using fusion techniques in the present problem, we compared the filter output for each motion with the use of individual sensors in terms of the error covariance for deflection. Table 4.3 compares the best filter and the best sensor for each motion. The contribution of fusing data from different sensors varies according to the motion regime. For both motions, the error covariances are better than any of the sensors individually. The improvement factor for bending motions is 2.2 and for plucking motions is 12.7.

Table 4.3 Filter performance in comparison to the best sensor for each motion. Bold font represents the best results.

filter versus single-sensor approach		error covariance for deflection $[10^{-3}\ mm^2]$
bending	filter	**5.4**
	SG	12
plucking	filter	**4.8**
	IR	61

Note that the lowest measurement error covariance for plucking motions ($6.1\,10^{-2}$ mm^2) is about five times worse than the lowest measurement error covariance for bending. Lastly, the most predictive physical behaviour is the one in which the sensor performance is the worst. Consequently, The Rulers is a good testbed to demonstrate that the proposed framework is satisfactory.

Additionally, it is worth comparing the proposed filter to a single-model filter approach.

In the case of a single-model, the most advantageous would be the one that reflects, at least partially, the physical behaviour of the system: damped sinusoidal function. The comparison is shown in Table 4.4. Even if the error covariance ranges are not significantly different, the bandwidth for the noisy sensor data is high, reflecting a disagreement between the selected process model and the motion being performed. Therefore, it is possible to conclude that the use of a multiple-model filter improves not only the error covariance for deflection but the robustness to sensor noise.

Table 4.4 Filter performance in comparison to the single-model approach. Bold font represents the best results.

filter versus single-model approach	error covariance for deflection $[10^{-3}\ mm^2]$	bandwidth
implemented filter	**4.8 – 5.4**	0.19 – 0.69
single-model approach	4.8 – 8.5	0.19 – 0.95

Comparison with other Bayesian methods

A comparison between Bayesian solutions for sensor fusion is far from trivial. A comparison itself implies common evaluation variables between all approaches. Some methods are based on explicit functions whereas others are based on simulation. Such characteristics produce different sets of variables, and most of them cannot be compared.

The algorithm error covariance given by different filter solutions can be the real measure of the error or an estimate of its value. Consequently, these variables cannot be used. Fortunately, there exists only one variable in all approaches that can be used for comparison: the estimate. The estimates given by different Bayesian methods can be compared to the true value, resulting in the real error of each method. However, it is hard to guarantee that this comparison would be fair. For instance, an optimal Kalman filter design cannot be

compared to a less rigorous particle filter design.

Each filter topology — Kalman, particle, etc — has several frameworks and enhancements for specific applications and goals (tracking, correction, error covariance reduction, etc). For example, Doucet and Johansen provided a tutorial on the particle filter, including several frameworks [178]. We strongly believe that one contribution does not dismiss another. All of them may be valuable for diverse cases. A comparison between frameworks within the realm of a single filter type is feasible, as multiple variables are present across frameworks. The same does not apply to comparison across filter topologies.

4.10 Applying the Framework

This section presents recommendations for filter designers who might be interested in replicating the framework.

4.10.1 Motion Segmentation

The main goal of segmenting motions is to define dedicated solutions (process and measurement descriptions) for each of the operation modes. The segmentation requires a strong knowledge of the system and its signals.

In some cases, the differences between the operation modes can be as clear as they were for The Rulers. On the other hand, sometimes the differences are less pronounced. An example is a human body segment moving in different modes: uniform velocity, uniform acceleration or having its acceleration changing over time. In this case, all modes are described by different order polynomial functions. Then, these functions describe different process models in a multiple-model filter design.

Among all the possible operation modes, there are the modes in which a physical model

is not possible to be determined, especially in human-computer interfaces. Therefore, after having a clear differentiation between all possible operation modes, each of them have to be labelled according to the knowledge of their process model. Next, all the modes that have a clear process model definition should be described by their physical model. Alternatively, unknown signals require evaluation of candidate process models, as will be described in section 4.10.4.

4.10.2 Classification

The more distinct the modes are, the easier it is to classify an incoming sample. We presented two different classification topologies. One classifies the sample just after its acquisition and therefore selects the correct filter design for the sample. Another classifies the sample based on the output of two filters running in parallel.

The classification can be designed in terms of physical parameters of the operation modes (frequency, amplitude, phase) or in terms of the residual analyses. In some cases, machine learning tools are recommended.

4.10.3 Multi-model Design

A multi-model design implies that every operation mode has its dedicated system, measurement description and tuning parameters. The description of system and measurements is composed of a state space matrix, process error covariance matrix, measurement matrix and measurement error covariance matrix.

In cases where the implemented classifier selects a single filter design at a time (online classifier), the feedback of the state estimate vector and the error covariance matrix alternates between the multiple filter models. Sometimes, the dimensions of these vectors and matrices are different and need to be adapted, as is well described in several studies [190, 129, 171].

4.10.4 Evaluation

The evaluation task is performed in order to select the best process model for each operation mode, especially for unknown signals. The evaluation occurs offline and requires a reference measuring system. The evaluation we proposed is based on a list of descriptors and their thresholds.

4.11 Conclusion

We have presented a sensor fusion technique based on a multiple-model linear Kalman filter for deflection estimation using strain gages, infrared and Hall effect sensors. The system of clamped beams has two distinguishable physical behaviours: a free damping motion (called plucking) and a driven motion controlled by the user (called bending). The problem lies in the unpredictability of bending motions, which make the physical modeling of this motion impossible.

Our solution derives from segmenting the motions according to the knowledge of their physical model, that is, according to their eligibility for physical modeling. Then, a classifier defines the gesture being performed and activates the correct measurement and process model parameters accordingly. This approach makes the design of a more predictive filter possible whenever the process model is known, i.e., free motions; while reducing the filter efficiency when the process model is impossible to be determined, i.e., user-driven motions.

The problem of selecting a process model for unknown signals is solved by defining a set of descriptors that evaluate candidate process models. Forcing threshold values for some of the descriptors exclude trials with low noise reduction and/or high risk of divergence. The remaining descriptors are used to select the model parameters. Therefore, this framework facilitates the process model selection for unknown signals and evaluates the robustness of

the filter design, inherently at high risk due to the limited knowledge of the process model.

Through experiments, it was shown that the suggested framework results in improved error estimate covariance for deflection compared to the measurement error covariance of any of the sensors individually. The application of fusion filters in the present case is appropriate, since the worst measurement errors happen for plucking gestures, whose process model is known.

We recommend the application of the framework in cases where one or more of the conditions apply:

- there are signals for which process model determination is unclear;
- the system has more than one operation mode and there is no clear transition between the modes;
- measurement functions and errors differ considerably between the operation modes;
- a better error covariance for the known signals estimate is desired, without compromising the estimate of unknown signals, and;
- a better error covariance for the unknown signals estimate is desired.

Although other works in NIME have used an implementation of sensor fusion, this work differs significantly from those. One example is the work by Benning et al., which used an IMM filter, an alternative mentioned in Section 4.2 [168, 169]. We have not pursued this path, since we intended to obtain a method for applying a fusion filter that would not be restricted to rules, probabilities, sequences or patterns. Their work is an example of a successful implementation of a type of Kalman filter, seen from a control engineering perspective. In contrast, our work is a framework for the implementation of a type of linear Kalman filter for cases that fit the criteria listed in Section 4.10, using the premises and requirements of signal processing research. In both cases, the Kalman filter formulations

are widely known. However, our framework includes not only this formulation, but also motion segmentation, classification, advanced regression, filter evaluation, process model selection, and optimization. Finally, a comparison between them does not hold because while Benning et al.'s work is a single-sensor filter with model selection driven by likelihood, our framework is multi-sensor with model selection given by motion classification, without any imposition of rules, patterns or probabilities.

Chapter 5

Conclusions

This dissertation focused on sensing design in input devices for musical expression. From reviewing five years of NIME publications, we have shown that there is room for improvement for instrumentation design and sensor signal processing in the context of Digital Musical Instruments. We believe that robust, reproducible, responsive, and accurate sensing design in DMIs can improve learnability and controllability [34]. Therefore, we proposed advanced instrumentation and sensor signal processing techniques which can improve sensing in DMIs. The main sensor signal processing technique explored was a sensor fusion algorithm: the linear Kalman filter.

The techniques presented might be obvious for sensing and controlling systems where human input is not the main variable. However, in systems where human input is the *raison d'être*, we have shown that other variables come into play. We focused on proposing techniques that could account for not only the robustness and reproducibility, but also the adaptability, i.e. allowing the user to attain full potential.

In Chapter 2, we intended to raise awareness of limitations and possibilities for instrumentation design and sensor signal processing. Given the review of DMI designs as

manifested in the NIME Conference from 2009 to 2013, we observed that most designs are based on uncomplicated sensing design. We offered possibilities to enhance instrumentation and signal processing for the most commonly used sensor technologies. We also reinforced the importance of calibration and coherent regression techniques for achieving measurements with quality [6]. In order to illustrate the panorama of sensing in DMIs, we cited successful and limited sensing choices in DMI design. The techniques briefly reviewed in Chapter 2 are further explored in the remaining chapters.

In Chapter 3, we chose one DMI used in performance—The Rulers—as a testbed to explore some of the techniques suggested in Chapter 2. The main advanced sensing technique explored in this chapter was the use of specialized sensors, strain gage sensing in this case. We also explored the analysis of quantitative and qualitative evaluation descriptors for sensing in the context of DMIs, and the introduction of techniques that can potentially improve response for low performance sensors, such as sensor placement and better regression analysis.

In Chapter 4, we performed the improvements mentioned in the previous chapter: better mechanical structure, sensor placement, calibration, and regression. Aside from this, in order to apply sensor fusion techniques to a DMI, we developed a method to deal with the unpredictable nature of human input. The method models the system and measurements according to the knowledge of their real behaviour. That is, the application of the method results in better error covariance improvement for non-driven motions, as compared with driven motions. Improvements on the error covariance of driven motions rely on the best measurements, with less correction given by the system model.

We claim that modeling gestures and DMI systems and signals require a deep knowledge of the system and its signals. Therefore, the techniques suggested in this thesis need to be adapted to the designer's problem. We attempted, as much as possible, to provide guidelines

and describe potential methods, in order for them to be reproduced in other HCIs.

5.1 Main Findings

In this section, we present the main findings of this thesis.

5.1.1 Trends in sensor use in DMIs

First, we reported that approximately 34% of sensor occurrences in DMIs are related to force assessment, using either an accelerometer or FSR sensors. The average use of accelerometers per year from 2009 – 2013 increased by more than 100% in comparison to the average use per year in the previous interval (2001–2008). The use of switches, buttons, and potentiometers in the 2009–2013 interval decreased to a third of the 2001–2008 interval's average use.

Unsurprisingly, we identified a substantial use of portable consumer electronic devices as input controllers: 71 occurrences in 266 publications. Also, this trend shows a monotonic increase on their use since 2010. The use of the embedded sensors in these devices is significant, especially the use of MARG sensors: a MARG sensor was used in 44 out of 71 occurrences for portable consumer electronic devices. A hypothesis for the decreasing trend of using video as a sensing technology might be related to the increasing trend of using the Kinect©.

Some sensors tend to be frequently used with other sensor types, whereas others tend to be applied alone. For instance, accelerometers, gyroscopes, and magnetometers tend to be applied concomitantly. Simple analog sensing techniques such as infrared, FSR, and potentiometers/switches present similar co-occurrence levels. That is, the amount of concomitant use for each of these sensors with other sensor types is similar. The highest co-occurrence belongs to the accelerometers and gyroscopes. The highest degree—the number of

sensor types with which one sensor can be concomitantly used—belongs to the accelerometer, followed by potentiometers and FSRs. The most obvious co-occurrence cluster involves the MARG sensors, followed by a cluster including accelerometers, potentiometers and FSRs. Another interesting cluster is the co-occurrence of light, video, and microphone—sensing tools which have been used in audio and video processing for decades [13, 1].

5.1.2 Specialized Sensors

In Chapter 2, we showed that the most common sensor types in DMIs measure kinetic parameters, e.g. force. Given the most common issues found in the application of these sensors, we suggested better instrumentation techniques for FSRs and better sensor signal processing for accelerometers. Also, through case studies, we indicated when the use of strain gages can be a valuable alternative for measuring kinetic parameters. In Chapter 3, we presented an in-depth review of strain gages, applying them to a DMI: The Rulers. The comparison between SGs and low performance sensors pointed to several advantages of SGs over their non-linear counterparts. In Chapter 4, we compared strain gages' performance to low performance sensors with improved instrumentation and sensor signal processing. Even if the quality of measurements supplied by ordinary sensors have improved drastically with those measures, the linear behaviour of SGs is a desired feature worth exploring. The cost of applying SGs lies on the complexity of their application to the specimen, as well as their intricate conditioning circuit.

Aside from that, considering the The Rulers as a testbed, the SG has promoted new mapping possibilities. In Chapter 4, we have shown that SG responses present the most significant difference across gestures being performed, which means that among the three sensor technologies used, the SG is the one whose responses to the two distinct gestures are the least similar. This has allowed for gesture classification, since the system response for

driven and free motions is different when it comes to the stress analysis of their mechanical structure.

5.1.3 Advanced Electronic Instrumentation

We introduced advanced electronic instrumentation in Chapter 2, by presenting an enhanced version of a voltage divider and the advantages of the use of buffers, instrumentation amplifiers, and comparators with hysteresis. In Chapter 3, we presented important factors to consider when it comes to selecting polarization resistors, as well as an in-depth application of the Wheatstone Bridge's principles - a balancing circuit whose output reflects the amount of variation in the sensing elements. Finally, in Chapter 4, we presented the importance of sensor placement and polarization resistors in order to obtain monotonic measurement ranges and an output free of saturation.

5.1.4 Advanced Sensor Signal Processing

Regarding advanced sensor signal processing, we first insisted on coherent calibration and data regression in Chapter 2. A discrete calibration and a regression using CSI is used in Chapter 3. Chapter 4 presented enhanced calibration—continuous and dynamic—and regression using DSI. This type of regression was essential in performing the multiple-model linear Kalman filter, resulting in a performance superior to that of a single model linear Kalman filter based on CSI. The choice for regression techniques is tied to the knowledge of system and measurement functions, as well as to what extent they differ from one gesture to another. Another possibility for improving regression errors is the use of DSI regression for high hysteresis sensors, as is the case for the Hall effect response in Chapter 3. For these cases, the reduction of the measurement error covariance is directly proportional to the hysteresis level.

In Chapter 3, we identified the advantages and disadvantages of each sensor type evaluated. We also showed that the requirements for stage context might differ from those for non-interactive systems. We concluded that none of the sensor types are superior in all evaluation descriptors. Therefore, the obvious solution would be to take advantage of each of the sensor technologies' positive features, and minimize the effects of the negative ones. This could be obtained by the use of sensor fusion. Among the sensor fusion techniques available, the fastest—for real-time purposes—is the weighted output of Complementary Filtering. However, we are interested in a more complex algorithm that could provide the error covariance of the estimates at each sampling time, accounting for each distinct gesture's system and measurements. Extended Kalman filters and particle filters were excluded as alternatives due to their processing time and cost. We ended up choosing a linear Kalman filter, as it offers optimal estimation with the requirement of accurate system and measurement variable knowledge.

In order to account for the high requirements imposed by the implementation of a linear Kalman filter, we developed a framework in Chapter 4 in order to apply the linear Kalman filter to human input signals, whose nature is inherently unpredictable and leads to signals that cannot be trivially modeled. Our solution is based on gesture segmentation and classification, along with multiple models for system and measurement functions. The framework proved to be efficient and stable: it improved the error covariance of the estimate by a factor of 2.2 for driven motions and 12.7 for free motions, compared to single-sensor filter design. Also, the comparison of multiple-model filtering with single-model filtering pointed to a smaller error covariance for the multiple-model approach.

Finally, better error covariance and more mapping possibilities are improvements brought by the framework, which is well-suited for multi-gesture devices where the system behaviour is only partially known. We believe that by segmenting and classifying gestures, we can

offer a flexible layer on top of an accurate measurement layer, providing adaptability for performance applications. The fusion of position- and force-related sensor data proved to be successful. The distinct kinetic and kinematic responses of systems and measurements seem to be fruitful when it comes to segmenting and classifying gestures, which characterizes the best scenario for the proposed framework's replication.

5.2 Contribution

In order to understand the unique contributions of this thesis, it is important to first develop an understanding of the context which has defined and made it necessary. First, the field of new interfaces for musical expression (NIME) is, as a formalized research domain, a rather young and strongly multidisciplinary area. Since the first NIME workshop in 2001, a yearly event has been held to discuss advances in this field coming from areas such as music performance and composition, electrical and computer engineering, design, and human-computer interaction. Because of these characteristics — augmented by the recent trend of Do-It-Yourself devices using user-friendly physical computing platforms and widely available, inexpensive sensors — the field of NIME tends to present a plethora of new devices that do not rely on advanced sensing systems [11]. In our view, these design choices present several limitations if used by skilled performers. It is commonly agreed upon that musicians rely on responsive and precise acoustic musical instruments to achieve a degree of expressiveness and perhaps virtuoso performance. Therefore, these devices with simple electronic instrumentation fall short in providing advanced characteristics such as robustness, and accuracy. We believe that this is one of many reasons hindering widespread and/or advanced musical use of such devices.

Secondly, it is extremely rare that new interfaces for musical expression are characterized

by their mechanical and/or electronic behaviour, as manifested by the NIME papers reviewed in this thesis. One exception is the Radio Baton, because of the extensive work by Andy Schloss and Peter Driessen group at University of Victoria. However, we are not aware of many other examples of the detailed characterization of sensing systems in DMIs, and in our opinion, it is imperative to perform such a characterization if one is to improve their response to fit musical performance requirements.

This thesis' main contribution relates to the design of sensing in DMIs. Although most of the techniques for instrumentation design used here are commonplace for instrumentation engineers, these techniques are not used in DMI design, as shown in a five-year review of NIME publications. In regards to sensor signal processing, our major contribution relies on the framework for a multiple-model linear Kalman filter application. To the best of our knowledge, this is a unique method to account for uncertainties in the knowledge of process and measurements, given the unpredictable nature of human input. Alternative methods rely on probability, rules, patterns, or sequences, which might limit user control to undesirable levels.

In this work, we have carefully reviewed all contributions—266 articles using sensing—in the last 5 years of the NIME conference (2009-2013). We then demonstrate the point that the engineering solutions applied to NIME devices are mostly suboptimal and many times inadequate. This inadequacy comes from misuse but also from the lack of proper characterization of the devices. Furthermore, we showed that most of the devices use only a few simple sensors, whereas many other options are available for similar instrumentation needs. We therefore set out to show how one can dramatically improve instrument response by using advanced sensors for musical instrumentation or by using techniques such as the Kalman filter for a system that includes multiple sensor measurements.

However, in order to make an efficient sensor fusion on unpredictable human input

signals, the popular implementation of a linear Kalman filter would not be possible, due to the limitations on describing the processes and their errors for unpredictable signals. Due to that, we have proposed a novel framework for a multiple-model multi-sensor linear Kalman filter for implementations where no probabilities, rules, patterns, or sequences are imposed on the human input. This framework contains a novel evaluation method for linear Kalman filters that can be applied for any Kalman filter implementation. This evaluation method not only tests the stability and convergency of the filter, but can also be used for selecting candidate process models. Our framework is based on judicious description of the observations, their measurement functions and errors, given by calibration.

These are novel contributions which improve upon previous work that applies a similar, albeit simpler, Kalman filter to another existing device, the Radio Baton [168, 169]. The main contribution of this thesis in comparison to Benning's publications is that we introduce a framework for the application of the Kalman filter on DMI signals, whereas Benning et al. present a Kalman filter implementation. Our framework includes sensor characterization, statistics for sensor data, gesture segmentation, gesture classification, selection of process model, filter evaluation, and filter optimization. We, as well as Benning et al., make use of multiple models to describe different gestures, but they tune the models arbitrarily while we have defined a method for evaluating and selecting candidate models. This evaluation method is novel for the Kalman filter field [59], and is a contribution to the works of Jwo, Cho, Zarchan, Musoff, Gelb and Maybeck [154, 188, 48, 190, 192, 129]. It includes evaluation descriptors proposed by these authors in a systematic and procedural manner, and introduces a novel descriptor. Also, Benning et al. make use of a single sensor technology, while we use three sensor technologies with different popularity levels among DMI designers. Finally, Benning's implementation uses model weighing according to the models' likelihood, whereas we use gesture classification driven by the similarity between sensor data and the

most predictive model. That is, gesture classification in our work does not impose rules, patterns, sequences, or probabilities for each model, or for the transition between them.

In summary, the uniqueness of this work is supported by the following summary of its major contributions:

- Careful review of 5 years of the main conference in this field (NIME 2009-2013, 266 papers in total), deriving hard evidence to support the claim of sub-optimal or inadequate engineering solutions applied in most devices (Chapters 1-2);
- Development of a novel framework for the use of a Kalman filter to unpredictable inputs (to differentiate between two very dissimilar gestures, plucking and bending) using all the three sensor solutions available in the device. This expands over previous papers that used related techniques to improve the response of one sensing technology (Chapter 4);
- Formalization of a method for evaluating candidate models and filter design, including evaluation techniques proposed by several authors and a novel technique created by us (Chapter 4);

These novel contributions shed new light into the design of DMIs and will hopefully be used by the NIME community to achieve advanced instrumentation solutions to improve novel and existing devices and eventually allow for responsive DMIs for expert musical use.

5.3 Future Directions

One interesting direction is the application of sensor fusion methods for human motion analysis. The current challenge is to fuse kinetics and kinematics to better analyze human motion. Our future work is devoted to algorithms for biomechanical analyses fusing positional

data—given by infrared-based motion capture—with sensor data—given by MARG sensors. Also, another publication currently being prepared proposes advanced instrumentation for low-performance sensors, such as FSRs and infrared [101].

Appendix A

Modular Design for Sensor Calibration and Placement

This section briefly discusses the benefits of using modular design, based on LEGOs and 3D printing, for sensing design. We build LEGO structures for sensor calibration and placement. This choice provides design flexibility and high dimension accuracy—LEGO company reports a "machine tolerance" as small as 0.01 mm [152]. A further development stage of our LEGO buildings is based on 3D printing. However, the LEGO choice tends to be cheaper, and allows for quicker modularization and changes.

Some examples of modular buildings used in this research follow:

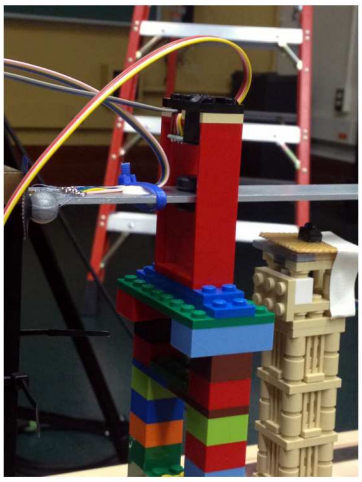

Fig. A.1 Early design of apparatus for sensor placement, based on LEGO bricks only. IR and Hall effect sensor placement above and below the beam suggest complementary behaviour for fusion. Limitation resides on approaching the two sensors.

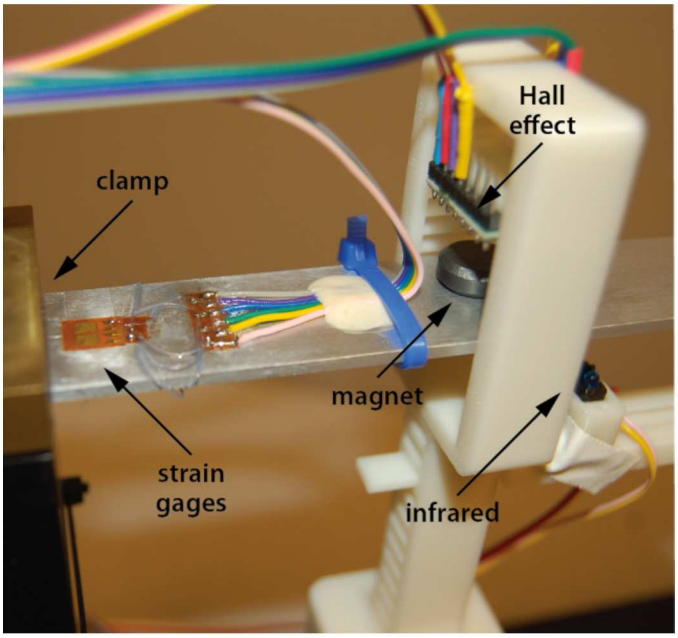

Fig. A.2 Apparatus for sensor placement for *The Rulers*: based on LEGO bricks and 3D printing. LEGO bricks are used to add flexibility (discrete adjustment of vertical position) and to reduce cost. Rail fitting allows continuous adjustment of longitudinal position for the Hall sensor. Apparatus design is a collaboration with Anthony Piciacchia. Photo by Vanessa Yaremchuk. Reproduced with permission.

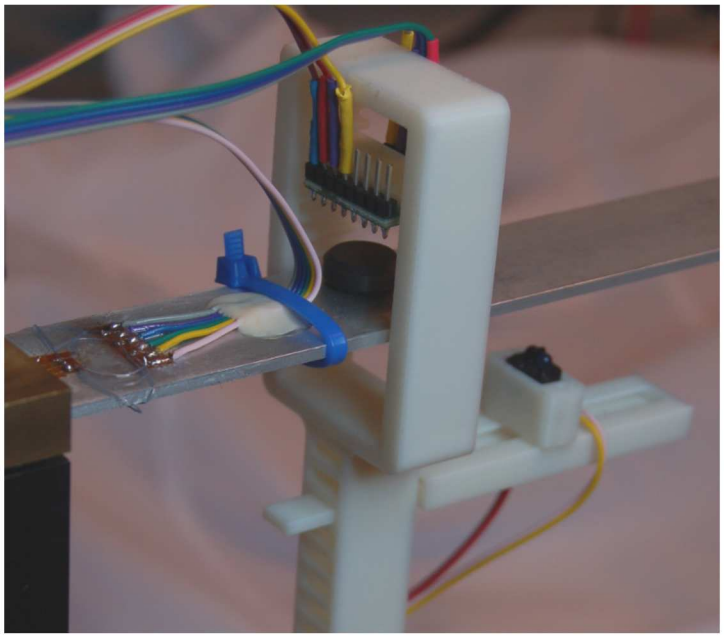

Fig. A.3 Detail of sensor placement for *The Rulers*. The following adjustments are available: independent discrete vertical position for IR and Hall effect sensors, and continuous longitudinal position for the IR sensor in relation to the Hall sensor longitudinal position. Apparatus design is a collaboration with Anthony Piciacchia. Photo by Vanessa Yaremchuk. Reproduced with permission.

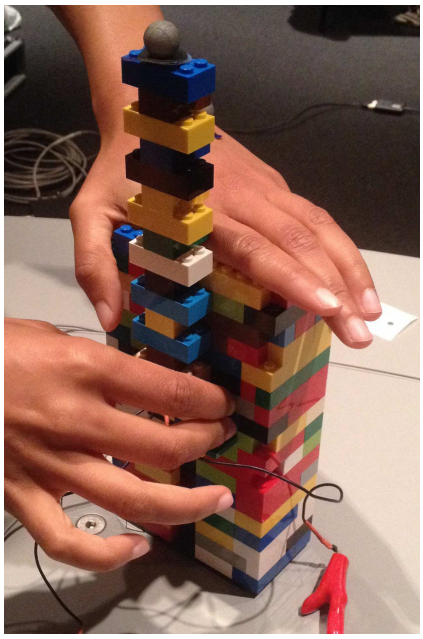

Fig. A.4 Building for infrared sensor calibration (assisted by Mailis Rodrigues). LEGO box blocks infrared light from the motion capture cameras. The right hand displaces the sensor inside the box, which fixture only allows vertical displacement. The left hand is the obstacle for the sensor's infrared light—common scenario in DMI applications. Pictured: Mailis Rodrigues. Reproduced with permission.

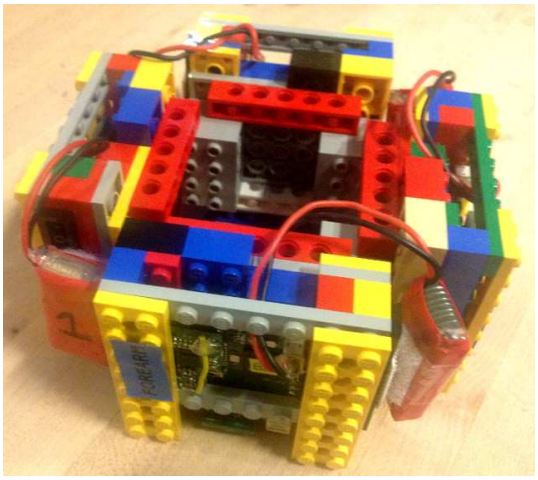

Fig. A.5 Building for MARG sensors calibration. The design has a space in the center for the hand. This allows the operator to perform random motions in all directions. The perpendicularity of the sensor placement allows verification of heading angle. Collaboration with MIT Media Lab Responsive Environments Group, Eric Berkson, and Tom Kepple.

Appendix B

IEEE Copyright Information

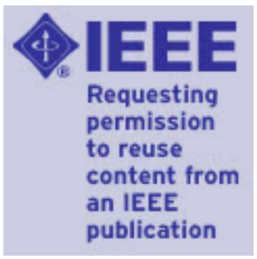

Title: Multiple-Model Linear Kalman Filter Framework for Unpredictable Signals
Author: Medeiros, C.B.; Wanderley, M.M.
Publication: IEEE Sensors Journal
Publisher: IEEE
Date: April 2014

Thesis / Dissertation Reuse

The IEEE does not require individuals working on a thesis to obtain a formal reuse license, however, you may print out this statement to be used as a permission grant:

Requirements to be followed when using any portion (e.g., figure, graph, table, or textual material) of an IEEE copyrighted paper in a thesis:

1) In the case of textual material (e.g., using short quotes or referring to the work within these papers) users must give full credit to the original source (author, paper, publication) followed by the IEEE copyright line © 2011 IEEE.
2) In the case of illustrations or tabular material, we require that the copyright line © [Year of original publication] IEEE appear prominently with each reprinted figure and/or table.
3) If a substantial portion of the original paper is to be used, and if you are not the senior author, also obtain the senior author's approval.

Requirements to be followed when using an entire IEEE copyrighted paper in a thesis:

1) The following IEEE copyright/ credit notice should be placed prominently in the references: © [year of original publication] IEEE. Reprinted, with permission, from [author names, paper title, IEEE publication title, and month/year of publication]
2) Only the accepted version of an IEEE copyrighted paper can be used when posting the paper or your thesis on-line.
3) In placing the thesis on the author's university website, please display the following message in a prominent place on the website: In reference to IEEE copyrighted material which is used with permission in this thesis, the IEEE does not endorse any of [university/educational entity's name goes here]'s products or services. Internal or personal use of this material is permitted. If interested in reprinting/republishing IEEE copyrighted material for advertising or promotional purposes or for creating new collective works for resale or redistribution, please go to http://www.ieee.org/publications_standards/publications/rights/rights_link.html to learn how to obtain a License from RightsLink.

If applicable, University Microfilms and/or ProQuest Library, or the Archives of Canada may supply single copies of the dissertation.

IEEE COPYRIGHT AND CONSENT FORM

To ensure uniformity of treatment among all contributors, other forms may not be substituted for this form, nor may any wording of the form be changed. This form is intended for original material submitted to the IEEE and must accompany any such material in order to be published by the IEEE.Please read the form carefully and keep a copy for your files.

TITLE OF PAPER/ARTICLE/REPORT, INCLUDING ALL CONTENT IN ANY FORM, FORMAT, OR MEDIA (hereinafter, "The Work"):**Multiple-model linear Kalman filter framework for unpredictable signals**

COMPLETE LIST OF AUTHORS:**BRUM Medeiros, Carolina; Mortensen Wanderley, Marcelo**

IEEE PUBLICATION TITLE (Journal, Magazine, Conference, Book):**IEEE Sensors Journal**

COPYRIGHT TRANSFER

1. The undersigned hereby assigns to The Institute of Electrical and Electronics Engineers,Incorporated (the "IEEE") all rights under copyright that may exist in and to: (a) the above Work,including any revised or expanded derivative works submitted to the IEEE by the undersigned based on the Work; and (b) any associated written or multimedia components or other enhancements accompanying the Work.

CONSENT AND RELEASE

2. ln the event the undersigned makes a presentation based upon the Work at a conference hosted or sponsored in whole or in part by the IEEE, the undersigned, in consideration for his/her participation in the conference, hereby grants the IEEE the unlimited, worldwide, irrevocable permission to use, distribute, publish, license, exhibit, record, digitize, broadcast, reproduce and archive, in any format or medium, whether now known or hereafter developed: (a) his,&er presentation and comments at the conference; (b) any written materials or multimedia files used in connection with his/her presentation; and (c) any recorded interviews of him/her (collectively, the "Presentation"). The permission granted includes the transcription and reproduction ofthe Presentation for inclusion in products sold or distributed by IEEE and live or recorded broadcast ofthe Presentation during or after the conference.

3. In connection with the permission granted in Section 2, the undersigned hereby grants IEEE the unlimited, worldwide, irrevocable right to use his/her name, picture, likeness, voice and biographical information as part of the advertisement, distribution and sale of products incorporating the Work or Presentation, and releases IEEE from any claim based on right of privacy or publicity.

4. The undersigned hereby warrants that the Work and Presentation (collectively, the "Materials") are original and that he/she is the author of the Materials. To the extent the Materials incorporate text passages, figures, data or other material from the works of others, the undersigned has obtained any necessary permissions. Where necessary, the undersigned has obtained all third party permissions and consents to grant the license above and has provided copies of such permissions and consents to IEEE.

[ ] Please check this box if you do not wish to have video/audio recordings made of your conference presentation.

See below for Retained Rights/Terms and Conditions, and Author Responsibilities.

AUTHOR RESPONSIBILITIES

The IEEE distributes its technical publications throughout the world and wants to ensure that the material submitted to its publications is properly available to the readership of those publications. Authors must ensure that their Work meets the requirements as stated in section 8.2.1 of the IEEE PSPB Operations Manual, including provisions covering originality, authorship, author responsibilities and author misconduct. More information on

IEEEs publishing policies may be found at http://www.ieee.org/publications_standards/publications/rights/pub_tools_policies.html. Authors are advised especially of IEEE PSPB Operations Manual section 8.2.1.B12: "It is the responsibility of the authors, not the IEEE, to determine whether disclosure of their material requires the prior consent of other parties and, if so, to obtain it." Authors are also advised of IEEE PSPB Operations Manual section 8.1.1B: "Statements and opinions given in work published by the IEEE are the expression of the authors."

RETAINED RIGHTS/TERMS AND CONDITIONS

General

1. Authors/employers retain all proprietary rights in any process, procedure, or article of manufacture described in the Work.

2. Authors/employers may reproduce or authorize others to reproduce the Work, material extracted verbatim from the Work, or derivative works for the author's personal use or for company use, provided that the source and the IEEE copyright notice are indicated, the copies are not used in any way that implies IEEE endorsement of a product or service of any employer, and the copies themselves are not offered for sale.

3. In the case of a Work performed under a U.S. Government contract or grant, the IEEE recognizes that the U.S. Government has royalty-free permission to reproduce all or portions of the Work, and to authorize others to do so, for official U.S. Government purposes only, if the contract/grant so requires.

4. Although authors are permitted to re-use all or portions of the Work in other works, this does not include granting third-party requests for reprinting, republishing, or other types of re-use.The IEEE Intellectual Property Rights office must handle all such third-party requests.

5. Authors whose work was performed under a grant from a government funding agency are free to fulfill any deposit mandates from that funding agency.

Author Online Use

6. Personal Servers. Authors and/or their employers shall have the right to post the accepted version of IEEE-copyrighted articles on their own personal servers or the servers of their institutions or employers without permission from IEEE, provided that the posted version includes a prominently displayed IEEE copyright notice and, when published, a full citation to the original IEEE publication, including a link to the article abstract in IEEE Xplore.Authors shall not post the final, published versions of their papers.

7. Classroom or Internal Training Use. An author is expressly permitted to post any portion of the accepted version of his/her own IEEE-copyrighted articles on the authors personal web site or the servers of the authors institution or company in connection with the authors teaching, training, or work responsibilities, provided that the appropriate copyright, credit, and reuse notices appear prominently with the posted material. Examples of permitted uses are lecture materials, course packs, e-reserves, conference presentations, or in-house training courses.

8. Electronic Preprints. Before submitting an article to an IEEE publication, authors frequently post their manuscripts to their own web site, their employers site, or to another server that invites constructive comment from colleagues.Upon submission of an article to IEEE, an author is required to transfer copyright in the article to IEEE, and the author must update any previously posted version of the article with a prominently displayed IEEE copyright notice. Upon publication of an article by the IEEE, the author must replace any previously posted electronic versions of the article with either (1) the full citation to the IEEE work with a Digital Object Identifier (DOI) or link to the article abstract in IEEE Xplore, or (2) the accepted version only (not the IEEE-published version), including the IEEE copyright notice and full citation, with a link to the final, published article in IEEE Xplore.

INFORMATION FOR AUTHORS

IEEE Copyright Ownership

It is the formal policy of the IEEE to own the copyrights to all copyrightable material in its technical publications and to the individual contributions contained therein, in order to protect the interests of the IEEE, its authors and their employers, and, at the same time, to facilitate the appropriate re-

use of this material by others.The IEEE distributes its technical publications throughout the world and does so by various means such as hard copy, microfiche, microfilm, and electronic media.It also abstracts and may translate its publications, and articles contained therein, for inclusion in various compendiums, collective works, databases and similar publications.

Author/Employer Rights

If you are employed and prepared the Work on a subject within the scope of your employment, the copyright in the Work belongs to your employer as a work-for-hire. In that case, the IEEE assumes that when you sign this Form, you are authorized to do so by your employer and that your employer has consented to the transfer of copyright, to the representation and warranty of publication rights, and to all other terms and conditions of this Form. If such authorization and consent has not been given to you, an authorized representative of your employer should sign this Form as the Author.

GENERAL TERMS

1. The undersigned represents that he/she has the power and authority to make and execute this form.
2. The undersigned agrees to identify and hold harmless the IEEE from any damage or expense that may arise in the event of a breach of any of the warranties set forth above.
3. In the event the above work is not accepted and published by the IEEE or is withdrawn by the author(s) before acceptance by the IEEE, the foregoing grant of rights shall become null and void and all materials embodying the Work submitted to the IEEE will be destroyed.
4. For jointly authored Works, all joint authors should sign, or one of the authors should sign as authorized agent for the others.

Carolina Brum Medeiros	**22-08-2013**
Author/Authorized Agent For Joint Authors	**Date(dd-mm-yy)**

THIS FORM MUST ACCOMPANY THE SUBMISSION OF THE AUTHOR'S MANUSCRIPT.
Questions about the submission of the form or manuscript must be sent to the publication's editor.Please direct all questions about IEEE copyright policy to:
IEEE Intellectual Property Rights Office, copyrights@ieee.org, +1-732-562-3966 (telephone)

Appendix C

Ethics Approval

Research Ethics Board Office
James Administration Bldg.
845 Sherbrooke Street West. Rm 429
Montreal, QC H3A 0G4

Tel: (514) 398-6831
Fax: (514) 398-4644
Website: www.mcgill.ca/research/researchers/compliance/human/

Research Ethics Board II
Certificate of Ethical Acceptability of Research Involving Humans

REB File #: 257-1213

Project Title: Comparison of Optical and Inertial System for Human Movement Analyses

Principal Investigator: Carolina Brum Medeiros **Department:** Schulich School of Music

Status: Ph.D. Student **Supervisor:** Prof. M. Wanderley

Co-Investigators/Other Researchers: Joseph Paradiso, Michael Lapinski, Eric Berkson

Approval Period: Dec. 12, 2013 to Dec. 11, 2014

The REB-II reviewed and approved this project by delegated review in accordance with the requirements of the McGill University Policy on the Ethical Conduct of Research Involving Human Participants and the Tri-Council Policy Statement: Ethical Conduct for Research Involving Humans.

Deanna Collin
Research Ethics Administrator

---

* All research involving human participants requires review on an annual basis. A Request for Renewal form should be submitted 2-3 weeks before the above expiry date.
* When a project has been completed or terminated a Study Closure form must be submitted.
* Should any modification or other unanticipated development occur before the next required review, the REB must be informed and any modification can't be initiated until approval is received.

References

[1] E. R. Miranda and M. M. Wanderley, *New Digital Musical Instruments:Control and Interaction Beyond the Keyboard*. A-R Editions, 2006.

[2] B. Buxton, "Artists and the art of the luthier," *SIGGRAPH Computer Graphics*, vol. 31, no. 1, pp. 10–11, Feb. 1997. [Online]. Available: http://doi.acm.org/10.1145/248307.248315

[3] International Bureau of Weights and Measures, Ed., *Vocabulary of Basic and General Terms in Metrology (VIM)*, 3rd ed. Joint Committee for Guides in Metrology (JCGM), 2012, standard.

[4] ——, *Evaluation of Measurement Data – Guide to the Expression of Uncertainty in Measurement (GUM)*. Joint Committee for Guides in Metrology (JCGM), 2008, standard. [Online]. Available: http://www.bipm.org/utils/common/documents/jcgm/JCGM_100_2008_E.pdf

[5] P. Stein, "The Unified Approach to the Engineering of Measurement Systems for Test and Evaluation - a Brief Survey," in *Instrumentation and Measurement Technology Conference Proceedings (IMTC 96)*, I. Q. Measurements, Ed., 1996.

[6] P. K. Stein, *The Unified Approach to the Engineering of Measurement Systems - Basic Concepts*. Stein Engineering Services, Inc, 1992.

[7] C. Dobrian and D. Koppelman, "The 'E' in NIME: Musical Expression with New Computer Interfaces," in *Proceedings of the International Conference on New Interfaces for Musical Expression (NIME 2006)*, 2006. [Online]. Available: http://dl.acm.org/citation.cfm?id=1142215.1142283

[8] P. Cook, "Principles for Designing Computer Music Controllers," in *Proceedings of the International Conference on New Interfaces for Musical Expression (NIME 2001)*, 2001.

[9] D. Kushner. (2011) The Making of Arduino. Accessed: May 2014. [Online]. Available: http://spectrum.ieee.org/geek-life/hands-on/the-making-of-arduino/0

[10] L. Buechley and H. Perner-Wilson, "Crafting technology: Reimagining the processes, materials, and cultures of electronics," *ACM Transactions on Computer-Human Interaction (TOCHI 2012)*, vol. 19, no. 3, pp. 21:1–21:21, Oct. 2012. [Online]. Available: http://doi.acm.org/10.1145/2362364.2362369

[11] M. T. Marshall, "Physical interface design for digital musical instruments," Ph.D. dissertation, McGill University, 2009.

[12] M. T. Marshall, M. Hartshorn, M. M. Wanderley, and D. J. Levitin, "Sensor Choice For Parameter Modulations In Digital Musical Instruments: Empirical Evidence From Pitch Modulation," *Journal of New Music Research*, vol. 38, no. 3, pp. 241–253, 2009.

[13] J. Chadabe, *Electric Sound: The Past and Promise of Electronic Music*. New Jersey, USA: Prentice Hall, 1997.

[14] J. Paradiso, K.-Y. Hsiao, and E. Hu, "Interactive Music for Instrumented Dancing Shoes," in *Proceedings of the International Computer Music Conference (ICMC 1999)*, Beijing, China, 1999.

[15] M. M. Wanderley and M. Battier, Eds., *Trends in Gestural Control of Music*. Paris, France: Ircam, 2000.

[16] J. Piringer. (2001. Accessed: May 2014) Elektronische musik und interaktivit at: Prinzipien, konzepte, anwendungen. Master Thesis Appendix: Liste der Instrumente. [Online]. Available: http://joerg.piringer.net/research/instruments.zip

[17] Troikatronix. Isadora. Accessed: July 2014. Troikatronix. [Online]. Available: http://troikatronix.com/isadora/about/

[18] C. B. Medeiros and M. M. Wanderley, "A Comprehensive Review of Sensors and Instrumentation Methods in Devices for Musical Expression," *Sensors*, vol. 14, no. 8, pp. 13 556–13 591, 2014.

[19] C. Chafe. Celletto. Accessed: July 2014. [Online]. Available: https://ccrma.stanford.edu/~cc/shtml/cellettoMusic.shtml

[20] D. Young, "The Hyperbow Controller: Real-Time Dynamics Measurement of Violin Performance," in *Proceeding of the International Conference on New Interfaces for Musical Expression (NIME 2002)*, Dublin, Ireland, May 2002.

[21] M. Waisvisz. 1984–1989 The Hand (first version). Accessed: August 2014. [Online]. Available: http://www.crackle.org/The%20Hands%201984.htm

[22] ——. 1989–2000 The Hand II. Accessed: August 2014. [Online]. Available: http://www.crackle.org/The%20Hands%202.htm

[23] L. Haken, E. Tellman, and P. Wolfe, "An Indiscrete Music Keyboard," *Computer Music Journal*, vol. 22, no. 1, pp. 30–48, 1998.

[24] M. Collicutt, C. Casciato, and M. M. Wanderley, "From Real to Virtual: A Comparison of Input Devices for Percussion Tasks," in *Proceedings of the International Conference on New Interfaces for Musical Expression (NIME 2009)*, Pittsburgh, USA, 2009.

[25] B. Bongers, "Exploring Novel Ways of Interaction in Musical Performance," in *Proceedings of the 3rd Conference on Creativity & Cognition*, ser. C&C '99. New York, NY, USA: ACM, 1999, pp. 76–81. [Online]. Available: http://doi.acm.org/10.1145/317561.317576

[26] M. Gurevich and A. Fyans, "Digital Musical Interactions: Performer-System Relationships and their Perception by Spectators," *Organised Sound*, vol. 16, no. 2, pp. 166–175, 2011.

[27] M. Gurevich, "Spectators of Mobile Musical Interactions: Opportunities and Challenges," in *Proceedings of the 9th ACM conference on Designing Interactive Systems. Workshop on Designing Musical Interactions for Mobile Systems.*, 2012.

[28] G. Welch and G. Bishop, "An Introduction to the Kalman Filter," in *SIGGRAPH Conference Proceedings*, 2001.

[29] R. Pallás-Areny and J. G. Webster, *Sensors and Signal Conditioning*. John Wiley & Sons, 2001.

[30] P. Horowitz and W. Hill, *The Art of Electronics*, 2nd ed. Cambridge University Press, 2004.

[31] M. T. Lapinski, E. Berkson, D. M. Scarborough, C. B. Medeiros, T. Kepple, T. J. Gill, and J. A. Paradiso, "A Wide-Range, Rapidly-Deployed, Wearable Wireless Inertial Motion Capture System For Sports Biomotion Analysis," *Journal of Biomedical and Health Informatics*, submitted.

[32] G. Essl and M. Rohs, "Interactivity for Mobile Music Making," *Organised Sound*, vol. 14, no. 2, pp. 197–207, 2009.

[33] B. Bongers, *Trends in Gestural Control of Music*. Centre Pompidou: Paris: IRCAM, 2000, ch. Physical Interfaces in the Electronic Arts. [Online]. Available: http://www.tufts.edu/programs/mma/emid/IRCAM/Bon.pdf

[34] M. M. Wanderley and N. Orio, "Evaluation of Input Devices for Musical Expression: Borrowing Tools from HCI," *Computer Music Journal*, vol. 26, no. 3, pp. 62–76, 2002.

[35] R. Begg and M. Palaniswami, *Computational Intelligence for Movement Sciences: Neural Networks and Other Emerging Techniques*. Idea Group Publishing, 2010.

[36] A. F. Page, H. D. Rosario, V. Mata, and A. Besa, "Rules of propagation of artifact to kinematic variables in human movement analysis: Effect of the angular displacement representation," *Journal of Biomechanical Engineering*, 2013.

[37] L. Naveda and M. Leman, "The spatiotemporal representation of dance and music gestures using Topological Gesture Analysis (TGA)," *Music Perception*, vol. 28, 2010.

[38] D. Lai, R. Begg, and M. Palaniswami, "Computational intelligence in gait research: A perspective on current applications and future challenges," *IEEE Transactions on Information Technology in Biomedicine*, vol. 13, no. 5, pp. 687 –702, 2009.

[39] T. Cloete and C. Scheffer, "Benchmarking of a full-body inertial motion capture system for clinical gait analysis," in *Annual International Conference of the IEEE Engineering in Medicine and Biology Society (EMBS 2008)*, 2008.

[40] J. Fraden, *Handbook of Modern Sensors: Physics, Design and Applications*, 3rd ed. Springer, 2004.

[41] K. Hoffmann, *An Introduction to Measurements Using Strain Gages*. HBM, 2012.

[42] Omega. Transactions in Measurement and Control - Volume 2: Data Acquisition. Accessed: July 2014. [Online]. Available: http://www.omega.com/literature/transactions/transactions_Vol_II.pdf

[43] C. Kitchin and L. Counts. A Designer's Guide to Instrumentation Amplifiers, 3rd Edition. Accessed: April 2014. Analog Devices. [Online]. Available: http://www.analog.com/static/imported-files/design_handbooks/5812756674312778737Complete_In_Amp.pdf

[44] T. Kugelstadt. Getting the most out of your instrumentation amplifier design. Accessed: July 2014. Texas Instruments. [Online]. Available: http://www.ti.com/lit/an/slyt226/slyt226.pdf

[45] R. Brown and P. Hwang, *Introduction to Random Signals and Applied Kalman Filtering*. New York City, USA: John Wiley & Sons, 1997.

[46] D. Hall and J. Llinas, *Handbook of Multisensor Data Fusion*. Boca Raton, USA: CRC Press, 2001.

[47] S. Haykin, *Kalman Filtering and Neural Networks*. New York City, USA: John Wiley & Sons, 2001, ch. Kalman Filters, pp. 1–22.

[48] P. Zarchan and H. Musoff, *Fundamentals of Kalman Filtering: A Practical Approach*. American Institute of Aeronautics and Astronautics, 2005, vol. 208.

[49] D. L. Hall and S. A. H. McMullen, *Mathematical Techniques in Multisensor Data Fusion*, 2nd ed. Artech House, 2004. [Online]. Available: http://portal.acm.org/citation.cfm?id=531406

[50] A. M. Sabatini, "Estimating Three-Dimensional Orientation of Human Body Parts by Inertial/Magnetic Sensing," *Sensors*, vol. 11, pp. 1489–1525., 2011.

[51] X. Yun, E. Bachmann, and R. McGhee, "A Simplified Quaternion-Based Algorithm for Orientation Estimation From Earth Gravity and Magnetic Field Measurements," *IEEE Transactions on Instrumentation and Measurement*, vol. 57, no. 3, pp. 638–650, 2008.

[52] X. Yun and E. Bachmann, "Design, Implementation, and Experimental Results of a Quaternion-Based Kalman Filter for Human Body Motion Tracking," *IEEE Transactions on Robotics*, vol. 22, no. 6, pp. 1216 –1227, 2006.

[53] J. Musič, R. Kamnik, and M. Munih, "Model based inertial sensing of human body motion kinematics in sit-to-stand movement," *Simulation Modelling Practice and Theory*, vol. 16, no. 8, pp. 933 – 944, 2008. [Online]. Available: http://www.sciencedirect.com/science/article/pii/S1569190X08001019

[54] V. Fohanno, F. Colloud, M. Begon, and P. Lacouture, "Estimation of the 3D kinematics in kayak using an extended Kalman filter algorithm: a pilot study," *Computer Methods in Biomechanics and Biomedical Engineering*, vol. 13, pp. 55–56, 2010.

[55] Y. Tao and H. Hu, "A novel sensing and data fusion system for 3-d arm motion tracking in telerehabilitation," *IEEE Transactions on Instrumentation and Measurement*, vol. 57, no. 5, pp. 1029 –1040, 2008.

[56] R. Zhu and Z. Zhou, "A real-time articulated human motion tracking using tri-axis inertial/magnetic sensors package," *Neural Systems and Rehabilitation Engineering, IEEE Transactions on*, vol. 12, no. 2, pp. 295 –302, June 2004.

[57] J. Marins, X. Yun, E. Bachmann, R. Mcghee, and M. Zyda, "An Extended Kalman Filter for Quaternion-based Orientation Estimation Using MARG Sensors," in *Proceedings of the International Conference on Intelligent Robots and Systems (RSJ 2001)*, vol. 4, 2001, pp. 2003–2011 vol.4.

[58] J. Farrell, *Aided Navigation: GPS with High Rate Sensors*. McGraw-Hill, 2008.

[59] C. Medeiros and M. M. Wanderley, "Multiple-Model Linear Kalman Filter Framework for Unpredictable Signals," *IEEE Sensors Journal*, vol. 14, no. 4, pp. 979–991, April 2014.

[60] L. Drolet, F. Michaud, and J. Cote, "Adaptable Sensor Fusion Using Multiple Kalman Filters," in *Proceedings of the International Conference on Intelligent Robots and Systems (IROS 2000)*, vol. 2, 2000, pp. 1434 –1439 vol.2.

[61] M. Lapinski, "A Platform for High-Speed Biomechanical Data Analysis using Wearable Wireless Sensors," Ph.D. dissertation, MIT, Cambridge, USA, 2013.

[62] D. Roetenberg, H. Luinge, C. Baten, and P. Veltink, "Compensation of Magnetic Disturbances Improves Inertial and Magnetic Sensing of Human Body Segment orientation," *IEEE Transactions on Neural Systems and Rehabilitation Engineering*, vol. 13, no. 3, pp. 395 –405, 2005.

[63] S. Madgwick, A. J. L. Harrison, and R. Vaidyanathan, "Estimation of IMU and MARG Orientation Using a Gradient Descent Algorithm," in *IEEE International Conference on Rehabilitation Robotics (ICORR 2011)*, June 2011, pp. 1–7.

[64] G. Vigliensoni and M. M. Wanderley, "A Quantitative Comparison of Position Trackers for the Development of a Touch-less Musical Interface," in *Proceedings of the International Conference on New Interfaces for Musical Expression Proceedings (NIME 2012)*, 2012.

[65] K. Nymoen, A. Voldsund, S. A. Skogstad, A. R. Jensenius, and J. Torresen, "Comparing Motion Data from an iPod Touch to an Optical Infrared Marker-Based Motion Capture System," in *Proceedings of the International Conference on New Interface for Musical Expression Proceedings (NIME 2012)*, 2012.

[66] S. A. Skogstad, K. Nymoen, Y. de Quay, and A. R. Jensenius, "OSC Implementation and Evaluation of the Xsens MVN suit," in *Proceedings of the International Conference on New Interfaces for Musical Expression (NIME 2011)*, 2011.

[67] B. Caramiaux and A. Tanaka, "Machine Learning of Musical Gestures," in *Proceedings of the International Conference on New Interface for Musical Expression Proceedings (NIME 2013)*, 2013.

[68] A. Tanaka, A. Parkinson, Z. Settel, and K. Tahiroglu, "A Survey and Thematic Analysis Approach as Input to the Design of Mobile Music GUIs," in *Proceedings of the International Conference on New Interfaces for Musical Expression (NIME 2012)*, 2012.

[69] J. Thibodeau and M. M. Wanderley, "Trumpet Augmentation and Technological Symbiosis," *Computer Music Journal*, vol. 37, no. 3, pp. 12–25, 2013.

[70] E. Guaus, J. Bonada, E. Maestre, A. Perez, and M. Blaauw, "Calibration Method to Accurately Measure Bow Force in Real Violin Performances," in *Proceeding of the International Computer Music Conference (ICMC 2009)*, 2009.

[71] N.-W. Gong, J. Steimle, S. Olberding, S. Hodges, N. Gillian, Y. Kawahara, and J. A. Paradiso, "PrintSense: A Versatile Sensing Technique to Support Multimodal Flexible Surface Interaction," in *ACM CHI Conference on Human Factors in Computing Systems (CHI 2014)*, 2004.

[72] R. Koehly, M. M. Wanderley, T. van de Ven, and D. Curtil, "In-House Development of Paper Force Sensors for Musical Applications," *Computer Music Journal*, vol. 28, no. 2, pp. 22–35, 2014.

[73] A. Hollinger, J. Thibodeau, and M. M. Wanderley, "An Embedded Hardware Platform for Fungible Interfaces," in *Proceedings of the International Computer Music Conference (ICMC 2010)*, 2010, pp. 56–59.

[74] T. Mitchell, S. Madgwick, and I. Heap, "Musical Interaction with Hand Posture and Orientation: A Toolbox of Gestural Control Mechanisms," in *Proceedings of the International Conference on New Interfaces for Musical Expression (NIME 2012)*, 2012.

[75] A. Hollinger and M. M. Wanderley. (2006, January) Evaluation of Commercial Force-Sensing Resistors. Accessed: July 2014. Internal Report IDMIL Laboratory, McGill University. [Online]. Available: http://idmil.org/_media/publications/hollinger_wanderley_fsrevaluation.pdf?id=publications

[76] G. Szekely and M. Rizzo, "Hierarchical Clustering via Joint Between-Within Distances: Extending Ward's Minimum Variance Method," *Journal of Classification*, vol. 22, pp. 151–183, 2005.

[77] Arduino playground. Accessed: May 2014. forum. [Online]. Available: http://playground.arduino.cc/Main/InterfacingWithHardware#InputTOC

[78] Threads on sensors in instructables portal. Accessed: May 2014. forum. [Online]. Available: http://www.instructables.com/tag/type-id/category-technology/channel-sensors/

[79] Sensorwiki. Accessed: May 2014. IDMIL. [Online]. Available: www.sensorwiki.org

[80] T. Kamada and S. Kawai, "An Algorithm for Drawing General Undirected Graphs," *Information Processing Letters*, vol. 31, 1989.

[81] R. A. Hanneman and M. Riddle, *Introduction to social network methods*, [Online], Ed. University of California, 2005. [Online]. Available: http://faculty.ucr.edu/~hanneman/nettext/

[82] T. Ahola, K. Tahiroglu, T. Ahmaniemi, F. Belloni, and V. Ranki, "Raja – A Multidisciplinary Artistic Performance," in *Proceedings of the International Conference on New Interfaces for Musical Expression (NIME 2011)*, 2011.

[83] E. Jessop, P. A. Torpey, and B. Bloomberg, "Music and Technology in Death and the Powers," in *Proceedings of the International Conference on New Interfaces for Musical Expression (NIME 2011)*, 2011.

[84] T. Todoroff, "Wireless Digital/Analog Sensors for Music and Dance Performances," in *Proceedings of the International Conference on New Interfaces for Musical Expression (NIME 2011)*, 2011.

[85] N. Gillian, "Gesture recognition for musician computer interaction," Ph.D. dissertation, School of Music and Sonic Arts, Queen's University Belfast, Belfast, Ireland, 2011.

[86] Analog devices. The Five Motion Senses: Using MEMS Inertial Sensing to Transform Applications. Accessed: May 2014. [Online]. Available: http://www.analog.com/static/imported-files/overviews/The_Five_Motion_Senses.pdf

[87] C. J. Fisher. Analog Devices Application Note on Using an Accelerometer for Inclination Sensing. Accessed: July 2014. Analog Devices. [Online]. Available: http://www.analog.com/static/imported-files/application_notes/AN-1057.pdf

[88] M. Park, "Error Analysis and Stochastic Modeling of MEMS based Inertial Sensors for Land Vehicle Navigation Applications," Ph.D. dissertation, The University of Calgary, 2004.

[89] Accelerometer for AHRS Application. Accessed: May 2014. Colibrys. [Online]. Available: http://www.colibrys.com/files/pdf/products/30N-AHRS.B.05.11.pdf

[90] R. Dorobantu and C. Gerlach, "Investigation of a Navigation Grade RLG SIMU type iNAV RQH," Ph.D. dissertation, Institut fur Astronomische und Physikalische Geodasie Technische Universitat Munchen, 2004.

[91] J. J. Allen, R. D. Kinney, J. Sarsfield, M. Daily, J. R. Ellis, J. Smith, S. Montague, R. Howe, B. Boser, R. Horowitz, A. Pisano, M. Lemkin, W. A. Clark, and T. Juneau, "Integrated micro-electro-mechanical sensor development for inertial applications," *IEEE Aerospace and Electronic Systems Magazine*, vol. 13, no. 11, pp. 36–40, Nov 1998.

[92] Kionix. An012 accelerometer errors. Accessed: April 2014. Kionix. [Online]. Available: http://www.kionix.com/sites/default/files/AN012%20Accelerometer%20Errors.pdf

[93] T. L. Grigorie, M. Lungu, I. R. Edu, and R. Obreja, "Concepts for Error Modeling of Miniature Accelerometers Used in Inertial Navigation Systems," in *Annals of the University of Craiova, Electrical Engineering series*, no. 34, 2010.

[94] M. Park and Y. Gao, "Error and Performance Analysis of MEMS-based Inertial Sensors with a Low-cost GSP Receiver," *Sensors*, no. 8, pp. 2240–2261, 2008.

[95] W. T. Ang, P. K. Khosla, and C. N. Riviere, "Nonlinear Regression Model of a Low-g MEMS Accelerometer," *IEEE Sensors Journal*, vol. 7, no. 1, 2007.

[96] T. Baba, M. Hashida, and H. Katayose, "'VirtualPhilharmony': A Conducting SySystem with Heuristics of Conducting an Orchestra," in *Proceedings of the International Conference on New Interfaces for Musical Expression (NIME 2010)*, 2010.

[97] S. L. Groux, J. Manzoli, and P. F. Verschure, "Embodied and Collaborative Musical Interaction in the Multimodal Brain Orchestra," in *Proceedings of the International Conference on New Interfaces for Musical Expression (NIME 2010)*, 2010.

[98] V. Yaremchuk and M. M. Wanderley, "Artificial Neural Networks for Movement Analysis of Musical Performance," in *Proceedings of the International Workshop on Movement and Computing (MOCO 2014)*, 2014.

[99] Interlink. Interlink Electronics FSR© Force Sensing Resistors. Accessed: February 2014. Interlink. [Online]. Available: http://akizukidenshi.com/download/ds/interlinkelec/94-00004_Rev_B%20FSR%20Integration%20Guide.pdf

[100] L. S. Pardue, A. Boch, M. Boch, C. Southworth, and A. Rigopulos, "Gamelan Elektrika: An Electronic Balinese Gamelan," in *Proceedings of the International Conference on New Interfaces for Musical Expression (NIME 2011)*, 2011.

[101] C. B. Medeiros and M. M. Wanderley, "Conditioning Circuits and Data Fusion for low Performance Sensors," [Working Paper].

[102] B. Carter, "Op amps and comparators - don't confuse them: Sloa067," Texas Instruments, Tech. Rep., 2001.

[103] A. Window, Ed., *Strain Gauge Technology*, 2nd ed. Elsevier Applied Science, 1993.

[104] W. N. Sharpe, Ed., *Springer Handbook of Experimental Solid Mechanics*. Springer, 2008.

[105] C. B. Medeiros and M. M. Wanderley, "Evaluation of Sensor Technologies for The Rulers: a Kalimba-like Digital Musical Instrument," in *Proceedings of the Sound and Music Computing Conference (SMC 2011)*, 2011.

[106] H. Leeuw, "The Electrumpet , a Hybrid Electro-Acoustic Instrument," in *Proceedings of the International Conference on New Interfaces for Musical Expression (NIME 2009)*, 2009. [Online]. Available: http://www.nime.org/proceedings/2009/nime2009_193.pdf

[107] L. Jenkins, W. Page, S. Trail, G. Tzanetakis, and P. Driessen, "An Easily Removable, Wireless Optical Sensing System (EROSS) for the Trumpet," in *Proceedings of the International Conference on New Interfaces for Musical Expression (NIME 2013)*, 2013.

[108] Fully Integrated Proximity and Ambient Light Sensor with Infrared Emitter and I2C Interface. Accessed: July 2014. Vishay. [Online]. Available: http://www.vishay.com/docs/83798/vcnl4000.pdf

[109] A. McPherson, "Portable Measurement and Mapping of Continuous Piano Gesture," in *Proceedings of the International Conference on New Interfaces for Musical Expression (NIME 2013)*, 2013.

[110] G. Shear and M. Wright, "Further Developments in the Electromagnetically Sustained Rhodes Piano," in *Proceedings of the International Conference on New Interfaces for Musical Expression (NIME 2012)*, 2012.

[111] J. R. Buschert, "Musician Marker: Play Expressive Music Without Practice," in *Proceedings of the 2012 Conference on New Interfaces for Musical Expression (NIME 2012)*, 2012.

[112] T. Grosshauser and G. Tröster, "Finger Position and Pressure Sensing Techniques for Strings and Keyboard Instruments ," in *Proceedings of the International Conference on New Interfaces for Musical Expression (NIME 2013)*, 2013.

[113] G. Shear and M. Wright, "The Electromagnetically Sustained Rhodes Piano," in *Proceedings of the International Conference on New Interfaces for Musical Expression (NIME 2011)*, 2011.

[114] L. S. Pardue and A. McPherson, "Near-Field Optical Reflective Sensing for Bow Tracking," in *Proceedings of the International Conference on New Interfaces for Musical Expression (NIME 2013)*, 2013.

[115] M. Marchini, P. P., A. Pérez, and E. Maestre, "A Hair Ribbon Deflection Model for Low-Intrusiveness Measurement of Bow Force in Violin Performance," in *Proceedings of the International Conference on New Interfaces for Musical Expression (NIME 2011)*, 2011.

[116] M. Demoucron, A. Askenfelt, and R. Caussé, "Measuring Bow Force in Bowed String Performance: Theory and Implementation of a Bow Force Sensor," *Acta Acustica united with Acustica*, no. 95, pp. 718–732, 2009.

[117] J. Wang, N. d'Alessandro, S. Fels, and B. Pritchard, "Squeezy: Extending a Multi-touch Screen with Force Sensing Objects for Controlling Articulatory Synthesis," in *Proceedings of the 2011 Conference on New Interfaces for Musical Expression (NIME 2011)*, 2011.

[118] A. Hollinger, "Optical Sensing, Embedded Systems, and Musical Interfaces for Functional Neuroimaging," Ph.D. dissertation, McGill University, March 2014.

[119] A. Hollinger and M. M. Wanderley, "MRI-Compatible Optically-Sensed Cello," in *Proceedings of IEEE SENSORS Conference*, 2013. [Online]. Available: http://idmil.org/fmri/cello

[120] ——, "Optoelectronic Acquisition and Control Board for Musical Applications," in *Proceedings of the International Conference on New Interfaces for Musical Expression (NIME 2012)*, 2012.

[121] J. A. Paradiso and N. Gershenfeld, "Musical applications of electric field sensing," *Computer Music Journal*, vol. 21, no. 2, pp. 69 – 89, 1997.

[122] N.-W. Gong, N. Zhao, and J. A. Paradiso, "A Customizable Sensate Surface for Music Control," in *Proceeding of the Internation Conference on New Interfaces for Musical Expression (NIME 2011)*, 2011.

[123] W. Elmenreich, "Sensor fusion in time-triggered systems," Ph.D. dissertation, Institut für Technische Informatik, Stuttgart, Germany 2002.

[124] J. Raol, *Multi-Sensor Data Fusion With MATLAB*. Boca Raton, USA: CRC Press, 2010.

[125] J. Llinas and D. Hall, "An Introduction to Multi-sensor Data Fusion," in *Proceedings of the IEEE International Symposium on Circuits and Systems (ISCAS 1998)*, vol. 6, may-3 jun 1998, pp. 537 –540 vol.6.

[126] L. Klein, *Sensor and Data Fusion: A Tool for Information Assessment and Decision Making*. Bellingham, USA: SPIE Press, 2004.

[127] E. L. Waltz and J. Llinas, *Multisensor Data Fusion*. Norwood, MA, USA: Artech House, Inc., 1990.

[128] C. Fowler, "Comments on the cost and performance of military systems," *IEEE Transactions on Aerospace and Electronic Systems*, vol. AES-15, no. 1, pp. 2 –10, 1979.

[129] P. Maybeck, *Stochastic models, estimation and control*. Waltham, USA: Academic Press, 1979.

[130] G. Cook, *Mobile Robots: Navigation, Control and Remote Sensing*, 1st ed. New York City, USA: John Wiley & Sons, Inc., 2011.

[131] M. Grewal and A. Andrews, *Kalman Filtering: Theory and Practice Using MATLAB*. New York City, USA: John Wiley & Sons, Inc., 2001.

[132] E. Arnaud and E. Memin, "An efficient Rao-Blackwellized particle filter for object tracking," in *Proceeding of the IEEE International Conference on Image Processing*, Genes, Italy, 2005. [Online]. Available: http://hal.inria.fr/inria-00306723

[133] A. Doucet and A. M. Johansen, "A Tutorial on Partical Filtering and Smoothing: Fifteen years After," The Institute of Statistical Mathematics, Oxford, UK, Tech. Rep., 2008.

[134] D. Comotti, M. Ermidoro, M. Galizzi, and A. Vitali, "Development of a Wireless Low-power Multi-sensor Network for Motion Tracking Applications," in *IEEE International Conference on Body Sensor Networks (BSN 2013)*, 2013. [Online]. Available: http://ieeexplore.ieee.org/xpl/mostRecentIssue.jsp?punumber=6573244

[135] J. Vasconcelos, G. Elkaim, C. Silvestre, P. Oliveira, and B. Cardeira, "Geometric Approach to Strapdown Magnetometer Calibration in Sensor Frame," *IEEE Transactions on Aerospace and Electronic Systems*, vol. 47, no. 2, pp. 1293–1306, April 2011.

[136] J. Malloch, D. Birnbaum, E. Sinyor, and M. M. Wanderley, "A New Conceptual Framework for Digital Musical Instruments," *Proc. of the 9th Int. Conference on Digital Audio Effects (DAFx-06)*, pp. 49–52, 2006.

[137] S. Ferguson and M. M. Wanderley, "The McGill Digital Orchestra: An Interdisciplinary Project on Digital Musical Instruments," *Journal of Interdisciplinary Music Studies*, vol. 4, pp. 17–35, 2010.

[138] A. S. Kobayashi, *Handbook on Experimental Mechanics*. New York City, USA: John Wiley & Sons, 1993.

[139] Fairchild. Qrd1113 datasheet. Accessed: July 2014. [Online]. Available: http://www.fairchildsemi.com/ds/QR/QRD1114.pdf

[140] Sharp. GP2Y0A02YK0F: Distance Measuring Sensor Unit. Accessed: November 2014. [Online]. Available: http://www.sharpsma.com/webfm_send/1487

[141] Honeywell. Datasheet SS49E/SS59ET Series: Economical Linear Position Sensor. Accessed: July 2014. Honeywell. [Online]. Available: http://sensing.honeywell.com/honeywell-sensing-ss39et-ss49e-ss59et-product-sheet-005850-3-en.pdf?name=SS49E

[142] Hall Effect Sensing and Application. Accessed: May 2014. Honeywell. [Online]. Available: http://sensing.honeywell.com/index.php?ci_id=47847

[143] J. Dias Pereira, P. Silva Girao, and O. Postolache, "Fitting Transducer Characteristics to Measured Data," *IEEE Instrumentation Measurement Magazine*, vol. 4, no. 4, pp. 26 –39, December 2001.

[144] D. Patranabis, S. Ghosh, and C. Bakshi, "Linearizing transducer characteristics," *IEEE Transactions on Instrumentation and Measurement*, vol. 37, no. 1, pp. 66 –69, March 1988.

[145] H. Erdem, "Implementation of software-based sensor linearization algorithms on low-cost microcontrollers," {*ISA*} *Transactions*, vol. 49, no. 4, pp. 552 – 558, 2010. [Online]. Available: http://www.sciencedirect.com/science/article/pii/S0019057810000364

[146] S. Khan, A. Alam, S. Ahmmad, I. Tijani, M. Hasan, L. Adetunji, S. Abdulazeez, S. Zaini, S. Othman, and S. Khan, "On the Issues of Linearizing a Sensor Characteristic Over a Wider Response Range," in *International Conference on Computer and Communication Engineering (ICCCE 2008)*, May 2008, pp. 72 –76.

[147] C. L. Dym and I. H. Shames, *Solid Mechanics: A Variational Approach, Augmented Edition*. New York, USA: Springer, 2013, ch. Theory of Linear Elasticity.

[148] L. L. Bucciarelli, *Engineering Mechanics for Structure*. Cambridge, USA: MIT Press, 2002, ch. Stresses: Beams in Bending.

[149] (2011, June) How Is Temperature Affecting Your Strain Measurement Accuracy? Accessed: July 2014. National Instruments. [Online]. Available: http://www.ni.com/white-paper/3432/en/#toc3

[150] K. F. Anderson, *The Constant Current Loop: A New Paradigm for Resistance Signal Conditioning*, ser. NASA Technical Memorandum 104260. National Aeronautics and Space Administration, 1992.

[151] T. T. S. of Measurement Group, Ed., *Strain Gage Based Transducer*. Raleigh, USA: Measurement Group, Inc., 1988.

[152] T. L. Group. (2010) Company Profile An Introduction to the LEGO Group 2010. Accessed: July 2014. The LEGO Group. [Online]. Available: http://cache.lego.com/upload/contentTemplating/AboutUsFactsAndFiguresContent/otherfiles/download98E142631E71927FDD52304C1C0F1685.pdf

[153] Arduino. Accessed: May 2014. Arduino Analog Input. [Online]. Available: http://playground.arduino.cc/CourseWare/AnalogInput

[154] D.-J. Jwo, "Remarks on the Kalman Filtering Simulation and Verification," *Applied Mathematics and Computation*, vol. 186, no. 1, pp. 159 – 174, 2007. [Online]. Available: http://www.sciencedirect.com/science/article/pii/S009630030600926X

[155] J. A. Farrell, *Aided Navigation: GPS with High Rate Sensors*. McGraw Hill, 2008.

[156] D.-J. Jwo, F.-C. Chung, and T.-P. Weng, *Sensor Fusion and its Applications*. Rijeka, Croatia: InTech, 2010, ch. Adaptive Kalman Filter for Navigation Sensor Fusion.

[157] C. Hu, W. Chen, Y. Chen, and D. Liu, "Adaptive Kalman Filtering for Vehicle Navigation ," *Journal of Global Positioning Systems*, vol. 2, no. 1, pp. 42–47, November 2003.

[158] Q. Xia, M. Rao, Y. Ying, and X. Shen, "Adaptive Fading Kalman Filter with an Application," *Automatica*, vol. 30, no. 8, pp. 1333–1338, 1994.

[159] C. Hide, T. Moore, and M. Smith, "Adaptive Kalman Filtering for Low-cost INS/GPS," *The Journal of Navigation*, vol. 56, pp. 143–152, 2003.

[160] K. P. Mohamed, A. H.; Schwarz, "Adaptive Kalman Filtering for INS/GPS," *Journal of Geodesy*, vol. 73, no. 4, pp. 193–203, December 1999.

[161] D.-J. Jwo and S.-H. Wang, "Adaptive Fuzzy Strong Tracking Extended Kalman Filtering for GPS Navigation," *IEEE Sensors Journal*, vol. 7, no. 5, pp. 778–789, 2007.

[162] F. Janabi-Sharifi and M. Marey, "A Kalman-Filter-Based Method for Pose Estimation in Visual Servoing," *IEEE Transactions on Robotics*, vol. 26, no. 5, pp. 939–947, October 2010.

[163] Y. Bar-Shalom, T. Kirubarajan, and X.-R. Li, *Estimation with Applications to Tracking and Navigation*. New York City, USA: John Wiley & Sons, Inc., June 2001.

[164] P. de Vallière and D. Bonvin, "Application of Estimation Techniques to Batch Reactor - III. Modelling Refinements Which Improve the Quality of State and Parameter Estimation," *Computers & Chemical Engineering*, vol. 14, no. 7, pp. 799 – 808, 1990. [Online]. Available: http://www.sciencedirect.com/science/article/pii/0098135490870876

[165] M. Agarwal and D. Bonvin, "Improved State Estimator in the Face of Unreliable Parameters," *Journal of Process Control*, vol. 1, no. 5, pp. 251 – 257, 1991. [Online]. Available: http://www.sciencedirect.com/science/article/pii/095915249185016C

[166] D. Dochain, "State and Parameter Estimation in Chemical and Biochemical Processes: a Tutorial," *Journal of Process Control*, vol. 13, no. 8, pp. 801 – 818, 2003. [Online]. Available: http://www.sciencedirect.com/science/article/pii/S095915240300026X

[167] L. Ljung, "Asymptotic Behaviour of the Extended Kalman Filter as a Parameter Estimator for Linear System," *IEEE Transactions on Automatic Control*, vol. 24, pp. 36–50, 1979.

[168] M. Benning, M. McGuire, and P. Driessen, "Improved Position Tracking of a 3-D Gesture-Based Musical Controller Using a Kalman Filter," in *Proceedings of the New Interfaces for Musical Expression (NIME 2007)*, 2007.

[169] M. S. Benning, "Kalman Filtering for Computer Music Applications," Master's thesis, University of Victoria, Department of Electrical and Computer Engineering, Victoria, British Columbia, Canada, August 2007.

[170] J. Kramer and A. Kandel, "Robust Small Robot Localization From Highly Uncertain Sensors," *IEEE Transactions on Systems, Man, and Cybernetics, Part C: Applications and Reviews.*, vol. 41, no. 4, pp. 509 –519, July 2011.

[171] E. Mazor, A. Averbuch, Y. Bar-Shalom, and J. Dayan, "Interacting Multiple Model Methods in Target Tracking: a Survey," *IEEE Transactions on Aerospace and Electronic Systems*, vol. 34, no. 1, pp. 103 –123, January 1998.

[172] X. Rong Li and Y. Zhang, "Multiple-model Estimation with Variable Structure - V. Likely-model Set Algorithm," *IEEE Transactions on Aerospace and Electronic Systems*, vol. 36, no. 2, pp. 448–466, 2000.

[173] M. Gabrea, "Robust Adaptive Kalman Filtering-based Speech Enhancement Algorithm," *Proceedings of the IEEE International Conference on Acoustics, Speech, and Signal Processing (ICASSP'04)*, vol. 1, 2004.

[174] E. A. Wan and R. van der Merwe, *Kalman Filter and Neural Networks*. New York City, USA: John Wiley & Sons, Inc., October 2001, ch. Dual Extended Kalman Filter Methods, pp. 175–220.

[175] S. Roweis and Z. Ghahramani, *Kalman Filter and Neural Networks*. New York City, USA: John Wiley & Sons, Inc., October 2001, ch. Learning Nonlinear Dynamical Systems Using the Expectation Maximization Algorithm, pp. 175–220.

[176] A. Zia, T. Kirubarajan, J. Reilly, D. Yee, K. Punithakumar, and S. Shirani, "An EM Algorithm for Nonlinear State Estimation With Model Uncertainties," *IEEE Transactions on Signal Processing.*, vol. 56, no. 3, pp. 921–936, March 2008.

[177] D. G. Dansereau, N. Brock, and J. R. Cooperstock, "Predicting an Orchestral Conductor's Baton Movements Using Machine Learning," *Computer Music Journal*, vol. Vol. 37, no. 2, pp. 28–45, 2013.

[178] A.Doucet and A. Johansen, *Oxford Handbook of Nonlinear Filtering*. Oxford University Press, 2011, ch. A Tutorial on Particle Filtering and Smoothing: 15 Years Later.

[179] A. Doucet, N. de Freitas, and J.Gordon, *Sequential Monte Carlo Methods in Practice*. New York: Springer-Verlag, 2001, ch. An Introduction to Sequential Monte Carlo Methods, pp. 3–13.

[180] M. Arulampalam, S. Maskell, N. Gordon, and T. Clapp, "A tutorial on particle filters for online nonlinear/non-gaussian bayesian tracking," *IEEE Transactions on Signal Processing*, vol. 50, no. 2, pp. 174 –188, feb 2002.

[181] A. Doucet, M. Briers, and S. Sncal, "Efficient Block Sampling Strategies for Sequential Monte Carlo," *Journal of Computational and Graphical Statistics*, pp. 693–711, 2006.

[182] A. Doucet, S. Godsill, and C. Andrieu, "On Sequential Monte Carlo Sampling Methods for Bayesian Filtering," *Statistics and Computing*, vol. 10, no. 3, pp. 197–208, 2000.

[183] R. Velmurugan, V. Cevher, and J. H. McClellan, "Implementation of batch-based particle filters for multi-sensor tracking," in *IEEE Computational Advances in Multi-Sensor Adaptive Processing (CAMSAP)*, 2007.

[184] A.Doucet, S. Godsill, and C. Andrieu, "On Sequential Monte Carlo Sampling Methods for Bayesian Filtering," *Statistics and Computing*, 2000.

[185] T. Schon, F. Gustafsson, and P. Nordlund, "Marginalized Particle Filters for Mixed Linear/Nonlinear State-space Models," *IEEE Transactions on Signal Processing*, 2005.

[186] TCRT5000 datasheet. Accessed: May 2014. Vishay. [Online]. Available: www.vishay.com/docs/83760/tcrt5000.pdf

[187] AD22151 datasheet. Accessed: August 2014. Analog Devices. [Online]. Available: www.analog.com/static/imported.../data_sheets/AD22151.pdf

[188] D.-J. Jwo and T.-S. Cho, "A Practical Note on Evaluating Kalman Filter Performance Optimality and Degradation," *Applied Mathematics and Computation*, vol. 193, no. 2, pp. 482 – 505, 2007. [Online]. Available: http://www.sciencedirect.com/science/article/pii/S0096300307004316

[189] D. Alazard, "Introduction au filter de Kalman," Institut Superieur d'Aeronautique et de l'Espace (ISAE), Tech. Rep., 2011.

[190] A. Gelb, Ed., *Applied Optimal Estimation*. Cambridge, USA: MIT Press, 1974.

[191] B. P. Gibbs, *Advanced Kalman Filtering, Least-Squares and Modeling: A Practical Handbook*. New York City, USA: John Wiley & Sons, Inc., 2011.

[192] P. Maybeck, *Stochastic Model, Estimation, and Control*. Waltham, USA: Academic Press, 1982, vol. 2.

[193] M. H. Beale, M. Hagan, and H. B. Demuth, *Neural Network Toolbox Users Guide*, Matlab, Natick, MA, October 2014, available Online. [Online]. Available: http://www.mathworks.com/help/releases/R2014b/pdf_doc/nnet/nnet_ug.pdf

[194] V. Yaremchuk, C. B. Medeiros, and M. M. Wanderley, "Classification of Sensor Outputs and Gestures for IMM and Kalman filter: a Machine Learning Approach," 2014, [Working paper].